Crosslinking studies of the bacterial RNase P holoenzyme and functional characterisation of the novel protein-only RNase P from *Arabidopsis thaliana*

Dissertation

zur

Erlangung des Doktorgrades

der Naturwissenschaften

(Dr. rer. nat.)

dem Fachbereich

Pharmazeutische Chemie

der Philipps-Universität Marburg

vorgelegt von

Liudmila Pavlova

aus Ardatov, Russland

Marburg an der Lahn, 2012

Vom Fachbereich Pharmazeutische Chemie
der Philipps-Universität Marburg als Dissertation am 01.08.2012 angenommen.

Erstgutachter: Prof. Dr. Roland K. Hartmann
Zweitgutachter: Prof. Dr. Peter Friedhoff

Tag der mündlichen Prüfung am: 02.08.2012

Crosslinking studies of the bacterial RNase P holoenzyme and functional characterisation of the novel protein-only RNase P from *Arabidopsis thaliana*

Dissertation

by

Liudmila Pavlova

in partial fulfillment of the requirements for
the degree of Doctor of Philosophy

Faculty of Pharmacy

Institute of Pharmaceutical Chemistry

Philipps University Marburg

Germany

Marburg an der Lahn, 2012

Table of contents

1.Introduction

1.1 RNase P

The ubiquitous endonuclease RNase P is responsible for the 5'-maturation of different precursor transfer RNA (ptRNAs) (Robertson et al., 1972; Schön et al., 1999; Kazantsev& Pace, 2006; Hartmann et al., 2009). RNase P was previously reported as a ribozyme: a single RNA subunit and one protein in Bacteria, or at least four proteins in Archaea, or up to ten protein subunits in Eukarya (Hartmann&Hartmann, 2003). The RNA moiety was shown to be the catalytic subunit of the enzyme (Guerrier-Takada et al., 1983). In Bacteria and some Archaea P RNA component is active *in vitro* without proteins (Guerrier-Takada et al., 1983; Pannucci et al., 1999). RNase P is indispensible for cell viability, as both P RNA and proteins are essential *in vivo.* Additionally, RNase P has been reported as a transcription factor (Reiner et al., 2006).

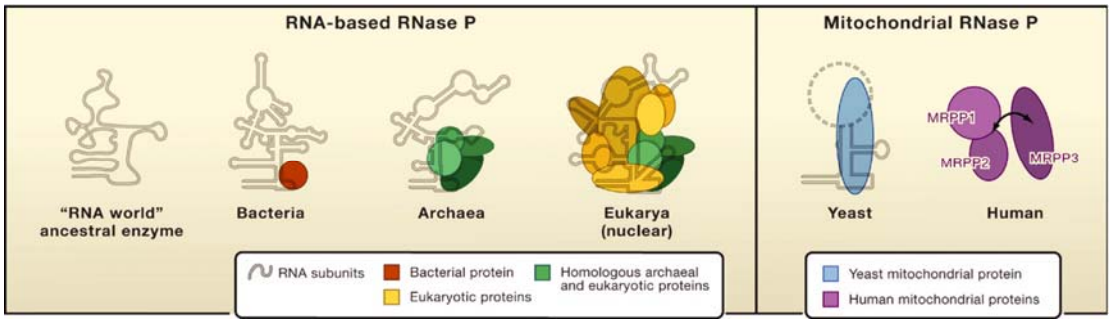

Figure 1.1. Diversity of RNase P from different species. On the left side is an assumed structure of ancestral RNA-only RNase P. RNA-protein interactions are presented schematically. On the right side are shown protein-only RNase P from yeast and human mitochondria (figure reproduced from Walker&Engelke, 2008).

Notwithstanding this general view, studies on RNase P activities from the organelles of some Eukarya are at odds with a general ribonucleoprotein nature of the enzyme. First evidence of protein-only RNase P was found in human mitochondria (Holzmann et al., 2008) and spinach chloroplast (Thomas et al., 1995). The same findings were reported for the trypanosomal mitochondrial RNase P (Salavati et al., 2001). Recently three protein-only RNase P enzymes, PRORP1, PRORP2 and PRORP3, were identified in *Arabidopsis thaliana* (Gobert et al., 2010). The smallest known free-living eukaryotic organism, green algae *Ostreococcus tauri,* harbours in its nucleus both *A.thaliana* PRORP1 homolog and bacterial RNase P-like protein, while

simultaneously its organelles encode bacterial RNase P-like RNAs (Lai et al., 2011). In contrast, *Cyanophora paradoxa* and *Porphyra purpurea* (red algae) as well as *Zea mays* and *Nephroselmis olivacea* (green plants) chloroplasts contain RNase P, which is a ribonucleoprotein similar to the archaeal/eukaryal nuclear RNase P (Baum et al., 1996; Cordier&Schon, 1999; Reith&Munholland, 1995; Turmel et al., 1999; Collins et al., 2000). RNase P is the only known natural model system with existing vestiges of different phases of evolution, ranging from the bacterial "almost RNA-alone" enzyme being close to the assumed "RNA World" state of early evolution, over intermediate states (archaeal and eukaryal nuclear RNase P with 4 to 10 proteins) to the protein-only RNase P enzymes.

1.2 Crystal structure of bacterial RNase P

Recently in 2010 the first high-resolution crystal structure of bacterial RNase P from *Thermotoga maritima* was resolved (Reiter et al., 2010). A comparison with previous three-dimensional P RNA model (Massire et al., 1998) and the holoenzyme models of *Escherichia coli* (Buck et al., 2005), *Bacillus subtilis* (Tsai et al., 2003; Niranjanakumari et al., 2007), and *Bacillus stearothermophilus* (Buck et al., 2005) are in good agreement with the crystal structure of the holoenzyme complex.

The structure of *T.maritima* RNase P consists of a large RNA subunit (338 nucleotides, ~110kDa, P RNA) and a small protein component (117 amino acids, ~14.3 kDa, P protein) in complex with tRNA (76 nucleotides, ~26 kDa). The acceptor stem of the tRNA is directed against RNase P and forms several tRNA- P RNA intermolecular contacts (Fig. 1.2a). The TΨC and D loops of the tRNA contact the S-domain of the P RNA, while the acceptor stem extends from the S-domain into the C-domain crossing the main P1/P4/P5 coaxial stem (Fig. 1.2b and 1.2c). The 3′-CCA end of the tRNA enters a tunnel formed by P6/P15/P16/P17 and base pairs with nucleotides in the L15-loop region (Fig. 1.2c). The 5′-end of the tRNA indicates the location of the active site, which is close to the region where P4, P5, and CR-IV intersect (Fig. 1.2c). The protein component is also adjacent to the 5′-end of the mature tRNA, but does not contact it.

The P protein contacts include the CR-IV and CR-V regions, the P15 stem, and the P2/P3 helix interface of the P RNA (Fig. 1.2c, protein not shown). The pre-tRNA leader makes extensive contacts with the P protein, but few with the P RNA.

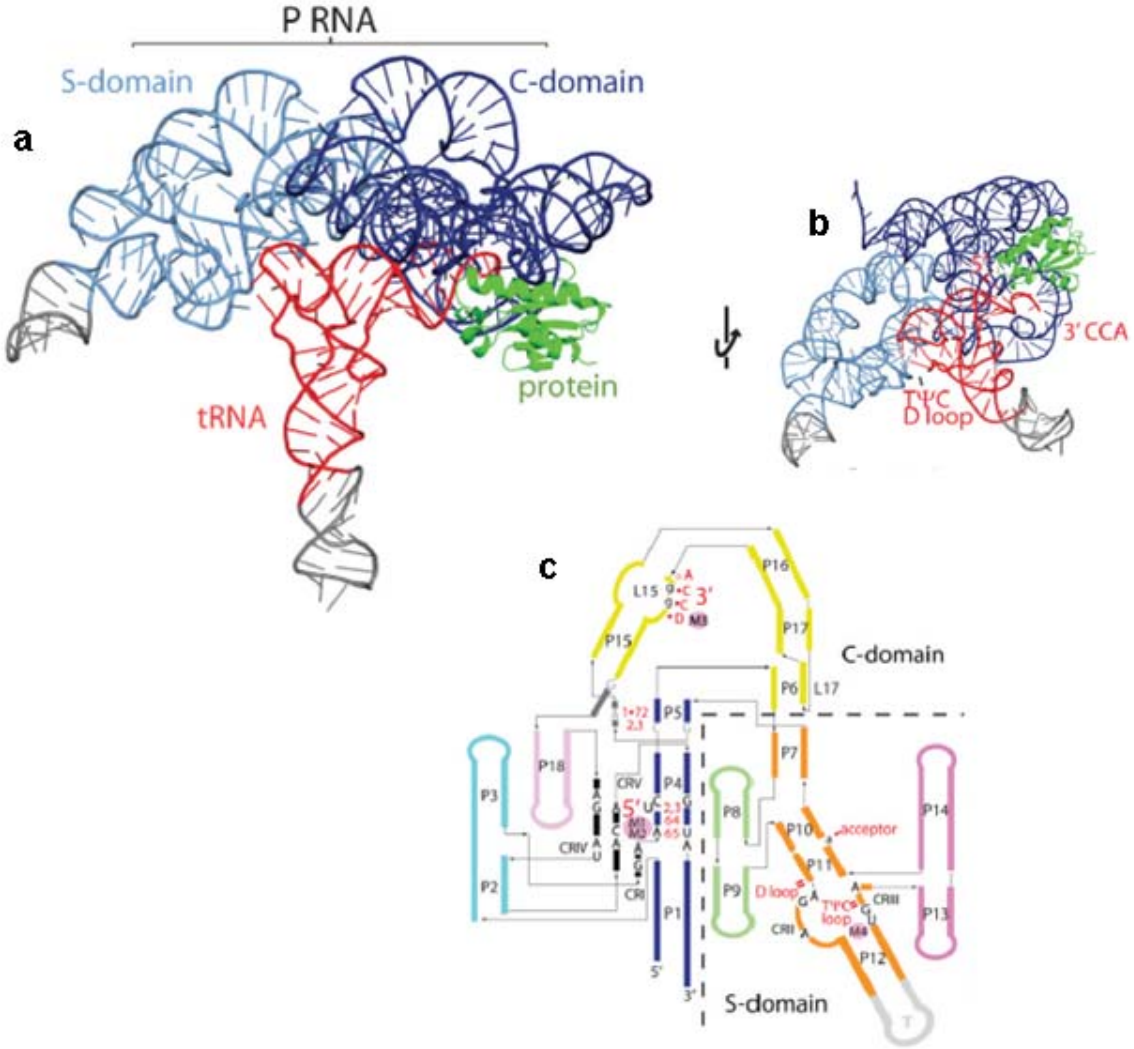

Figure 1.2. Crystal structure of the *T. maritima* RNase P holoenzyme in complex with tRNA.

a. The RNA subunit contains the catalytic C-domain (blue) and specificity S-domain (light-blue) domains. The RNase P protein (green) binds the 5′ -leader region of the ptRNA (red). **b.** The tRNA recognition regions: the 5′ -end and the highly conserved TΨC and D loop regions of ptRNA, the 3′-CCA end of ptRNA. **c.** Scheme of the P RNA secondary structure mapping the tRNA-P RNA contacts observed in the crystal structure (figure assumed from Reiter et al., 2010).

1.3 tRNA recognition

Among various RNase P substrates are some viral RNAs (Guerrier-Takada et al., 1988; Mans et al., 1990; Hartmann et al., 1995), 4.5S RNA (Peck-Müller et al.,1991), bacteriophage ø-induced RNA (Bothwell et al., 1976), precursor of transfer messenger RNA (tmRNA)

(Komine et al., 1994), mRNAs (Alifano et al., 1994; Li&Altman, 2003), and some riboswitches (Altman et al., 2005). These alternative substrates of RNase P were not well characterized, but most likely they structurally imitate the l-like shape of the main substrate (tRNA). So far, genetically encoded synthesis of leaderless ptRNA was discovered only in *Nanoarchaeum equitans* (Randau et al., 2008).

In the *T.maritima* holoenzyme complex, the 3′-end of the tRNA is separated from the 5′-end and enters a tunnel shaped by P6/P15/P16/P17, which can barely host a single stranded RNA molecule (Fig. 1.3a).

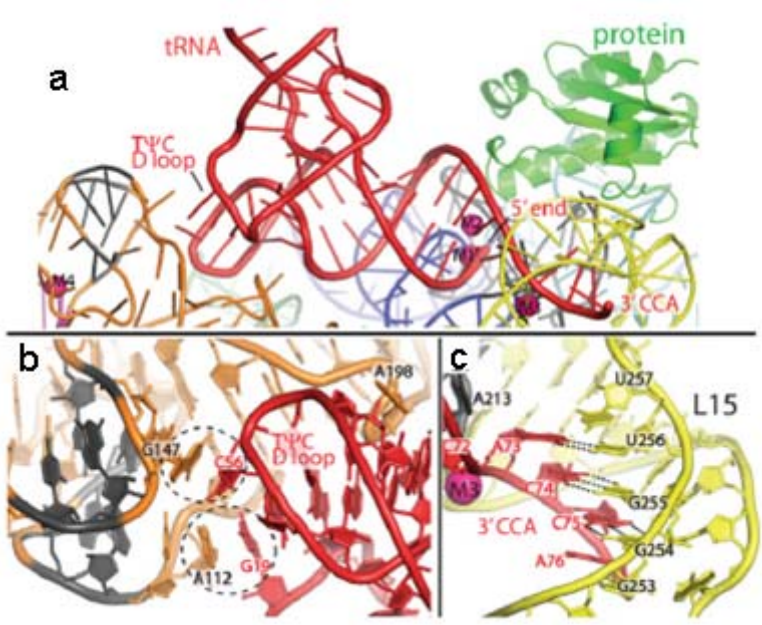

Figure 1.3. tRNA recognition by RNase P RNA observed in the crystal structure.

a. Recognition of precursor tRNA (red) by the P RNA of RNase P. **b.** tRNA-TΨC/D loop recognition by the S-domain of RNase P. **c.** Recognition of the tRNA 3'-CCA by the C-domain (figure adapted from Reiter et al., 2010).

The observed RNA-RNA interactions involved in substrate recognition include:

1) Stacking between bases in the tRNA TΨC and D-loops and the P RNA S-domain: G19-A112 and C56-G147 (Fig. 1.3b);

2) The second major interaction involves a highly conserved unstacked adenosine A198 in the P11 stem entering the minor groove of the tRNA acceptor stem (Fig. 1.3b);

3) The formation of canonical base pairing between the tRNA 3′-CCA D-motif and the L15 loop. This interaction is likely conserved in all bacterial and most archaeal RNase Ps, but not in organisms where CCA is added post-transcriptionally (Hartmann et al., 2009).

1.4 Protein/RNA interactions

An alignment of bacterial RNase P protein sequences (about 120 amino acids) reveals that the protein has a large, highly conserved area. Heterologous reconstitution of RNase P using an RNA from one source (organism) and a protein from another source indicated that bacterial RNase P proteins structurally are very similar to each other (Guerrier-Takada et al., 1983; Morse&Schmidt, 1992; Pascual&Voique, 1996), although they have little similarity to the protein components of Archaea and Eukarya (Liu&Altman(eds.), 2010).

Up to date three-dimensional structures of *Bacillus subtilis, Thermotoga maritima and Staphilococcus aureus* RNase P proteins were solved (Stams et al., 1998; Kazantsev et al., 2003; Spitzfaden et al., 2000). The crystal structure of the *T.maritima* holoenzyme agrees with biochemical data (Niranjanakumari et al., 1998; Kurz et al., 1998).

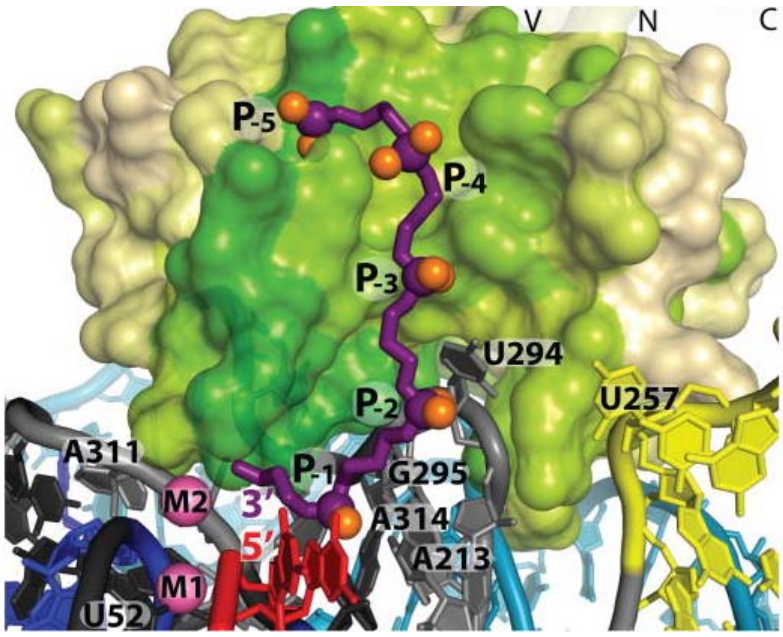

Figure 1.4. P protein-precursor tRNA interactions in the *T.maritima* RNase P crystal structure. Surface representation of the P protein (green). Pre-tRNA modeled as a phosphate chain (violet). 5'-leader of ptRNA (red) (figure adopted from Reiter *at al.,* 2010). The violet sequence is 5'-leader which was soaked after the cleavage, while it is so short and flexible that only phosphate backbone was possible to detect. 5'-end (+1 nt) of mature tRNA is marked in red (figure adopted from Reiter et al., 2010).

In the holoenzyme-ptRNA complex, the P protein is near the 5′-end of mature tRNA, but is too far away (over 6 Å) to make direct contacts. The P protein is located between the P15 and P3 stems and also contacts the CR-IV and CR-V loop regions of P RNA (Fig. 1.4). The structure shows that the leader contacts residues Phe17, Phe21, Lys51, Arg52, and Lys90 and likely interacts with Ser26, Gln28, Lys56, Arg89 (Fig. 1.4). The 3′-end of the leader is located

adjacent to the 5′-end of tRNA and near two conserved residues (Arg52 and Lys56) of the P protein. Consequently the main role of the protein subunit is stabilization of the leader to align the pre-tRNA in the complex.

1.5 Holoenzyme models of bacterial RNase P

Several bacterial RNase P holoenzyme models were proposed before the first holoenzyme crystal structure was solved. *E.coli* (Buck et al., 2005), *B.subtilis* (Tsai et al., 2003; Niranjanakumari et al., 2007) and *B.stearothermophilus* (Buck et al., 2005) holoenzyme models are based on the footprinting experiments, crosslinking studies and individual three-dimensional structures (Fig. 1.5).

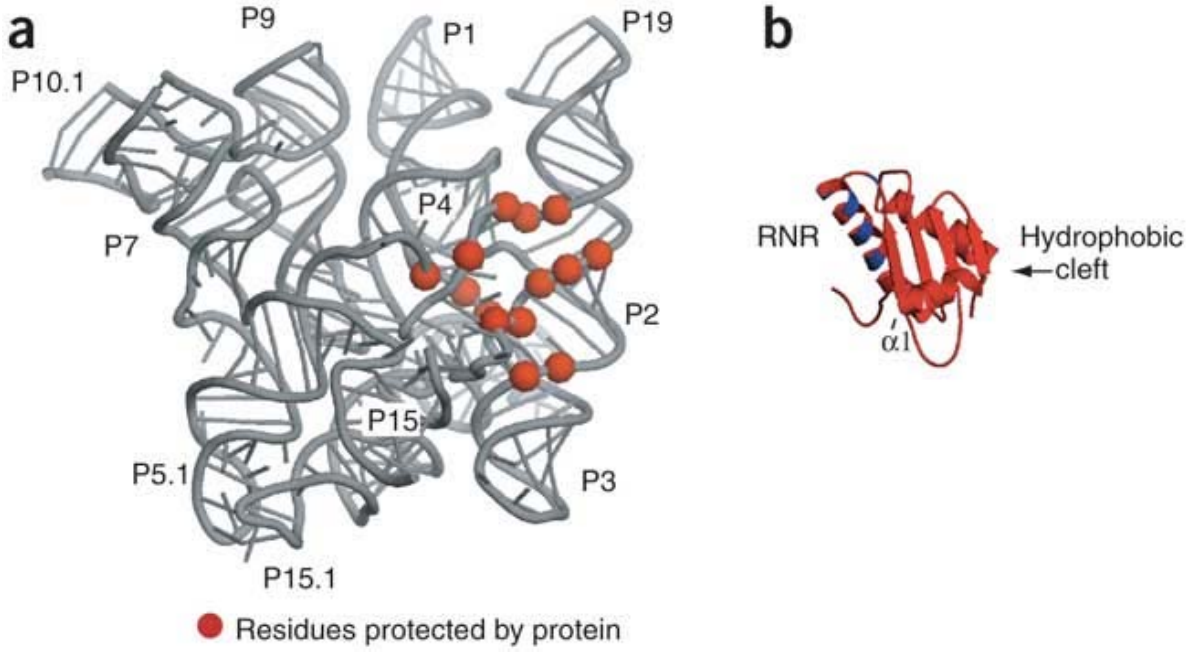

Figure 1.5. Holoenzyme model of *B.stearothermophilus* RNase P RNA and *B.subtilis* P protein. The residues marked as magenta spheres are protected by the P protein (adopted from Buck et al., 2005).

The holoenzyme model of *B.stearothermophilus* RNase P (Buck et al., 2005) is grounded on the crystal structure of *B.stearothermophilus* RNase P RNA (Kazantsev et al., 2005) and comparative footprinting studies with *E.coli*, *B.subtilis (*Stams et al., 1998) and *T.maritima* (Kazantsev et al., 2003) RNase P proteins (Buck et al., 2005). These studies showed up to 23 residues (ex. C23, C26, A49) in helices P2 and P3, P5 and P15 and loop L15 that are protected by the P protein.

1.6 Active site structure

The location of the active site is expected to be from the 5′-end of the mature tRNA (Figs. 1.6a and 1.6b). The phosphate backbone of tRNA nucleotides (+1 to +3) sits on the major groove of the P4 stem (near A50, G51, and U52) and places the tRNA 5′-end next to the P4 phosphate backbone and nucleotides A313 and A314 (Figs. 1.6a and 1.6b). The universally conserved U52 nucleotide is unstacked from the P4 stem and faces the tRNA 5′ -end. In addition, the tRNA 1•72 base pair is stabilized by an adenosine stack with A213, a nucleotide conserved in all bacteria.

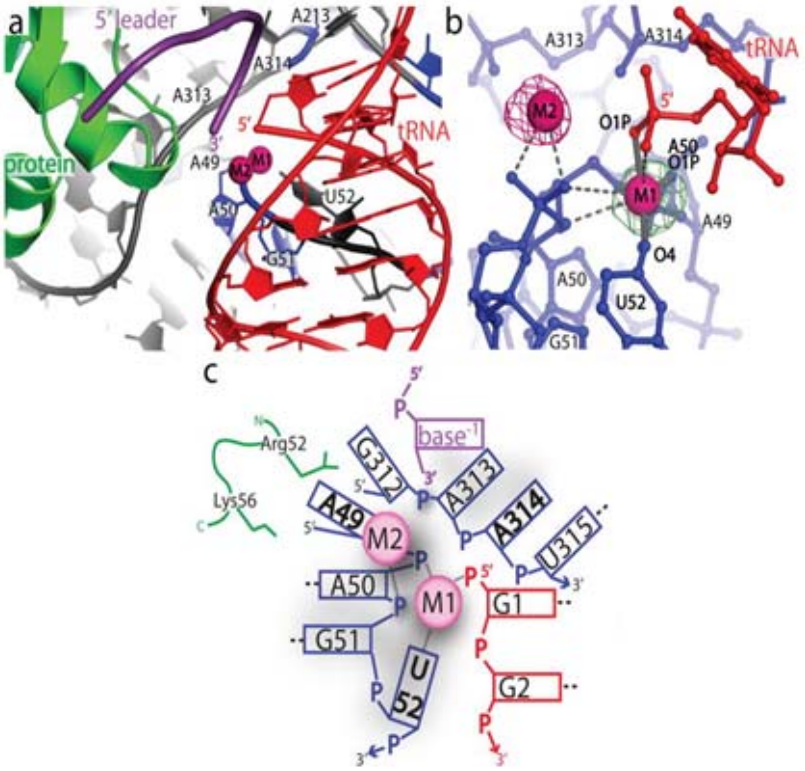

Figure 1.6. **Structure of the RNase P active site environment.**

a. The mature tRNA (red), the 5'-leader (purple), the P protein subunit (green), and the P RNA (blue and grey). A group of conserved P RNA nucleotides (A49 -U52, A213, A313, and A314) and two metal ions (magenta spheres) shape part of the active site. **b.** The two active site metal ions (M1 and M2) make contacts with tRNA and P RNA oxygens. Possible ligands are marked by dashed grey lines **c.** The schematic diagram represents all residues within 8 Å of the 5′ -phosphorus atom of tRNA. Metal ligand distances within 2.2 Å are marked by short dashed lines and canonical base pairs are shown in longer dashed lines. Universally conserved nucleotides in the P RNA are bold. The P RNA, tRNA, 5′ -leader, and protein side chains are marked in blue, red, purple and green, respectively (figure reproduced from Reiter et al., 2010).

The structure indicates that the active site includes at least two metal ions upon complex formation with pre-tRNA. The first metal ion M1 participates in catalysis by direct binding of

P RNA and the 5′-phosphate of tRNA. The metal ion M1 contacts with the A50 non-bridging phosphoryl oxygen, the O4 oxygen of the U52 nucleobase, and the O1P oxygen at the 5′ - termini of tRNA (Fig. 1.6c) (Reiter et al., 2011).

The second metal ion M2 is in close proximity to the phosphoryl oxygens of G51, the O3′ of the 5’ - leader, and the 5′-end of tRNA. The M2 metal ion could make additional contacts with both, the tRNA and the P RNA, during catalysis. A fully occupied M2 site is observed only in the presence of leader, suggesting that a local metal-dependent conformation change may occur, as previously reported (Hsieh et al., 2010). The distance between M1 and M2 metal ions is ~4.8 Å and both have a distance of 4 Å from the 5′ -phosphate of the tRNA.

1.7 The mechanism of RNase P catalysis

Antecedent biochemical (Guerrier-Takada et al., 1986; Smith&Pace, 1993; Warnecke et al., 1996; Chen et al., 1997) and recent structural (Reiter et al., 2010) studies are consistent with proposed nucleophilic substitution (in-line S_N2) reaction mechanism for the endonucleolytic cleavage of pre-tRNA by RNase P. The enzyme catalysis the hydrolysis of a phosphodiester bond: a monophosphate is generated at the 5’-termini of the mature tRNA and the 5’-flank is released with a uniform 3‘-OH termini (Fig. 1.7).

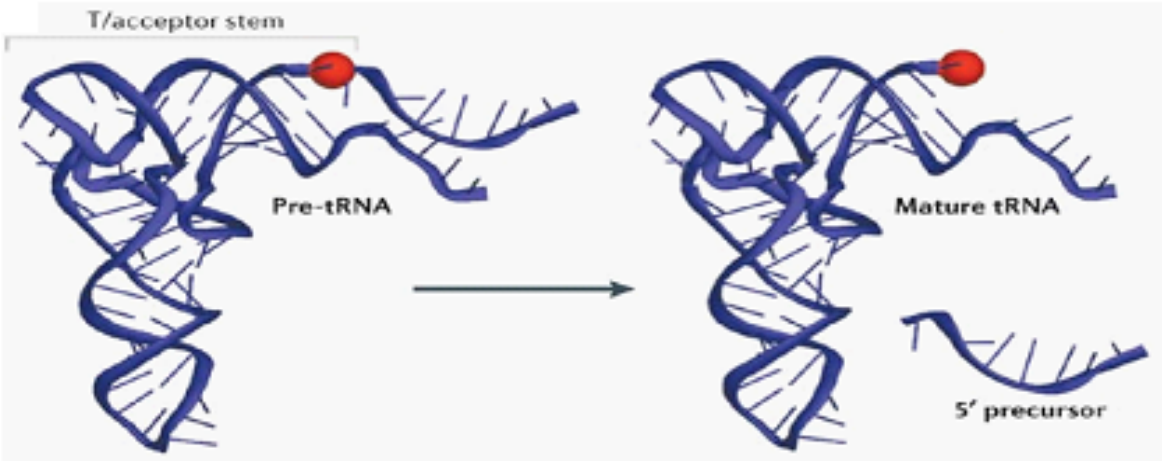

Figure 1.7. RNase P cleaves ptRNA. Schematic representation of precursor tRNA (on the left) and cleavage products (the mature tRNA and the 5’-precursor) (on the right side). The phosphate at the cleavage site is represented by a magenta sphere (figure adopted from Kasantsev&Pace, 2006).

According to the obtained crystal structure of the enzyme-product (E-P) complex (Reiter et al., 2010), the first metal ion M1 activates a hydroxyl nucleophile for an in-line nucleophilic substitution. That leads to formation of a new bond and shifting of the 3′-scissile

phosphate oxygen (Fig. 1.8). Consequently the stereochemistry of the phosphorus atom subjects an inversion of the configuration. As detected by biochemical studies, the metal ion is coordinated by the *pro-R*p (O2P) oxygen in the E-S complex during catalysis. This would allow the *pro-S*p (O1P) oxygen to coordinate the metal ion in the E-P complex, as it was observed in the crystal structure. Product release could be performed by activated OH^-.

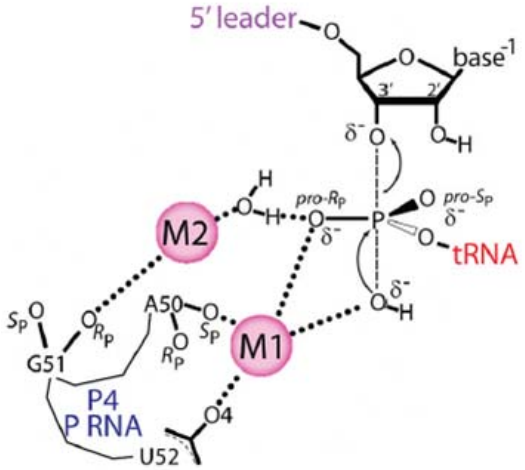

Figure 1.8. **Schematic representation of the proposed reaction mechanism for the 5'- maturation of pre-tRNA by RNase P** (figure adopted from Reiter et al., 2010).

1.8 Metal ion rescue experiments for RNase P studies

Metal ion rescue is an attractive technique for studying the functions of specific atoms as ligands for catalytic metal ions within ribozymes. The method utilizes differential affinities of two or more metal ions for two different ligands. The substitution of the original ligand that interacts weakly with the metal ion is proposed to diminish that function. That followed restitution of activity upon addition of a metal ion that binds to the substituted atom more strongly. This means the metal ion-ligand interaction was re-established, or "rescued". The rescuing metal ions are transition metals such as Mn^{2+}, Zn^{2+}, Cd^{2+}, Co^{2+}. The higher polarizability and d-orbitals allow them to interact more strongly with sulfur or nitrogen than Mg^{2+}, which binds oxygen ligands exclusively. The rescuing metal ions have different sizes and coordination geometries: Mg^{2+} ion and Mn^{2+} ion have similar ionic radii (0,72Å and 0,67Å, respectively), the more thiophylic Cd^{2+} ion is significantly larger (0.95Å), and Zn^{2+} is more thiophylic than Mn^{2+} (Frederiksen&Piccirilli, 2009).

Phosphorothioate substitution of nonbridging *pro*-Rp-oxygen on ptRNA at the canonical cleavage site -1/+1 reduces the reaction rate in the presence of Mg^{2+} by 1000-10000 fold (Fig.

1.9). The addition of Cd^{2+} or Mn^{2+} restores this activity, indicating that *pro*-Rp nonbridging oxygen directly coordinates a divalent ion during catalysis (Warnecke et al., 1996, 1999, 2000, Pfeiffer et al., 2000; Chen et al., 1997). In contrast, sulphur substitution of either *pro*-Sp oxygen or the 3'-bridging oxygen at the cleavage site shifts cleavage to the next unmodified phosphodiesther linkage in the 5'-direction (-1/-2 position) (Warnecke et al., 1996, 1999, 2000, Pfeiffer et al., 2000). In the unmodified reaction the rate of miscleavage is less than the rate of canonical cleavage. Softer metal ions have minor effect on the reaction rate and do not change the site of cleavage.

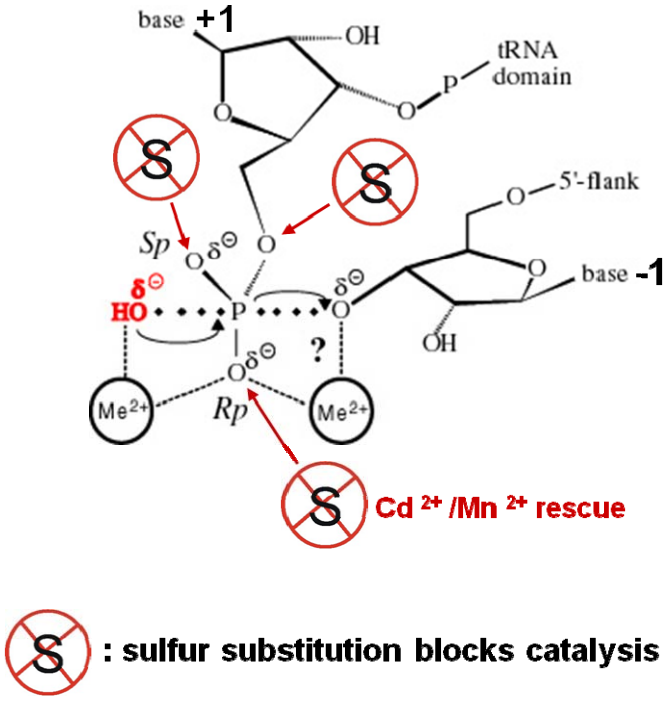

Figure 1.9. **Summary of thio effects on *E.coli* P RNA reaction.** (figure based on Warnecke et al., 1996, 1999, 2000 ; Pfeifer et al., 2000; Zuleeg et al., 2001 ; Persson et al., 2003. Figure courtesy: Prof.Dr.Roland Hartmann, Philipps University Marburg).

Catalytic metal ion-ligand interactions within group I introns (Szewczak et al., 2002; Adams at al., 2002), the hammerhead ribozyme (Peracchi et al., 1997; Martick et al., 2006) and bacterial RNase P (Warnecke et al., 1996, 1999, 2000 ; Pfeifer et al., 2000 ; Zuleeg et al., 2001 ; Persson et al., 2003 ; Reiter et al., 2010) were characterized by metal ion rescue experiments and later confirmed by structural studies. As example, in the case of protein enzymes for the homing endonuclease PI-*Sce*I, the involvement of aspartates in the cofactor binding was detected by metal ion rescue experiments (Christ et al., 1999; Schöttler et al., 2000), although substitution of individual atoms within proteins is a challenge.

1.9 Protein-only RNase P

1.9.1 Human mitochondrial RNase P

Early reports on the protein nature of some RNase Ps from human mitochondria, spinach chloroplast and trypanosomal mitochondria were met with scepticism (Rossmanith&Karwan, 1998; Rossmanith et al., 1995; Thomas et al., 1995; Wang et al., 1988), since none of the individual proteins were identified. Breakthrough came only in 2008 when three proteins of human mitochondrial RNase P (MRPP1, MRPP2 and MRPP3), were affinity-purified (Holzmann et al., 2008). In the presence of all three proteins the enzymatic ptRNA processing activity was reconstituted. This was the first evidence of ribozyme-free 5'-maturation of ptRNA. None of the proteins alone, nor combinations of any two of them, demonstrated ptRNA cleavage. Crystal structures of MRPP proteins are not presently available. MRPP1 is one of three vertebrate homologs to yeast TRM10 (tRNA m^1G methyltransferase), which is responsible for methylation of guanosine at position 9 of tRNAs (Jackman et al., 2003). It was assumed that MRPP1 is involved in substrate recognition, contributing specific tRNA-binding capacity to mtRNase P. Overexpression of MRPP1 protein alone augmented mtRNase P activity drastically.

MRPP2 is a member of the short-chain dehydrogenase/reductase (SDR) family. The NAD^+-binding domain of MRPP2, which is a well-conserved structure and proposed common RNA-binding motif, probably contributes to tRNA binding of the stable MRPP1/MRPP2 complex.

MRPP3 has two pentatricopeptide repeats which consist of approximately 35 amino acids and are assumed to mediate RNA-binding activity. No other structural motifs could be identified so far. Interaction of MRPP3 with the MRPP1/MRPP2 complex is unstable and dissociated under low salt conditions.

In spite of all three proteins contributing to RNA-binding, their tertiary structure is not known as well as their role in substrate recognition and catalysis. All three proteins are essential for 5'-maturation of mitochondrial pre-tRNA, in contrast to the recently discovered singular PRORP1 enzyme from *A. thaliana*.

1.9.2 PRORP protein family

In *Arabidopsis thaliana* a new family of proteins - PRORP (proteinaceous RNase P, Fig. 1.10) - was discovered (Gobert et al., 2010). Three proteins were identified (PRORP1,

PRORP2, PRORP3) that are orthologs of the human mitochondrial RNase P protein MRPP3, whereas no candidates for MRPP1 and MRPP2 were found. The overall identity between human MRPP3 and land-plant PRORP proteins is approximately 17 ± 1.6%.

In PRORP proteins the C-terminal part is the most conserved. It contains the catalytic domain NYN (N4BP1, YacP-like nuclease), which characterizes the PRORP proteins as metallonucleases (Anantharaman & Aravind, 2006). NYN domain is connected to zinc-finger-like motif and two or three pentatricopeptide repeats (PPR) that could be involved in RNA binding (Lurin et al., 2004). The N-terminal part is less conserved and only mitochondrial matrix-targeting sequence was recognized so far (Fig. 1.10). Two aspartates are conserved in the C-terminal domain and are responsible for the endonucleolytic activity of the enzymes. Mutation of these residues into alanines resulted in loss of activity for PRORP1, PRORP2 and PRORP3 (Gobert et al., 2010; Gutmann et al., 2012). So far, crystal structures of PRORP proteins are not available.

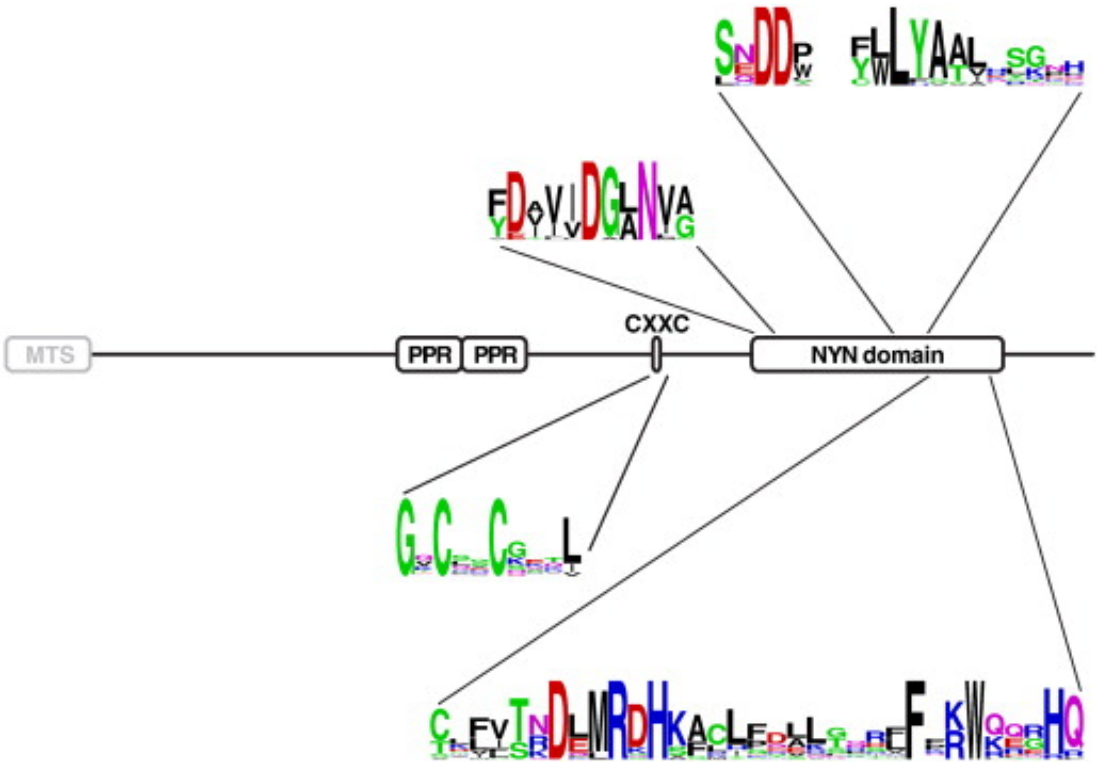

Figure 1.10. Structure of proteinaceous RNase P (PRORP). MTS-mitochondrial targeting sequence, PPR-pentatricopeptide repeat, CXXC-zinc-finger-like motif, NYN domain-N4BP1-YacP-like metallonuclease domain (figure adopted from Rossmanith, 2011)

PRORP1 is localized in mitochondria and chloroplasts, while PRORP2 and PRORP3 are harbored in the nucleus. Recombinant purified PRORP1 demonstrated *in vitro* efficient cleavage of mitochondrial $ptRNA^{Cys}$ and chloroplastic $ptRNA^{Phe}$ at the canonical site -1/+1 and generated tRNAs with 5′-phosphate ends as with other previously characterized RNase P types. Moreover PRORP1 cleaved tRNA-like structures of mRNAs called t-elements correctly at 3'-ends, indicating that the enzyme is also involved in the maturation of mRNAs in plant mitochondria (Gobert et al., 2010). Beyond involvement of PRORP2 and PRORP3 in tRNA 5'-maturation in nucleus, enzymes process small nucleolar RNA snoR43 and perform 3'-maturation of *nad6* mRNA (Gutmann et al., 2012).

Organellar RNase P PRORP1 is absolutely essential for plant viability, while involved in maturation of tRNAs and therefore in translation (protein synthesis is indispensible for photosynthesis and oxidative phosphorylation in plastids and mitochondria). In contrast, human mitochondrial RNase P is active only as a combination of three proteins *in vitro*, and all of them are involved in 5'-maturation of ptRNA *in vivo* (Holzmann et al., 2008). Moreover *Arabidopsis* PRORP1 can functionally replace *E. coli* RNase P *in vivo* (Gobert et al., 2010). Complementation studies demonstrated that the lethal knockdown of RNase P RNA in the *E. coli* mutant strain BW (Wegscheid & Hartmann, 2006) was rescued by PRORP1.

As was reported recently (Placido et al., 2010), two $tRNA^{His}$ biogenesis pathways coexist in plant mitochondria. The G_{-1} residue is absolutely essential for recognition by histidyl-tRNA synthetase. In the direct pathway the G_{-1} nucleotide of histidyl-tRNA is encoded by mitochondrial genome and PRORP1 cleaves at position -2/-1. The second pathway involves PRORP1 clevage at -1/+1 and the subsequent addition of a guanosine at the 5′-end of histidyl-tRNA (corresponding to position –1) by an enzymatic guanylyl transferase activity. This fact demonstrates that PRORP1 is less flexible and efficient than ribozyme-type RNase P in the processing of mitochondrial $tRNA^{His}$. Proteinaceous RNase P PRORP1 and bacterial RNase P may have a similar two-metal ion catalytic mechanism, as speculated previously for RNA- and protein-based metallonucleases (Steitz&Steitz, 1993; Auletta et al., 2011).

1.9.3 Spinach chloroplast RNase P

In a few publications by Peter Gegenheimer group (Wang et al., 1988; Thomas et al., 1995, 2000; Gegengeimer, 2000) *Spinacia oleracea* chloroplast RNase P was reported to be a protein enzyme, lacking the RNA subunit common to all other characterized RNase Ps. This assumption is based on the fact that the buoyant density of partially purified spinach

chloroplast RNase P corresponds to protein and not to RNA. Moreover micrococcal nuclease treatment of crude or partially purified spinach chloroplast RNase P had no affect on catalytical activity of the enzyme whereas the same treatment of RNA-based RNase P completely abolishes enzyme activity. The partially purified enzyme cleaves maize chloroplast pre-$tRNA^{Phe}$ (which lacks an encoded 3'-CCA sequence) and yeast nuclear pre-$tRNA^{Phe}$ at the canonical site for RNase P (position -1/+1).

The catalytic mechanism of a proteinaceous and RNA-based RNase P was compared. Partially purified preparations of chloroplast RNase P were tested for their ability to cleave a substrate molecule containing a phosphorothioate substitution at the scissile bond. In striking contrast to bacterial ribozyme, RNase P from spinach chloroplasts can accurately and efficiently cleave phosphorothioate-containing pre-tRNAs at the correct position. The ability of the chloroplast enzyme to hydrolyze an Rp-sulfur-containing phosphodiester bond suggests that Mg^{2+} is not coordinated, directly or indirectly, by the substrate *pro*-Rp oxygen during the chloroplast RNase P reaction

.

1.9.4 Diverse RNase Ps in *Ostreococcus tauri*

Recently genomes of some Prasinophyceae (*Micromonas pusilla, Ostreococcus lucimarinus, Ostreococcus tauri*) were sequenced. These unicellular green algae are ancient relatives of land plants and have small genome sizes (e.g. the nuclear genome of *O. tauri* is one of the smallest and most compact among eukaryotes).

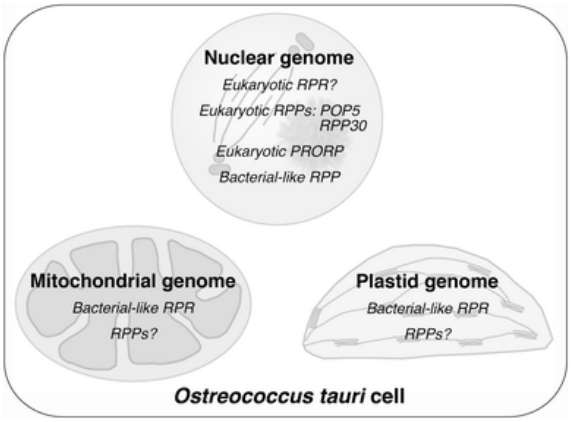

Figure 1.11. Summary of identified diverse RNase P components in *O. tauri* (figure reproduced from Lai et al., 2011).

Diverse variants of RNase P were discovered in *O. tauri* (Lai et al., 2011) (Fig. 1.12). First, a bacterial RNase P-like protein encoded by nuclear genome was found. Second, organelle (mitochondrial and chloroplast) genomes encode bacterial RNase P-like RNAs (269 nt and 327 nt respectively). Cleavage activity of these *O. tauri* RNase P RNAs was not detected even in the presence of *O. tauri* or bacterial RNase P proteins. Subsequently, a set of eukaryal nuclear RPPs was found (thus only POP5 and RPP30 were identified so far). Moreover, the *O. tauri* nuclear genome encodes a 57 kDa protein that is a homolog of *A. thaliana* PRORP1. The recombinant *O.tauri* PRORP cleaves pre-tRNA^{Gly} and pre-tRNA^{Leu} accurately *in vitro*. The presence of PRORP variants in organella of *O. tauri* was not yet investigated.

2. Goals

Crosslinking studies of the bacterial RNase P holoenzyme

Understanding the RNA-protein interactions is of fundamental value for molecular biology. Crosslinking is one of the best methods to investigate individual contacts between amino acids and nucleotides. Previously, crosslinking approaches to study the binding interfaces in RNA-protein complexes have utilized photoreactive base analogs or long-range crosslinkers attached to the phosphate. Short-range photoreactive groups at the 2'-ribose position have not yet been explored for RNA. The development of short-range ribose 2'-functionalities for crosslinking would extend the repertoire of tools to identify contacts at RNA-protein binding interfaces and would improve the resolution of the determined RNA-protein distance maps.

RNA-protein crosslinking by use of reactive 2'-ribose functionalities will be initially established and evaluated for the biochemically well-characterized bacterial RNase P, which consists of a catalytic RNA subunit (ca. 130 kDa) and a small basic protein (ca. 13 kDa). For crosslinking to Lys residues, RNAs with site-specific 2'-cis-diol functionalities will be activated by oxidation with sodium periodate.

The aims of this project include enzymatic synthesis of *Bacillus stearothermophilus* P RNA fragments and ligation with synthetic 2’-modified ribooligonucleotides to reconstitute full-lengh P RNA. Since the long RNA ligation (ca. 414 nts) is a challenge, the main effort will be to establish efficient ligation protocol. Enzymatic activity of ligated modified and unmodified ribozymes will be investigated. Crosslinking experiments and detection of sites of crosslinking in RNA and protein moieties will be conducted. The concrete question to be answered: will site-specific ribose 2'-aldehyde functions in the RNA react with Lys residues of the protein subunit in a specific manner? Since 2'-aldehyde functions are highly reactive, there is a risk of non-specific reactions with Lys residues before the genuine RNA-protein complex has formed. Here, the main effort will be to establish conditions that avoid damage of the RNA-protein complex during periodate oxidation treatment.

Functional characterisation of the novel protein-only RNase P from *Arabidopsis thaliana*

Ribonuclease P has been predominantly identified as a ribonucleoprotein that is responsible for the 5'-maturation of precursor tRNA (ptRNA). RNA-containing RNase P enzymes are present in all domains of life (Bacteria, Archaea and Eukarya). The majority of RNase P enzymes consist of one RNA subunit and at least one or up to ten protein subunits. The RNA moiety has been shown to be the catalytic subunit of the ribonucleoprotein enzymes.

Notwithstanding this general view, studies on RNase P activities from the organelles of some Eukaryotes are at odds with a general ribonucleoprotein nature of the enzyme. Human mitochondrial, spinach chloroplast and trypanosomal mitochondrial RNase P are composed of protein only. Recently three protein-only RNase P enzymes were identified in *Arabidopsis thaliana*, of which one (PRORP1) localizes to mitochondria and chloroplasts, whereas the other two (PRORP2 and PRORP3) are exclusively present in the nucleus. Recent data have demonstrated that *Arabidopsis* PRORP1 is able to replace the bacterial ribonucleoprotein *in vivo.*

The goal of this project is to characterise the function of the novel protein-only RNase P enzymes PRORP1, PRORP2 and PRORP3 from *Arabidopsis thaliana in vitro.* First, these protein enzymes have to be compared with the classical RNA-based RNase P enzyme from *Escherichia coli* in terms of kinetic parameters and cleavage mechanism. In order to identify functional groups in protein-based RNase P, we use a chemogenetic approach that involves altering single functional groups in the ptRNA substrate to identify coordination ligands of catalytic metal ions.

3. Methods

3.1 Bacterial cell culture

All media, buffers, glass pipettes and flasks used for bacterial cell culture were autoclaved for 20 minutes at 121°C and 1 bar. Alternatively, heat labile solutions were sterile filtrated via 0.2µm membrane filters, glassware was sterilized at least 3 hours at 180°C.

3.1.1 Bacterial cell culture in liquid medium

LB (Luria Bertani) medium	
Peptone	10 g/l
Yeast extract	5 g/l
NaCl	10 g/l
adjust pH to 7.5 (with NaOH)	

TB medium Solution *A*	
Tryptone	12 g
Yeast extract	24 g
Glycerol	4 ml
Total volume	1 l
TB medium Solution B	
KH_2PO4	170 mM
K_2HPO4	720 mM
Total volume	1 L
Do not adjust pH, app. 7.0	

E. coli cells were grown in LB at 37°C or TB medium at 19°C. For inducible promoter systems the media were supplemented for effective expression with IPTG (1 mM endconcentration). For selection of antibiotic resistance genes, growth media were adjusted to the appropriate antibiotic concentration (see Table 1).

Table 2.1. Antibiotic concentrations in these studies

Antibiotic	Bacteria	Concentration [µg/ml]	plasmid
ampicillin	*E. coli*	100	pSP64, pSBpt3'hh
kanamycin	*E. coli*	50	pET28b(+)], pET28-At-PRORP1-His, pET28-At-PRORP2-His, pET28-At-PRORP3-His,

For overnight cultures 3 ml LB/TB medium were inoculated either directly from a glycerol stock or with a single colony from an agar plate, and incubated while shaking (180-220 rpm, GFL 3033 shaking incubator) at 37°C.
Glycerol stocks were prepared by mixing sterilized 500 µl 99% (v/v) glycerol and 500 µl bacterial overnight culture. Glycerol stocks were frozen in liquid nitrogen and then stored at –80°C.

3.1.2 Cell growth on agar plates

In order to prepare agar plates, 12 g of agar-agar was added to 1 L of liquid LB / TB medium before autoclaving. After sterilization the medium was cooled down to approximately 50°C, then the appropriate antibiotic was added and Petri dishes were filled with small aliquots (15 – 20 ml) of the warm liquid. As soon as agar medium became solid, dishes were kept at 4°C until usage. Appropriate dilutions of cell suspension (~100 – 200 µl) were streaked on the agar plates using a sterile glass stick until the surface became dry. The plates then were turned upside-down and incubated overnight at 37°C.

3.1.3 Transformation of *E. coli* cells

3.1.3.1 Preparation of chemically competent cells

Ability of bacterial cells to accept external plasmid DNA is called competence. Incubation with $CaCl_2$ and cold treatment affects permeability and structure of the cell wall.
E.coli DH5α or BL21(DE3) strain was directly streaked from frozen glycerol stocks on agar plates and incubated overnight at 37°C. On the next day a single colony was picked and transfered into 3 ml LB medium and incubated under shaking (180 – 220 rpm) overnight. Next morning 1 ml was transferred into 1L Erlenmeyer flask with 400 ml LB or TB medium and was shaken in the incubator until OD_{600} reached 0.6-0.8. Then cell culture was poured into 500 ml plastic flask, kept on ice for 10 min and centrifuged at 3200xg (10 min and 4°C). The supernatant was discarded and the pellet resuspended in 100 ml ice-cold 100 mM $CaCl_2$. Cell suspension was divided in two 50 ml flasks and centrifuged at 12000 x g (10 min and 4°C). Pellets were resuspended in 7.5 ml cold 75 mM $CaCl_2$ / 25% (v/v) glycerol buffer, aliquoted in 200µl portions, frozen in liquid nitrogen and stored at -80°C.

3.1.3.2 Transformation of *E.coli* cells

Transformation is a process of changing cell genotype and phenotype as a result of uptaking exogeneous DNA.

SOC Medium	
Peptone	20 g
Yeast extract	5 g
NaCl	0.6 g
KCl	0.17 g
adjust to pH 7.5 with NaOH and autoclave	
Glucose (autoclave separately)	20 mM
$MgCl_2$	10 mM
$MgSO_4$	10 mM
Total volume	1 L
Magnesium salts (sterile filtered stock solutions) are added prior to use	

Competent cells were thawed on ice, 50µl cell suspension was mixed with 20 ng plasmid DNA or 5 µl DNA ligation reaction (see DNA ligation section) and incubated on ice for 30 min. Then they were heated 1 min at 42°C and chilled on ice for 2 min. 1000 µl SOC medium was added and reaction tubes were incubated 1 h in the thermo-mixer under gentle shaking at 37°C. After short centrifugation (4000 rpm) 800 µl of supernatant was removed, the cell pellet was resuspended in the remaining 200 µl of medium. Finally, the cell suspension was streaked out on an agar plate supplemented with appropriate antibiotic(s) (see Table 1).

3.2 General nucleic acid techniques

Electrophoresis is defined as the migration of a charged particle in an electric field. Under conditions of constant velocity, the driving force on a particle is the product of the charge on the particle and the applied field strength. This force is counteracted by the frictional resistance of the separation medium, which is proportional to its sheer velocity. The frictional resistance also depends on the additional factors, such as gel density and particle size (Dunn M.J.1993).

3.2.1 Agarose gel electrophoresis

5 x TBE buffer	[c]End	5 liters
Tris	445 mM	269.54 g
Boric acid	445 mM	137.57 g
EDTA	10 mM	18.61 g

5 x DNA sample buffer	
Bromophenol blue (BPB)	0.25 % (w/v)
Xylene cyanol blue (XCB)	0.25 % (w/v)
Glycerol	25 % (w/v)

In 5 x TBE buffer; pH 8.0

Agarose gels were mainly used for separation of DNA fragments. Agarose is a polysaccharide (composed of galactose and galactose derivatives). Agarose was dissolved in 1 x TBE buffer by heating (e.g. in a microwave). The gel solution was cooled down to about 50-60°C, ethidium bromide or RothiSafe® was added to a final concentration of 40 µg/100 ml, and the solution was poured into a gel tray with comb. Agarose concentrations are chosen according to the size of the expected fragments (see Table 2). Electrophoresis chambers were filled with 1 x TBE buffer. Gels were run at 7.5 mA/cm.

Table 2.2. Separation range of DNA fragment in agarose gels

% agarose (w/v)	DNA fragment size (kbp)
0.5	1.0-30
0.7	0.8 - 12
1.0	0.5 - 7
1.2	0.4 – 6.0
1.5	0.2 – 3.0
2.0	0.1 – 2.0

3.2.2 Detection of nucleic acids from PAA gels

3.2.2.1 Crystal violet gels

Mutagenic is either ethidium bromide itself or UV visualization. To handle these problems, crystal violet staining was used as it binds to DNA via electrostatic interactions. Crystal violet final concentration is 10 µg/ml in agarose gel and running buffer. DNA is visible as a dark

violet band. Staining with crystal violet is less sensitive compared to ethidium bromide staining. In some cases the cloning efficiency could be improved by this procedure.

3.2.2.2 Ethidium bromide staining

In agarose gel electrophoresis, DNAs were visualized by ethidium bromide staining. Ethidium bromide intercalates between the stacked bases of DNA and RNA. It emits fluorescent light at 590 nm (orange) when exposed under UV light between 254 nm (short wave) and 366 nm (long wave). Ethidium bromide (final concentration 0.4 mg/ ml) was added to agarose gel solution, therefore DNA could be visualized directly after or even during electrophoresis under UV transilluminator. Finally the gel was placed on a UV-transilluminator and nucleic acids were visualized and documented using a digital camera system.

3.2.3 Polyacrylamide gel electrophoresis

Polyacrylamide gel is formed by the polymerization of monomers of acrylamide in the presence of a suitable concentration of the bifunctional cross-linking agent *N, N'*-methylene-*bis*-acrylamide. The length of the polymer chains and therefore the pore size is dictated by the concentration of acrylamide used, which is typically between 3.5 and 20 %, and by the ratio of acrylamide –bisacrylamide (48:2 in our lab). Further, the concentration of acrylamide determines elasticity, density, and mechanical strength of the gel. Gel polymerization is initiated with ammonium persulfate (APS), the polymerization is accelerated with *N,N,N,N,*-tetramethylendiamine (TEMED). It is important to be aware that acrylamide is an accumulative neurotoxin.

3.2.3.1 Denaturing PAGE

Denaturing gels are supplemented with 8 M urea before polymerisation, hence, the native structure of macromolecules that run within the gel is disrupted.

PAA gel solution	c_{End}	20 %	10 %
5 x TBE	1 x TBE	200 ml	200 ml
Acrylamide (48 %)/ Bisacrylamide (2 %)	in appropriate concentration	400 ml	200 ml
Urea	8 M	480 g	480 g
H_2O		ad 1000 ml	ad 1000 ml

3 x Stock solution sample buffer	
Urea (end concentration = 8 M)	0.48 g
5 x TBE	200µl
Bromophenol blue (BPB)	0.001 % (w/v)
Xylene cyanol blue (XCB)	0.001 % (w/v)
H_2O	ad 1 ml

For gel preparation glass plates were cleaned with 70 % ethanol and assembled with spacers. For PAA gel solutions of < 20 %, the 20 % PAA gel solution (see above) was diluted by addition of the appropriate volume of 8 M urea in 1 x TBE. Polymerisation was initiated by mixing with 1/100 volume 10 % (w/v) APS and 1/1000 volume TEMED. The gel solution was poured between the clamped glass plates, and a comb was inserted between the glass plates at the top, to create pockets for later sample loading. After polymerisation (approximately 1 h), the comb was removed, and pockets were immediately rinsed using a syringe filled with 1 x TBE buffer to remove urea that diffuses from the gel matrix and tends to accumulate in the pockets, and to avoid later polymerisation of unpolymerised acrylamide within the pockets. The glass plates containing the gel were fixed in the electrophoresis chamber to bridge the buffer reservoirs filled with 1 x TBE buffer and electrophoresis was performed at 5–30 mA (depending on gel size and PAA concentration).

Table 2.3. The size of single-stranded DNA/RNA fragments comigrating in denaturing PAGE (given in base pairs)

% Polyacrylamide	Bromophenol blue	Xylene cyanol
5	35	130
6	26	106
8	19	70-80
10	12	55
20	8	25

3.2.3.2 Native polycrylamide gels

Native gels do not contain any denaturing agents. Usually they are applied for the separation of double-stranded DNA or folded RNAs. The migration mobility depends on the size and tertiary structure of a nucleic acid. This results in migration differences between fragments of the same size, but different structure.

Table 2.4. The size of DNA fragments (bp) comigrating in non-denaturing PAGE

% polyacrylamide	Bromophenol blue	Xylene cyanol
3.5	100	460
5	65	260
8	45	160
12	20	70
20	12	45

3.2.4 Detection of nucleic acids from PAA gels

Nowadays several fluorescent dyes for detection of nucleic acids are available. Their sensitivity is summed up in the Table 2.5.

Table 2.5. Sensitivity of general nucleic acid stains per band (table adopted from Tuma.R. 1999)

Nucleic acid	Gel type	Ethidium bromide staining	SYBR Gold staining	SYBR Green staining	Crystal violet staining
dsDNA	agarose	140 pg	34 pg	38 pg	50 ng
	PAGE	290 pg	35 pg	46 pg	
ssDNA	Urea-PAGE	870 pg	110 pg	430 pg	
oligos	Urea-PAGE	29 ng	1.5 ng	3.7 ng	
RNA	Formaldehyde-agarose	34 ng	4 ng	23 ng	
	agarose	3.2 ng	0.48 ng	7.0 ng	

3.2.4.1 Ethidium bromide staining

In case of DNA/RNA in PAA gels, glass plates were reassembled after electrophoresis. Gels were carefully inserted into plastic bags, incubated in ethidium bromide staining solution (0.5 µg/ml in 1 x TBE) for 10 min at room temperature under shaking. Staining solution was carefully removed and gels were analysed under UV transilluminator.

3.2.4.2 SYBR Gold staining

SYBR Gold stain is greater than 10-fold more sensitive than ethidium bromide for detecting dsDNA, ssDNA, oligos or RNA in gels. We routinely detect as little as 34 pg of dsDNA or 4 ng of RNA per band using a 300 nm UV transilluminator. Detection with SYBR Gold is possible in many gel types, including high-percentage agarose, glyoxal/agarose,

formaldehyde/agarose, native polyacrylamide– and urea–polyacrylamide gels. No wash step is required in order to achieve maximal sensitivities. 10.000×fold stock SYBR Gold stain was diluted to 1×fold solution in 5×TBE-buffer instead of 1× TBE-buffer, because in our hands the stability of light-sensitive solution was rather higher during a period of 2 weeks. Though the best results were obtained with fresh staining solution. For 1 mini-gel 50 ml of 1×staining solution is sufficient. This amount is enough to stain up to 20 mini-gels. In the staining container protected from light gels were agitated gently 40-60 min at room temperature. Stained gels were viewed with 300 nm UV transilluminator and photographed.

3.2.4.3 Radioluminography

^{32}P- labelled RNA or DNA was detected using a phosphoimager. For this purpose, the gel was wrapped in cellophane and exposed to imaging plate in closed cassette. Depending on the amount of radioactivity, exposition times varied (e.g. a 1-min exposure for labelling reactions and overnight exposure for kinetic analyses or ligation). The imaging plates were scanned by BIO-imaging analyser BAS 1000 (Raytest, Fujifilm) and the PC-BASR software. Further evaluation was done using software AIDA 4.5.

3.2.5 Photometric concentration determination of nucleic acids

The concentration of nucleic acids was determined by measuring the absorption at 260 nm. Concentration could be calculated according to the Lambert Beer law:

$A = \varepsilon \cdot c \cdot d$

(**A**: Absorbance; c: molar concentration of DNA/RNA [mol/l]; **ε**: molar extinction coefficient [1/(M·cm)]; **d:** path length of the cuvette [cm])

Samples were diluted 1:100 –1:400 in water (depending on the expected concentration) and the absorbance at 260 nm was measured against water using a UV spectrophotometer. The concentration was calculated using the known values c(1 A_{260}) that represent the concentration corresponding to one absorbance unit at 260 nm (1 A_{260}):

1 A_{260} **double-stranded DNA**	corresponds to a c(1 A_{260}) of ~ 50 µg / ml
1 A_{260} **single-stranded DNA**	corresponds to a c(1 A_{260}) of ~ 33 µg / ml
1 A_{260} **RNA**	corresponds to a c(1 A_{260}) of ~ 40 µg / ml

This results in a general formula for RNA/DNA concentration calculation:

$$c[\mu g/\mu l] = \frac{A_{260} \cdot c(1\,A_{260}) \cdot D_f}{1000}$$

(**c** is concentration in µg/µl, $\boldsymbol{D_f}$ is the dilution factor).

3.2.6 Isolation of DNA from agarose gels

To isolate double-stranded DNA from agarose gels, bands containing the DNA fragment of interest were cut out under UV lamp. Commercially available QIAquick Gel Extraction Kit from Qiagen was used for further purification. DNA binds to a silica membrane of spin column. Contaminations and salts were removed by several washing steps. Finally pure DNA was eluted under low ionic strength conditions. The procedure was carried out according to the original protocol.

3.2.7 Isolation of RNA from polyacrylamide gels

RNAs from PAA gels were isolated by diffusion elution. The band of interest was detected by UV shadowing or using a phosphoimager (for radiolabelled RNA), cut out and transferred into a 1.5 ml reaction tube (or 50 ml falcon e.g. for preparative scale T7 transcriptions) containing elution buffer. The volume of buffer depends on the size of gel slice. For example a standard 15 µl labelling reaction was eluted in 500 µl buffer or in a buffer volume which efficiently covered the gel piece. Samples were shaken overnight at 4°C.

Elution buffer	
NaOAc pH 5.0	1 M

3.2.8 Precipitation of nucleic acids

3.2.8.1 Ethanol precipitation

Ethanol precipitation is a widely-used method to concentrate nucleic acids and remove salts. A precipitate of DNA/RNA formed at low temperature (-20°C or less) is recovered by centrifugation and redissolved in double-distilled or an appropriate buffer. Salts remain predominantly in the ethanol supernatant. For short DNA or RNA (< 30 nucleotides) or very small amounts of DNA/RNA, 20-40 µg glycogen was added as carrier. 1/10 volume of 3 M NaOAc pH 5.0 was added to one volume of DNA/RNA solution (for precipitation), followed

by mixing with 2.5 volumes of absolute ethanol. Samples were kept at least for 30 min at –80°C and centrifuged at least 30 min at 4°C, 13.000 rpm (Heraeus Biofuge fresco). For more efficient removal of salts, the pellet was eventually washed with 70 % (v/v) ethanol and centrifuged for another 15 min at 13.000 rpm. The supernatant was discarded. The pellet was dried at room temperature or at 37°C for ~2-5 min and dissolved in an appropriate volume of double-distilled water or an appropriate buffer for downstream application.

3.2.8.2 Isopropanol precipitation

Larger volumes of DNA/RNA solutions were precipitated by adding 0.8 volumes of isopropanol at room temperature. Samples were centrifuged as described for ethanol precipitation and if necessary washed with 70 % ethanol.

3.2.9 Phenol/Chloroform extraction

Phenol/chloroform extraction is a common technique used to purify DNA or RNA samples. Such extractions are used whenever it is necessary to inactivate or remove enzymes. The procedure capitalizes on the fact that deproteinisation is more efficient when two different organic solvents are used instead of one. The final extraction with chloroform also removes residual phenol. An equal volume of phenol (pH 7.5-8.0) is added to an aqueous DNA solution or acidic phenol (pH 4-4.5) was used for RNA purification (this keeps the RNA in the aqueous solution) pRNA. Probes were vigorously vortexed (2 min) and then centrifuged (3min, 13.000 rpm at room temperature) to split up phases. The upper aqueous layer was removed and transferred into a new tube under avoidance of the protein-containing interface. The lower organic layer and interface are discarded. The aqueous phase was extracted a second time using phenol and then once using chloroform. The aqueous layer is also the upper one in chloroform extractions. Afterwards DNA/RNA was concentrated by ethanol precipitation (chapter 3.2.8.1).

3.2.10 Gel filtration

3.2.10.1 NAP gel filtration

The NAP 5 columns (GE Healthcare) used in this study are filled with Sephadex 25. They are commonly applied to remove salts and single nucleotides from reaction mixtures. The columns were equilibrated with double-distilled water according to the manufacturer's protocol. The sample (500 µl) was loaded onto the column the volume had to be adjusted to the specified total volume if smaller) and entered the gel matrix by gravity flow. The sample was concentrated by ethanol precipitation.

3.2.10.2 Gel filtration on PD SpinTrap G-25

PD SpinTrap G-25 (GE Healthcare) is a single-use microspin column that is designed for desalting and buffer exchange of biological sample using a standard microcentrifuge. The column is prepacked with 500 µl Sephadex G-25. The applied sample was 25 µl. In this work columns were used for oligonucleotide purification from free γ-^{32}P ATP after 5'- end labelling (chapter 3.4.4.1).

3.2.11 Gel drying

For some techniques the PAA gel has to be dried because it is placed in direct contact with an X-ray film. Thin gels were dried in the vacuum dryer at 60°- 80°C. Therefore gels cast on filter paper (GB002, Schleicher and Schuell) were placed on a dryer support beneath which is a heating block. The gel was covered with cellophane and a silicone rubber cover sheet of the apparatus, above which a vacuum seal forms (Biorad Slab dryer model 483). The device is then connected to a vacuum pump. To minimize cracking of the middle size gel the procedure should take at least 1 hour.

3.3 DNA techniques

3.3.1 Preparation of plasmid DNA

The technique for plasmid DNA isolation is based on a modified alkaline lysis procedure (Birnboim and Doly, 1979; Birnboim, 1983). Under low salt and specific pH conditions plasmid DNA binds to an anion exchange resin or a silica membrane. All impurities (RNA, proteins, low-molecular dyes) are removed by a wash at intermediate ionic strength. Finally plasmid DNA is eluted in high salt buffer, concentrated and desalted by isopropanol precipitation.

3.3.1.1 Analytical scale preparation of plasmid DNA from *E.coli* cells ("Mini prep")

For isolation of plasmid DNA for analytical purposes the commercially available GenJET® Plasmide Miniprep Kit (Thermo Scientific) was used according to the supplied protocol. 3 ml (for cells containing high-copy plasmids like pSP64 or pUC19 derivatives) of an overnight culture (chapter 3.1.1) was lysed under alkaline conditions. Cell suspension was neutralised and adjusted to high-salt binding conditions in one step after lysis. Therefore, a sample was ready for purification on a spin column with a silica membrane. Elution was performed under low ionic strength conditions, and the eluted DNA could be directly used for e. g., digestion by restriction enzymes (chapter 3.3.2) or sequencing.

3.3.1.2 Preparative plasmid DNA isolation from *E.coli* cells

Commercially available Plasmide DNA Purification Nucleobond® PC500 kit (Macherey-Nagel) was applied for plasmid DNA isolation as described in manuals. Midi-preps and Maxi-preps were usually done starting from 50-100 ml bacterial culture or 400 ml respectively (high copy plasmids). Cell pellets were resuspended in RNase A containing buffer. After an SDS/alkaline lysis step, solution was neutralised and finally applied onto an anion exchange resin. Pure plasmid DNA was eluted in a high salt buffer. Plasmid DNA was concentrated by isopropanol precipitation (chapter 3.2.8.2) and washed using 70 % ethanol.

Buffers used for preparative plasmid preparation (Plasmide DNA Purification Nucleobond® PC500 kit, Macherey-Nagel)	
Cell resuspension buffer	50 mM Tris / HCl, pH 8.0 10 mM EDTA 100 µg/ml RNase A
Lysis buffer	200 mM NaOH 1 % (w/v) SDS
Neutralisation buffer	3 M KOAc, pH 5.5
Column equilibration buffer	750 mM NaCl 50 mM MOPS pH 7.0 15 % (v/v) Isopropanol 0.15 % (v/v) Triton X-100
Washing buffer	1 M NaCl 50 mM MOPS pH 7.0 15 % (v/v) Isopropanol
Elution buffer	1.25 M NaCl 50 mM Tris / HCl pH 8.5 15 % (v/v) Isopropanol

3.3.2 Restriction digest of DNA

Digestion of DNA with restriction endonucleases is a routine procedure to prepare DNA for analysis. This yields DNA products of a convenient size for further manipulations. Type ll restriction endonucleases bind and cleave DNA at specific target sites, consisting of short palindromic sequences. Isoschizomers are different enzymes that share the same specificity, in some cases, the same cleavage pattern. Compatibility of reaction conditions, fragment size, methylation sensitivity, blunt-ended/sticky-ended fragments need to be considered when choosing suitable restriction enzymes. Some restriction enzymes generate DNA fragments with either 5'- or 3'-overhangs (sticky ends) or some cut in the middle of their recognition site creating blunt ends. 3'-hydroxyl and 5'-phosphate termini are generated.

Restriction digest (exemplary)	
DNA (ca. 0.5 µg)	x µl
10 x buffer	2 µl
Restriction enzyme	0.2 - 2 µl
H_2O	ad 20 µl
	Σ 20 µl

The volume of restriction enzyme does not exceed more than 10 % of the total reaction volume to avoid relaxed cleavage specificities (star activities) and inhibition of digestion by the glycerol. Buffer conditions and incubation temperature depend on the specific restriction

enzyme. Incubation time varies from 1-3 h for analytical digestion to 4 –12 h for the preparative scale.

After digestion DNA was analysed on agarose gels (chapter 3.2.1). For some downstream applications it is necessary to heat-inactivate (temperature/time depends on the used restriction enzyme) the enzyme after digestion. For DNA ligation the digested sample was heat-inactivated for 20 min at 65°C. Optional, enzyme, primers, small cleavage fragments or uncut plasmid was removed by phenol/chloroform extraction (chapter 3.2.9) or gel purification (chapter 3.2.6).

3.3.3 Dephosphorylation of DNA

Removal of 5'-phosphates from linearized vector DNA can help prevent vector self-ligation and improve ligation efficiency. Calf intestinal alkaline phosphatase (CIAP) catalyses the removal of terminal 5'-phosphates from DNA, RNA and ribo- and deoxyribonucleotide triphosphates.

Dephosphorylation reaction		
DNA	x µl	1-10 µg
10 x CIAP buffer	3 µl	
CIAP 1 U/µl	3 µl	
H_2O	ad 30 µl	
	Σ 30 µl	30 min 37°C
10 x CIAP buffer	+ 2 µl	
H_2O	+ 16 µl	
CIAP 1 U/µl	+ 2 µl	
	Σ 50 µl	30 min 50°C, 30 min 37°C

Linearized plasmid DNA was mixed with the appropriate ATP-containing buffer and CIAP, as specified above, and then incubated for 30-60 min at 37°C. After 30 min incubation at 37°C, the reaction volume was increased by adding 10 x buffer, water and additional enzyme; the sample was incubated for another 30 min at 50°C and after adding of the second portion for 30 min at 37°C. Dephosphorylation was performed prior to gel purification (chapter 3.2.6) of the plasmid. Alternatively, the phosphatase was removed by phenol/chloroform extraction (chapter 3.2.9) and the DNA was concentrated by ethanol precipitation (chapter 3.2.8.1).

3.3.4 5'-phosphorylation of DNA

T4 Polynucleotide Kinase (T4 PNK) is a polynucleotide 5'-hydroxyl kinase that catalyses the transfer of the γ-phosphate from ATP to the 5'-OH group of single- and double-stranded DNA and RNA (forward reaction) or transfers the 5'-phosphate of DNA/RNA to ADP and rephosphorylates the 5'-OH of DNA/RNA generated in the first step (exchange reaction).

For subsequent ligation of PCR products, primers were 5'-phosphorylated prior to the PCR reaction or the DNA fragment was phosphorylated directly following the PCR reaction. The DNA oligonucleotide (primer) or double-stranded DNA fragment was phosphorylated as specified below.

Phosphorylation reaction		
DNA	x µl	10-1000 pmol
100 mM ATP	0.5 µl	
10 x T4 PNK buffer A (forward) (Thermo Scientific)	2 µl	
T4 PNK 20U/ml (Thermo Scientific)	1 µl	
H_2O	ad 20 µl	
	Σ 20 µl	1 h 37°C

The phosphorylated primers could be used directly in the PCR reaction after cooling down. If necessary, the enzyme was removed by phenol/chloroform extraction (chapter 3.2.9) and the DNA was concentrated by ethanol precipitation (chapter 3.2.8.1).

Radioactive labelling of DNA oligonucleotides was done using γ-^{32}P ATP according to the protocol for 5'-labelling of RNA (chapter 3.4.4.1).

3.3.5 Ligation

The individual components of the desired DNA can be joined together with DNA ligase. T4 DNA ligase catalyses formation of a phosphodiester bond between juxtaposed 5'-phosphate and 3'-hydroxyl termini in DNA duplex with blunt or cohesive termini. Insert DNA (5'-phosphorylated) and plasmid vector (dephosphorylated) were incubated with DNA ligase. Prior to ligation, DNA fragments and plasmid vectors were gel purified (chapter 3.2.6).

Concentration estimation based on an ethidium bromide agarose gel. Then the products of the ligation mixture were introduced into competent cells (chapter 3.1.3.2). Afterwards transformants are identified by appropriate genetic selection. A typical ligation reaction is shown below. A plasmid only control reaction with and without DNA ligase allowed monitoring for inefficient dephosphorylated and the presence of uncut plasmid, respectively. Molar ratios of vector: insert were usually 1:3 or 1:9.

Ligation reaction	**control**	**1:3**	**1:9**	
Vector	2 µl	2 µl	2 µl	30-100 ng
Insert	-	1 µl	3 µl	90-300 ng
5 x T4 DNA ligase buffer	2 µl	2 µl	2 µl	
ddH_2O	5 µl	4 µl	2 µl	
T4 DNA ligase	1 µl	1 µl	1 µl	
	Σ 10 µl	Σ 10 µl	Σ 10 µl	1h;37°C or overnight 16°C or 4°C

Ligation of DNA with 'sticky ends' was incubated overnight at 37°C. T4 DNA ligase was heat inactivated for 10 min at 65°C and then the ligation reaction was directly transformed into competent cells (chapter 3.1.3.2).

3.3.6 Polymerase chain reaction (PCR)

PCR is a powerful tool that allows amplification of specific DNA sequences. PCR is performed *in vitro* as a single step, requiring only two oligonucleotide primers, a polymerase, and temperature cycling of the DNA template in the presence of deoxyribonucleotides and Mg^{2+}ions.

For cloning experiments a thermostable DNA polymerase, usually *Pfu* or *Taq* polymerases (different features as speed, proof-reading etc.) were used, it exhibits a proofreading activity (3'→ 5' exonuclease activity) and does not produce 3'-overhangs. For efficient PCR reaction the primer and Mg^{2+} concentration in the PCR buffer and annealing temperature of the reaction has to be optimized. The reaction is basically performed in three steps:

Denaturation of the double-stranded DNA at 95°C.

Annealing of primers to the DNA template at a temperature specific for the primers used.

Elongation at 68-72°C for 5'→ 3' elongation of the annealed primer; elongation velocity is 1 min/1 kb using *Taq* polymerase and 2 min/1 kb using *Pfu* polymerase.

The components listed below were mixed in a PCR reaction tube. Polymerase was added during the initial denaturation step at 95°C to prevent unspecific elongation (hot start PCR).

PCR program			
Initial denaturation	95 °C	2 min	
denaturation	95 °C	30 s	
annealing	45- 65°C	30 s	
elongation	68 –72°C	30 s – 5 min	25-30 cycles
Final elongation	68 –72°C	5 min	

PCR reaction		
template	x µl	single bacterial colony, 10 ng plasmid or 500 ng genomic DNA
10 x PCR buffer MBI (–$MgCl_2$, + KCl)	5 µl	
25 mM $MgCl_2$	3 µl	or c_{End} = 1.5 – 4.5 mM
10 mM dNTPs each	0.5 µl	
Primer forward 100 pmol/µl	0.5 µl	
Primer reverse 100 pmol/µl	0.5 µl	
ddH_2O	ad 49.5 µl	
Pfu/*Taq* (5 U/µl)	+ 0.5 µl	added at 95°C during initial denaturation step
	Σ 50 µl	

5 µl aliquot of each reaction was checked on agarose gel (chapter 3.2.1). If the PCR fragment was used for cloning, the PCR reaction was concentrated by ethanol precipitation (chapter 3.2.8.1), digested with restriction enzymes (chater 3.3.2) if required and gel purified (chapters 3.3.2 and 3.2.6) prior to ligation (chapter 3.3.5).

3.4 RNA techniques

3.4.1 T7 RNA transcription

RNA can be transcribed *in vitro* on DNA template using RNA polymerases (e. g. T7 RNA polymerase). T7 phage promoter sequence (5'-TAA TAC GAC TCA CTA TA -3'; sense strand) is recognised by T7 RNA polymerase. Polymerisation occurs downstream in 5'→ 3' direction until the elongation complex falls off the template end during run-off transcription (i.e. polymerisation is compleated when the RNA polymerase reaches the end of the template). Either linearized plasmids or PCR products were used as templates. RNA for further 5'-end labelling with γ-^{32}P ATP was transcribed in the presence of guanosine (to

provide 5'-hydroxyl group). Guanosine was applied in excess to compete with GTP for incorporation at the 5'-end (suggesting a template encodes a G residue in position +1, otherwise T7 transcription would not function. The guanosine stock solution was dissolved at 75°C.

T7 transcription reaction

	c_{Stock}	c_{End}	small scale reaction	preparative reaction
HEPES pH 8.0	1 M	80 mM	4 µl	80 µl
DTT	100 mM	15 mM	2.5 µl	50 µl
$MgCl_2$	3 M	33 mM	0.55 µl	11 µl
Spermidine	100mM	1 mM	0.5 µl	10 µl
NTP mix	25 mM each	3.75 mM each	7.5 µl	150 µl
BSA	20 mg/ml	0.12 mg/ml	0.3 µl	6 µl
Template (linearised plasmid)	1 µg/µl	40 µg/ml	4 µl	80 µl
Guanosine	30 mM	9 mM	15 µl	300 µl
Pyrophosphatase	200 U/ml	2 U/ml	0.25 µl	5 µl
T7 RNA Polymerase	200 U/µl	4000 U/ml	1 µl	20 µl
RNase-free water			ad 50µl	ad 1000 µl
			Σ 50 µl	Σ 1000 µl

The guanosine stock solution was only added if the transcribed RNA was used for 5'-end labelling.

All components were mixed up in a 1.5 ml reaction tube, finally T7 RNA polymerase was added, followed by incubation at 37°C, after 2-4 h a second portion (2µl) of T7 RNA Polymerase was added. For optimizing transcription efficiency and higher yield, small scale (50 µl) reactions were performed (for better thermal equilibration). For efficiency analysis and concentration estimation, 2 µl aliquots were analysed in parallel with a defined amount of control RNA as a size marker on denaturing PAGE (chapter 3.2.4). After successful transcription, RNA transcript was purified. Therefore proteins were removed by phenol/chloroform extraction (chapter 3.2.9) and the eluate was concentrated by ethanol precipitation (chapter 3.2.8.1). Then the pellet was dissolved in double-distilled water and the sample was purified by denaturing PAGE on 1 mm thick gels. The pocket size was chosen according to the efficiency of T7 transcription (for example, 1 ml reaction sample was loaded into a 2x10 cm pocket). Gel percentage was adapted to the size of the RNA transcript. Gels were run at 15-20 mA to avoid heating until xylen cyanol reached 12 cm from the slot. Bands were cut out under UV lamp and eluted in 1 M NaOAc (pH 5.0) overnight at 4°C under

shaking (chapter 3.2.7). If the yield of elution was low, a second elution step was optional. RNA was concentrated by ethanol precipitation and resuspended in double-distilled water. Concentration was measured as described in chapter 3.2.5. The quality of purified RNA was checked by denaturing PAGE (chapter 3.2.3.1).

3.4.2 T7 RNA transcription of chemically modified RNAs

The T7 RNA polymerase mutant Y639F (Padilla&Sousa, 2002) is able to incorporate efficiently modified nucleotides such as 2´-ribose modifications (2'-deoxy, 2'-NH_2, 2'-F), *S*p-NTPαS analogs and *R*p-NTPαS because it has enhanced tolerance toward substitution of functional groups in the minor groove. *In vitro* T7 transcription with *S*p-NTPαS analogs resulted in *R*p-phosphorothioate-modified RNAs, which are produced due to converse of configuration at the phosphorus atom. Many phosphorothioate nucleotides are commercially available. For our studies all-Rp- phosphorothioate modified $ptRNA^{Gly}$ were synthesized with guanosine-5'-(α-thio)-monophosphate (GTPαS) (Jena Bioscience, Germany) and inosine-5'-(α-thio)-monophosphate (ITPαS). For stability of phosphorothioate nucleotides it is recommended to keep stock solutions at -80°C up to 12 months. To reach the highest yield of reaction the homogeneity of phosphorothioate nucleotides is required: only *Sp*-isomers, instead of random mixture. The 5'-OH termini is a prerequisite for 5'-end labelling that's why T7 transcription reaction was initiated with guanosine (chapter 3.4.1). Before pipetting, the frozen guanosine stock solution was pre-warmed at 75°C in a thermoshaker.

T7 transcription reaction

	[c]Stock	[c]End
RNase-free water		ad 50 µl
HEPES pH 8.0	1 M	80 mM
DTT	100 mM	15 mM
$MgCl_2$	2 M	20 mM
Spermidine	100 mM	1 mM
ATP, UTP, CTP	100 mM each	3.75 mM each
GTPαS or ITPαS	100 mM each	3.75 mM each
BSA	20 mg/ml	0.12 mg/ml
Template (linearised plasmid)	1 µg/µl	50 µg/ml
Guanosine	30 mM	9 mM
Pyrophosphatase	200 U/ml	2 U/ml
T7 RNA Polymerase Y639F (our lab)	self-prepared	2-4 µl
Total		50 µl

The reaction mix was prepared by adding the components – except for guanosine and T7 RNA polymerase – at room temperature in the order they are listed above and afterwards the mixture was pre-warmed to 37°C before adding guanosine. An appropriate amount of the pre-heated guanosine solution was quickly added to the reaction mix, which was vortexed immediately to avoid guanosine precipitation. The reaction was started by addition of pyrophosphatase and T7 RNA polymerase. After 2 hours of incubation at 37°C an additional portion of T7 RNA polymerase (2 µl in 50 µl total volume) was added to each reaction. The reaction mixture was incubated overnight at 37°C. Reaction efficiency was analyzed on 10 % denaturing polyacrylamide gel (chapter 3.2.3.1). To verify correct size of the sample, unmodified $ptRNA^{Gly}$ was loaded as a control. RNA transcripts were purified as described for unmodified RNAs (chapter 3.4.1).

3.4.3 Homogeneous 5' - and 3' - ends of T7 RNA transcripts

T7 RNA polymerase tends to append a few non-templated nucleotides to the 3'-end of the transcript product. For synthesis of RNAs with homogeneous 3' and 5' ends several approaches were established. For example, to one or both termini hammerhead or Hepatitis delta virus (HDV) ribozymes can be appended. They are small autocatalytic RNA motifs, originally identified in pathogenic plant viroids and virusoids, that catalyse phosphodiester bond hydrolysis at a single defined position immediately after synthesis and folding into an active conformation (Mg^{2+} ions have to be at high concentrations). A prerequisite for the application of hammerhead ribozymes at 3'-ends of RNA transcripts is the presence of a trinucleotide upstream of the cleavage site, optimally 5′-GUC. Hammerhead *cis*-cleavage generates products with 2', 3' cyclic phosphate at the 3' ends (ribozyme part) and 5'-hydroxyls. This is very useful if the RNA of interest has to be labeled at the 5' -end for further analysis. We sometimes observed reduced cleavage efficiency due to interaction of RNA product with HDV ribozyme. That problem was solved by incubating reaction tube for 3 min at 60°C and 3 min at 25°C (10 cycles).

3.4.4 Radiolabeling of RNA

3.4.4.1 5'-end labelling of RNA

For 5'- end labelling a 5'-hydroxyl group is essential. Consequently RNA transcripts have to be started with guanosine or have to be dephosphorylated prior to the reaction (chapter 3.3.3). T4 polynucleotide kinase (T4 PNK) from *E. coli* phage T4 was applied for this procedure.

5'- end labelling reaction	
10 x T4 PNK buffer A (forward reaction)	1.5 µl
25 mM DTT	1.5 µl
RNA	x µl (30 pmol)
RNase-free water	ad 11 µl
γ-^{32}P ATP (3000 Ci/mmol, 10 µCi/µl, 3.3 µM)	3.0 µl
T4 PNK (10 U/µl)	1.0 µl
	Σ 15 µl

Components were mixed in a reaction tube (T4 PNK was mixed up very promptly) and incubated for 1 h at 37°C. Sample volume was adjusted to 25 µl with RNA sample buffer and purified by denaturing PAGE (chapter 3.2.3.1) using thin (< 1mm) spacers. For localization of labelled RNA bands, small stickers were fixed on the cellophane covering the gel and marked with the rest of labelling reaction and detected using imaging plates. The printout of the image was confronted with the gel and bands of interest were cut out and eluted by diffusion (chapter 3.2.7), then ethanol precipitated in the presence of 10 µg glycogen as a carrier, and finally resuspended in 10 µl double-distilled water. Efficiency of labelling was measured with 1 µl sample by Cherenkov counting.

3.4.4.2 3'-end labeling of RNA

3'- end labelling is performed by T4 RNA ligase, which add a ^{32}P-pCp to the 3'-OH termini of the RNA (England and Uhlenbeck, 1978).

3'- end labeling reaction	
10 x T4 RNA ligase buffer	0.6 µl
1.5 mM ATP (use fresh dilution)	0.33 µl
RNA (purified by denaturing PAGE)	x µl (5-10 pmol)
[5'-^{32}P] pCp (3000 Ci/mmol, 10 µCi/µl,)	3.0 µl
T4 RNA Ligase (10 U/µl)	1.0 µl
ddH_2O	ad 6 µl

Components were mixed in a reaction tube in the order listed above and incubated overnight at 6°C. 19 µl RNA loading buffer was added and the radiolabelled RNA was purified by denaturing PAGE (chapter 3.2.3.1). The band of interest was cut out, eluted and concentrated by ethanol precipitation as described for 5'- end labelling of RNA (chapters 3.2.7, 3.2.8.1 and 3.4.4.1).

3.4.3 RNA ligation

Routine chemical synthesis of RNA is limited nowdays to 60- to 100-nt oligomers. Longer RNAs containing internal, site-specific chemical modifications could be prepared with T4 RNA ligase or T4 DNA ligase (Moore et al., 1992). T4 DNA ligase is able not only to join two DNA molecules, but also to catalyze formation of a phosphodiesther bond between two RNA molecules as well as RNA and DNA molecules. Two-way approach allows joining together two RNAs (or three-way - to ligate three RNA molecules) aligned and held together on a complementary bridging DNA oligonucleotide ("DNA splint").

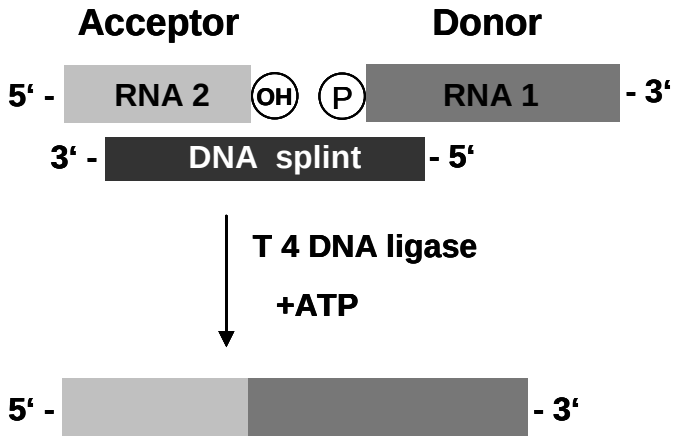

Figure 12.1. The scheme of the RNA ligation with T4 DNA ligase. DNA bridging oligonucleotide (black) hybridizes with two RNA molecules (light-gray and dark-gray) and shapes a double helical structure.

The most important prerequisites for ligation are 5'-phosphate of the donor and 3'-OH group of acceptor, as well as DNA splint without any bulges or gaps at the point of junction. T4 DNA ligase allows avoiding formation of circularized RNA structures and obtaining higher ligation efficiency in comparison to T4 RNA ligase.

To quantify the total yield of ligation it is recommended to include trace amounts of radiolabeled RNA (at 5' or 3'-end which should not be joined) in the reaction. In GRAFIT software intensity of ligated product compared to the total amount of radioactively labeled RNA can be calculated.

10x T4 DNA ligation buffer (Thermo Scientific)	
Tris-HCl pH 7.5	500mM
$MgCl_2$	100 mM
DTT	200 mM
ATP	10 mM

Two-way ligation reaction	
	[c]End
RNA 1 (donor)	1 µM
RNA 2 (acceptor)	3 µM
γ-^{32}P RNA 2 (trace amounts of 5'-labeled RNA 2)	≤1nM
DNA splint	2 µM
DTT	5 µM
ATP (fresh dilution)	1 mM
RNase inhibitor (Thermo Scientific)	40 U or 0.1µg/ml
T4 DNA ligase	7.5 U
10x T4 DNA ligase buffer	2 µl
ddH_2O	ad 20 µl
total	20µl

All components except RNase inhibitor, T4 DNA ligase and ATP were mixed at room temperature and heated up to 92°C for 1 min. Then reaction tube was cooled down at 25°C for 5 min. Afterwards T4 DNA ligase, RNase inhibitor and ATP were added and ligation reaction was performed at 28°C overnight. In general for design of the ligation reaction temperature (starting at 20°C up to 37°C) and incubation time (for example, 4h, 6h, 8h, 15h) should be optimized. In our hands this protocol resulted in the highest ligation yield of approximately 20% after 15 h incubation.

Product was analysed on 8% denaturing PAA gel with RNA marker or RNA of respective size in parallel. If the size was verified, whole amount of the probe was purified on 8% denaturing PAA gel (to remove DNA splint) and eluted in 1M NaOAc (pH 5.0) overnight as described in chapter 2.2.7. The yield of reaction was calculated using GRAFIT software.

3.4.4 Annealing of oligonucleotides

For crosslinking studies between RNase P RNA and RNase P protein *in vitro* transcribed fragments of RNase P RNA were annealed to corresponding synthetic 2'-aldehyde modified

oligoribonucleotides. Then, activity tests were performed to demonstrate that functional RNA subunits formed by annealing procedure.

RNA annealing	
in vitro transcript	40 or 50 pmol
5'-^{32}P-labeled synthetic oligoribonucleotides	2 - 2.5 pmol
KN4.5-buffer	10 µl

Annealing buffer	
HEPES-KOH, pH 7.4	50 mM
NH_4OAc	150 mM
β-Mercaptoethanol	4 mM
$MgCl_2$	4.5 mM

In vitro-transcribed RNA and 5'-^{32}P-labeled oligoribonucleotides in ratio 20:1 respectively were incubated for 5 min at 55 °C, then for 30 min at 37°C in 10 µl annealing buffer (50 mM HEPES-KOH, pH 7.4, 150 mM NH_4OAc, 4.5 mM $MgCl_2$, 4mM β-mercaptoethanol). The annealed RNase P RNA was directly used for kinetic studies and cross-linking assays.

3.4.6 Mass spectrometry: MALDI-TOF

Matrix-assisted laser desorption/ionization time-of-flight (MALDI-TOF) type of spectrometry is the most widely used technique for analysis of large biomolecules. For our studies all MALDI-TOF mass spectra were produced in the group of Prof. Sabine Müller at Ernst Moritz Arndt University, Greifswald. MALDI-TOF mass spectra were registered using Bruker Microflex (Bruker, Germany). The mixture of 3-hydroxypicolinic acid and aqueous ammonium citrate was used as a matrix. Prior to analysis samples were purified on cation-exchange resins in order to remove alkali and alkaline earth metals.

3.5 Protein methods

3.5.1 Protein staining methods

3.5.1.1 Sensitivity of general protein stains

The sensitivity of silver staining is considered to be 20-200 times higher than methods using Coomassie (CBB) and about 0,1 ng of protein per band could be detected. The high sensitivity makes this method ideal for the detection and analysis of protein samples that are

available in only limited quantities or for the detection of protein-nucleic acids complex formation.

Sensitivity of general protein stains	per band
Coomassie brilliant blue staining	0.2-0.5 µg
Fluorescent staining	10 ng
Silver staining	0.1 ng

3.5.1.2 Silver staining

A variety of commercial kits for silver staining are available from several manufactures. In these studies Silver Staining Kit (Thermo Scientific) was used to alleviate problems of excessive background staining or poor reproducibility that were experienced using silver staining recipes from the literature.

3.5.1.3 Coomassie staining

Coomassie brilliant blue R250 requires an acidic medium for electrostatic interaction between the dye molecules and the amino groups of protein. The time required for staining depends on the thickness of the gel and its polyacrylamide concentration. Gels of 10-13% were stained for about 2 hours. In practice, immersion of the gel in staining solution overnight is often convenient.

Gel staining solution	
Methanol	40 % (v/v)
Acetic acid	10 % (v/v)
Coomassie Brilliant Blue R250	0.5 % (w/v)

Destaining solution
Same composition, but without Coomassie

The process of destaining can take up to 24 hours, but can be accelerated by using several changes of the destaining solution.

3.5.2 Sodium dodecyl sulfate-polyacrylamide gel electrophoresis (SDS-PAGE)

SDS-PAGE is currently the most commonly used electrophoretic technique for the analysis of proteins. This is due to the ability of the strong anionic detergent SDS in combination with

disulfide bond cleaving reagents (DTT, ß-mercaptoethanol) to solubilise, denature, and dissociate most proteins to produce single polypeptide chains. The resulting SDS-protein complexes can then be separated according to molecular size by electrophoresis in gels containing SDS.

After reaction initiation with ammonium persulfate (APS), the polymerization was accelerated with *N,N,N',N'*-tetramethylendiamine (TEMED). The separation gel solution was poured between the glass plates and overlaid with isopropanol to smooth out the gel surface. The optimum temperature is in the range 25-30°C, then the reaction generally occurs within 40 minutes. After polymerization of the separation gel, the stacking gel solution was poured in, then a 0.75 mm comb was inserted. Slab gels were cast in a slab gel cassette and inserted into the apparatus which holds them in a vertical position (Mini Protean® 3 cell chamber system (Biorad)). The electrode reservoirs were filled in with appropriate buffers.

After electrophoresis, the gel is removed from the apparatus for detection of the separated polypeptides. Gloves should be worn during procedures involving any handling of the gels, as contact with the skin can lead to the production of the artifacts or ceratine contamination during staining, particularly in the case of sensitive methods such as silver staining and crosslinking.

Heating the protein sample with 3 volumes of 4x SDS-PAGE loading buffer for at least 3 min at 95°C is important to ensure optimal reaction with SDS. For size control a protein marker (prestained protein marker Thermo Scientific) was loaded in parallel.

Until Bromphenol Blue (BPB) had reached the border of stacking/separating gel the voltage was 40-50 V, later it was increased to 90 V.

3.5.2.1 Schägger-Jagow SDS-PAGE

Small peptides/proteins (< 20000 Da) can not be separated by standard SDS-PAGE procedure because they aggregate in SDS-protein complexes of the same size and charge, which then migrate together during SDS-PAGE. This problem can be overcome by adding high concentrations of urea to a loading buffer. Else small polypeptides can be effectively separated using a tricine buffer system. This protocol was established by Schägger and Jagow (Schägger H., 1987).

For the analysis of *E.coli* and *B.subtilis* RNase P protein 4% stacking and 13% separation gels were used.

3x Gel buffer	
Tris/HCl pH 8.45	3 M
SDS	0.4 % (w/v)

5x Anode buffer	
Tris/HCl pH 8.9	1 M

5x Cathode buffer	
Tris/HCl pH 8.25	0.5 M
Tricine	0.5 M
→ 1 x concentrated buffer has to be supplemented with 0.1 % (w/v) SDS!	

4x SDS-PAGE loading buffer (Schägger)	
Tris/HCl pH 6.8	100 mM
SDS	8 % (w/v)
Glycerol	24 % (v/v)
β-mercaptoethanol	4 % (v/v)
→ after adjustment of pH, 0.04 % (w/v) bromophenol blue is added	

SDS-PAGE (Schägger)	Stacking gel (4 %)	Separation gel (13 %)
Acrylamide (48 %)/ bisacrylamide (2 %)	400 µl	2.6 ml
3x Gel buffer	1.25 ml	3.35 ml
demin. H_2O	3.3 ml	4.05 ml
TEMED	5 µl	10 µl
APS (10 %)	50 µl	100 µl

3.5.2.2 Laemmli SDS-PAGE

For the analysis of *Arabidopsis thaliana* RNase P (PRORP) Laemmli SDS-PAGE system was used.

4x Separation gel buffer (Laemmli)	
Tris/HCl pH 8.8	1.5 M

8x Stacking gel buffer (Laemmli)	
Tris/HCl pH 6.8	1 M

5x Gel running buffer (Laemmil)	
Tris/HCl pH 8.3	20 mM
Glycine	0.25 M
SDS	0.1 % (w/v)

4x SDS-PAGE loading buffer (Laemmli)	
SDS	4 % (w/v)
Glycerol	20 % (w/v)
β-mercaptoethanol	5 % (w/v)
Tris/HCl pH 6.8	250 mM
Bromophenol blue	0.001 %

SDS-PAGE gels (Laemmli)

Separation gel (5 ml)	10 %	13 %	15 %	17 %
Acrylamide (48 %)/ bisacrylamide (2 %)	1 ml	1.3 ml	1.5 ml	1.7 ml
4x Separation gel buffer (Laemmli)	1.25 ml	1.25 ml	1.25 ml	1.25 ml
20 % (w/v) SDS	25 µl	25 µl	25 µl	25 µl
demin. H_2O	2.73 ml	2.45 ml	2.23 ml	2.03 ml
10 % (w/v) APS	50 µl	50 µl	50 µl	50 µl
TEMED	5 µl	5 µl	5 µl	5 µl

Stacking gel (5 ml)	4 %
Acrylamide (48 %)/ bisacrylamide (2 %)	400 µl
8x Stacking gel buffer (Laemmli)	625 µl
20 % (w/v) SDS	25 µl
demin. H_2O	3.95 ml
10 % (w/v) APS	50 µl
TEMED	5 µl

3.5.4 Western blotting

Blotting technique, in which by SDS-PAGE separated proteins are transferred onto the surface of a matrix, is known as a Western blotting. The most popular matrices are nitrocellulose and polyvinylidene difluoride (PVDF). As a result, immobilized proteins are accessible to interaction with antibodies and other ligands.

Transfer buffer	
Tris base pH ~ 9.2 (pH was not adjusted)	48 mM
Glycine	39 mM
Methanol	20 % (v/v)
SDS	0.04 % (v/v)

SDS-PAGE gels were pre-transfer washed 10 minutes with transfer buffer to remove SDS and other gel constituents that can cause problems during transfer. This also minimizes shrinking or swelling of the gel during transfer and allows possible protein renaturation. The PVDF

matrix (Immobilon P, Millipore) was moistened with methanol and rinsed with ddH_2O, then equilibrated in transfer buffer for 5 minutes. In the blotting apparatus (SammyDry, Schleicher & Schuell) filter papers (GB004, Schleicher & Schuell) moistened with transfer buffer were organized in the following order: graphite cathode, 2 layers of filter paper, gel, PVDF membrane, 3 layers of filter paper, graphite anode (air bubbles should be avoided). Graphite plates were moistened with ddH_2O. 1 mA/mm^2 for 75 minutes was applied (the voltage was 6 mV at the start and increased to 30 mV at the end of the transfer).

3.5.5 Immunodetection

Immunodetection is the reaction with specific antibody or ligand and visualization of the protein in the sample. Usually an indirect or sandwich approach involving labeled secondary antibody reagents was used. The secondary antibody can be fluorescently labeled, radiolabeled or conjugated to an enzyme. The best substrate system to visualize alkaline phosphatase (AP)-conjugated secondary antibodies is a mixture of 5-bromo-4-chloro indolyl phosphate (BCIP) and nitroblue tetrazolium chloride (NBT). BCIP is an AP substrate, which gives a purple dye as oxidation product as well as reduced NBT.

5x TBS Buffer	
Tris/HCl pH 7.6	100 mM
NaCl	2.5 M

Washing Buffer	
TBS	1 x final concentration
Skim milk powder	0.5 % (w/v)
Tween 20	0.1 % (v/v)

Blocking Buffer	
TBS	1 x final concentration
Skim milk powder	5 % (w/v)

Substrate Buffer	
Tris/HCl pH 9.5	100 mM
NaCl	100 mM
$MgCl_2$	50 mM

Colour reagents for AP	
NBT in 70 % DMF (Promega)	25 mg/ml
BCIP in 70 % DMF (Promega)	25 mg/ml

A PVDF matrix was moistened with methanol after the blotting procedure. Incubation in blocking buffer for 30 min at room temperature was followed by washing twice in 1x TBS buffer for 5 min. Then the membrane was incubated with 0.5 % (w/v) skim milk powder solution in 1x TBS buffer for 1.5 h under gentle shaking at room. *E. coli* RNase P protein-specific antibodies were diluted 1:900; those specific for the *B. subtilis* RNase P protein were diluted 1:2500. For *B. subtilis* RNase P protein immunodetection, unspecific background bands could be reduced by incubating the primary antibody with 3 ml *E. coli* cell lysate (11 mg protein/ml) in 27 ml TBS/0.5 % skim milk powder for 30 min at room temperature prior to incubation with the PDVF membrane. Afterwards the PVDF matrix was washed twice in washing buffer for 5 min and equilibrated for 10 min in substrate buffer. The staining reaction was initiated by adding of BCIP (1:750) and NBT (1:375) in substrate buffer. As soon as the colour of the immundetected bands became dark blue/purple, the reaction was stopped by transferring the membrane into distilled water. For data collection the membrane was air dried and scanned.

3.5.6 Expression and purification of recombinant *B.subtilis* and *E. coli* RNase P protein

Sonication buffer SB	
Tris-HCl, pH 8.0	50 mM
NaCl	0.3 M
Triton X-100	0.1% (v/v)
1M NH_4Cl	1 M
Washing buffer	
Tris-HCl, pH 8.0	50 mM
imidazol	30 mM
Triton X-100	0.1% (v/v)
Urea	8 M

Elution buffer	
Tris-HCl, pH 7.0	50 mM
imidazol	0.3 M
Urea	7 M
Glycerol	10 % (v/v)
EDTA	20 mM

Dialysis buffer	
Tris-HCl, pH 7.0	50 mM
Glycerol	10 % (v/v)
NaCl	0.1 M

Recombinant *E. coli* and *B. subtilis* RNase P protein has an N-terminal His-tag (His-tagged peptide leader: MRGSHHHHHHGS, encoded in plasmid pQE-30 in *E. coli* JM109) and was expressed as described (Rivera-León *et al.*, 1995) and purified as described (Wegscheid and Hartmann, 2006).

Cell cultures (LB medium contains 100 µg/ml ampicillin) were grown to an OD_{600} of 0.6, then isopropyl-β-D-thiogalactopyranosid (IPTG) was added to a final concentration 1 mM. After 3 h growth at 37°C shaking under 180rpm cells were harvested (OD_{600} ~ 2.5) by centrifugation (10 min at 5000 rpm in a desktop centrifuge at 4°C). The posterior manipulations were performed at 4°C or on ice, and 40 µg/ml phenylmethylsulfonyl fluoride (PMSF) was added to all buffers. Then cells were resuspended in 15 ml sonication buffer SB (50 mM Tris-HCl, pH 8.0, 0.3 M NaCl, 0.1% triton X-100, 1M NH_4Cl).

After sonication (Branson Sonifier 250, output 2, duty cycle 50%, 15 min on ice, the sample was centrifuged for 30 min (4°C, 12000 rpm in a desktop centrifuge), and the supernatant was mixed with Ni-NTA agarose (Qiagen) (400 µl of the Ni-NTA slurry for 2 liters of cell culture) which had been pre-equilibrated in SB buffer. Under gentle rotating the sample was incubated for 2 h at 4°C.

The Ni-NTA agarose slurry was washed three times (centrifugation-resuspension cycles; centrifugation at 4°C, 3000 rpm in a desktop centrifuge) with 500 µl ice-cold washing buffer (30 mM imidazol, 50 mM Tris-HCl, pH 8.0, 8 M urea, 0.1% triton X-100); the supernatant after each washing step was removed carefully, as RNase P proteins started to precipitate during this procedure.

Proteins were then eluted with 500 µl elution buffer (50 mM Tris-HCl, pH 7.0, 10% glycerol, 7 M urea, 20 mM EDTA, 0.3 M imidazol) for 45 min under gentle rotating at 4°C. After centrifugation the supernatant was dialyzed twice for 1 h and additionally overnight against 500 ml dialysis buffer (50 mM Tris-HCl, pH 7.0, 0.1 M NaCl, 10% glycerol, dialysis bags (Roth, MWCO: 12.000 – 14.000); during dialysis a white precipitate forms.

The content of dialysis bags was removed to a 2-ml Eppendorf tube and centrifuged for 20 min at 4°C and 12000 rpm .

The supernatant containing RNase P protein devoid of any RNase P RNA contamination, whereas the pellet included traces of RNase P RNA and was therefore discarded. Fractions of all purification steps were analyzed on 17% SDS-PAGE (chapter 3.5.2.1) to estimate the

purity of the protein preparations. Concentration of *E.coli* and *B.subtilis* P protein was determined using absorbance at 280nm.

3.5.7 Purification of recombinant *Arabidopsis thaliana* PRORP1, PRORP2 and PRORP3

IMAC A buffer	
Tris-HCl pH 7.4	50 mM
NaCl	150 mM
glycerol	10 % (v/v)
DTT	1 mM

IMAC B buffer	
Tris-HCl pH 7.4	50 mM
NaCl	150 mM
glycerol	10 % (v/v)
DTT	1 mM
Imidazole	500 mM

IMAC C buffer	
Tris-HCl pH 7.4	50 mM
NaCl	1 M
glycerol	10 % (v/v)
DTT	1 mM

TB medium Solution A	
Tryptone	12 g
Yeast extract	24 g
glycerol	4 ml
Total volume	1 L
TB medium Solution B	
KH_2PO4	170 mM
K_2HPO4	720 mM
Total volume	1 L
Do not adjust pH, app. 7.0	

PRORP cDNAs were cloned in pET28-b(+) (Novagen) to obtain C-terminal fusions with 6x His-affinity tags (Gobert et al., 2010). The encoded PRORP enzymes represent the presumably mature mitochondrial / chloroplast (PRORP1, 537 aa) and nuclear (PRORP2, 528 aa and PRORP3, 517 aa) form, respectively. For purification of PRORP, *E. coli* BL21(DE3) (New England Biolabs) containing the respective expression vector was grown in 20 ml TB medium (900 ml solution A [per liter 12 g tryptone, 24 g yeast extract, 4 ml glycerol] were combined with 100 ml solution B [170 mM KH_2PO_4, 720 mM K_2HPO_4] immediately before

use) and grown overnight at 37°C / 180 rpm. Next morning, 250 ml pre-warmed TB medium was inoculated with 5 ml of the overnight culture and incubated at 30°C / 180 rpm until the culture reached an OD_{600} of 2.0 – 2.5. Then the culture was transfered to 19°C and grown for another 90 min at 180 rpm. Addition of isopropyl-β-D-thiogalactopyranosid (IPTG) to an end concentration of 0.25 mM enabled expression of PRORP for further 16 – 18 h at 19°C / 180 rpm. Next, the 250 ml-culture was split in two equal portions and cells were pelleted by centrifugation (15 min at 3000 g / 4°C). For further protein purification each cell pellet was washed once by resuspension in 40 ml of a mixture of 90 % buffer IMAC A (50 mM Tris-HCl pH 7.4, 150 mM NaCl, 10 % (v/v) glycerol, 1 mM DTT) and 10 % buffer IMAC B (50 mM Tris-HCl pH 7.4, 500 mM imidazole, 150 mM NaCl, 10 % (v/v) glycerol, 1 mM DTT). After centrifugation (s.o.) each cell pellet (each corresponds to 125 ml of cell culture) was resuspended in 4 ml ice-cold mixture of 90 % IMAC A / 10 % IMAC B supplemented with 0.2 % (v/v) protease inhibitor cocktail P8849 (Sigma Aldrich) and 4 µl 10 mg/ml DNase I. After sonication in an ice-water bath (Vienna preparation: Bandelin sonoplus GM70, 5 min duty cycle 30 %, 70 % power, 3 cycles, 1 min pause inbetween each cycle / Marburg preparation: Branson Sonifier 250, 15 min duty cycle 50 %, output 2) the crude cell lysate was centrifuged for 35 min at 18.000 g / 4°C. The thus obtained supernatant was filtrated via a membrane filter (0.2 µm pore size) for application to a HisTrap HP column (GE Healthcare). The affinity chromatograhic purification was performed with a ÄKTA™ FPLC-System (Amersham Biosciences). Before application of the probe the column was pre-equilibrated with 5 volumes of 90 % IMAC A / 10 % IMAC B at a flow rate of 1 ml / min. After loading the probe (flow rate: 0. 4 ml / min) the column was washed: for purification of PRORP1 with 10 column volumes of 90 % IMAC A / 10 % IMAC B and 3 column volumes of 100 % buffer IMAC A; for purification of PRORP2 / PRORP3 with 10 column volumes of 90 % IMAC A / 10 % IMAC B, 7 column volumes of 100 % IMAC C (50 mM Tris-HCl pH 7.4, 1 M NaCl, 10 % (v/v) glycerol, 1 mM DTT) and 3 column volumes of 100 % IMAC A. For elution of PRORP1 / PRORP2 5 column volumes of 100 % IMAC B (flow rate: 0. 8 ml / min) and for elution of PRORP3 5 column volumes of 50 % IMAC A / 50 % IMAC B (flow rate: 1 ml / min) were applied. The eluate was fractionated in 1, 5 ml portions and immediately frozen in liquid nitrogen for storage at -80°C. Fractions of all purification steps were analyzed on 12% SDS-PAGE to estimate the purity and concentration of *A. thaliana* PRORP1, PRORP2 and PRORP3 proteins. Protein concentrations were determined with Bio-Rad protein assay, based on the method of Bradford (chapter 3.5.8.1).

3.5.8 Protein concentration determination

3.5.8.1 Bradford method

The Bio-RAD protein assay is based on the method of Bradford (Bradford et al., 1976). It is a simple and accurate procedure to determine concentration of solubilized protein. The assay bases on a colour change after dye-binding to protein. Primarily the blue dye binds to basic and aromatic amino acid residues shifting the absorbance maximum from 465 nm to 595 nm. Detection limit is approximately 2 µg. First standard curve was established using Bovine Serum Albumin (BSA) solution. BSA solution was diluted in the same buffer as respective protein to final concentration of 100 µg/ml. Appropriate dilution of protein was prepared in respective buffer.

Protein solutions were normally assayed in duplicate:

1. 800µl H_2O
2. 780µl H_2O + 20 µl BSA
3. 760µl H_2O + 40 µl BSA
4. 720µl H_2O + 80 µl BSA
5. 700µl H_2O + 100 µl BSA
6. 650µl H_2O + 150 µl BSA
7. 799µl H_2O + 1µl undiluted protein
8. 795µl H_2O + 5µl protein dilution (1:20)
9. 790µl H_2O + 10µl protein dilution (1:20)

200 µl Bio-RAD reagent was added to each test tube, shaken and incubated at room temperature for at least 5 min. Absorbance will increase over time; hence samples should incubate at room temperature for no more than 1 hour.

3.5.8.2 Protein concentartion determination using absorbance at 280nm

Determination of protein concentration by ultraviolet absorption (260 to 280 nm) depends on the presence of aromatic amino acids in proteins. Tyrosine and tryptophan residues absorb at approximately 280 nm. Higher orders of protein structure also may absorb UV light or modify the molar absorptivities of tyrosine and tryptophan and thus the UV detection is highly sensitive to pH and ionic strength at which measurement is taken. Many other cellular components, and particularly nucleic acids, also absorb UV light. The ratio of A_{280}/A_{260} is often used as a criterion of the purity of protein or nucleic acid samples during their

purification. The real advantages of this method of determining protein concentration are that the sample is not destroyed and that it is very rapid. Although different proteins will have different amino acid compositions and thus different molar absorptivities, this method can be very accurate when comparing different solutions of the same protein preparations. To make an accurate determination of protein concentration, a standard curve (A_{280}) with known amounts of purified protein was produced. A blank that is appropriate for the sample and contains the same concentrations of buffer and salts as the sample was provided. Concentration was calculated according to the Lambert-Beer equation. A handy equation to estimate protein concentration (Pace *et al,* 1995) that is often used is:

$$\mathbf{A = \varepsilon_{280nm} \times c \times d} \qquad \Rightarrow \qquad \mathbf{c = A / \varepsilon_{280nm} \cdot d}$$

c: a protein concentration, [mg/mL]; **d**: a cuvette path length, [cm]; $\boldsymbol{\varepsilon}_{280nm}$: the theoretical extinction coefficient at 280nm, **[**1/M·cm**]**, $\boldsymbol{\varepsilon}_{280nm}$ can be estimated using the equation:

$\boldsymbol{\varepsilon}_{280nm} = \mathbf{N_{Try}} \cdot 5500 + \mathbf{N_{Tyr}} \cdot 1490 + \mathbf{N_{Cys}} \cdot 125$

$\mathbf{N_{Try}}$: number of tryptophan residues; $\mathbf{N_{Tyr}}$: number of tyrosine residues; $\mathbf{N_{Cys}}$: number of cysteine residues

The main disadvantage of this method is low sensitivity. For increased sensitivity, the wavelength can be lowered to the range of 210 to 225 nm.

3.6 Kinetic analysis

Kinetic experiments allow to analyse dependence of substrate processing by RNase P on buffer conditions, chemical modifications, deletions and mutations. Using appropriate reaction conditions, individual steps of catalysis can be explored.

Using an excess of substrate relative to enzyme (Michaelis-Menten conditions), the measured reaction velocity is dependent on the slowest reaction step. Each enzyme molecule runs through the reaction cycle many times (*multiple turnover*). The rate-determining step is the dissociation of mature tRNA from the enzyme complex.

$$E + S \underset{k_{-1}}{\overset{k_1}{\leftrightarrows}} ES \xrightarrow{k_2} EP \underset{k_{-3}}{\overset{k_3}{\leftrightarrows}} E + P$$

where ***E*** is P RNA; ***S*** is ptRNA and ***P*** is tRNA.

If the enzyme is in excess relative to the substrate ([E] □□ [S]) each enzyme molecule can maximally process one substrate molecule, therefore it runs through the reaction cycle only

once (*single turnover*). Under these conditions product release does not contribute to the speed of substrate conversion. Consequently, the reaction velocity depends on substrate binding k_1, k_{-1} or on the rate of the chemical step k_2. Performing *single turnover* experiments, three different constants could be determined:

$\mathbf{K_M}$ is an enzyme concentration at the half-maximal cleavage rate;

$\boldsymbol{k_{obs}}$ is a rate constant observed in the single turnover reaction at a certain enzyme concentration;

$\boldsymbol{k_{react}}$ is a rate constant corresponding to the highest possible reaction velocity in a *single turnover* reaction. This condition is met when enzyme concentration becomes saturating.

In this work almost all kinetic experiments were performed under *single turnover* conditions and at enzyme concentrations in the saturating range where $\boldsymbol{k_{obs}} = \boldsymbol{k_{react}}$. Standard protocols for performing *single turnover* kinetic experiments are described below.

3.6.1 Kinetic analysis of PRORP (protein-only RNase P)

KN buffer(without Me2+) (Dinos et al., 2004)	
Hepes-KOH, pH 7.4	20 mM
NH_4OAc	150 mM
Spermidine	2 mM
Spermine	0.05 mM
β-Mercaptoethanol	4 mM

For kinetics with proteinaceous RNase P KN buffer without bivalent metal ions was prepared. That allowed us to vary easily metal ion conditions (Mg^{2+}, Mn^{2+}, Cd^{2+} and combinations of them) in reaction. We observed that activity of proteinaceous RNase P enzymes from *Arabidopsis thaliana* drastically decreased after approximately 6-9 month storage in the freezer at -20°C, therefore we recommend to store the enzymes at -80°C in small aliquots enough for a one-day set of experiments. Before starting kinetic the aliquots of enzyme were briefly thawed in hands and kept on ice before pipetting. They were pre-incubated separately in the same 1x KN buffer for 5 min at 37°C. Longer incubation is not recommended.

Substrate mix contains 5'-^{32}P-labelled substrate (app. 2000 cpm pro time point) in 1x KN buffer and respective bivalent ions. The substrate mix was incubated for 5 min at 55°C and 25 min at 37°C.

Processing reactions were started by combining 16 µl enzyme mix and 4µl substrate mix and assayed at 37°C. 4 µl aliquots were collected at different time points, mixed with 16 µl PPF

buffer (19 µl for control) and analysed on PAA gel. Zero control (in omission of enzyme) was withdrawn at the end of the experiment.

3.6.2 Kinetic analysis of *in vitro* assembled RNase P holoenzyme

10x KN buffer	
Hepes-KOH, pH 7.4	20 mM
$Mg(OAc)_2$	10 mM
NH_4OAc	150 mM
□-Mercaptoethanol	4 mM

We determined holoenzyme and RNA-alone kinetics of bacterial RNase P under single turnover conditions ([E] □□ [S]) at 4 10 mM Mg^{2+} and pH 7.4.

RNase P RNA were preincubated in assay 1x KN buffer for 5 min at 55°C and 55 min at 37°C to resolve potential folding traps and to fold annealed P RNA correctly. Then RNase P protein was added and incubated for 5 min at 37°C. Substrate mix contains 5'-^{32}P-labeled substrate (app.2000 cpm pro time point) in 1x KN buffer and was pre-incubated 5 min at 55°C and 25 min at 37°C. Processing reactions were started by combining 16 µl enzyme mix and 4µl substrate mix and assayed at 37°C. 4µl aliquots including zero control (in omission of enzyme) were collected at different time points mixed with 16 µl PPF buffer (19 µl for control) and analysed on PAA gel.

3.6.3 Evaluation of kinetic analysis

Samples were analysed on 20 % denaturing PAA gels, imaging plates were exposed to the gel overnight and scanned with Bio-Imaging System (Raytest). Bands corresponding to uncleaved ptRNA or released 5'-flank were quantified using software AIDA and all further evaluation was done using the software GRAFIT 3.0.

The processed amount of RNA could be calculated as follows:

$$tRNA_{processed} = \frac{[5'-flank]}{[5'-flank]+ptRNA}$$

To calculate the k_{obs} values by fitting, a single oder rate equation was applied:

$$A_t = A \cdot \left(1/e^{-kobs} \cdot t\right)$$

At is an amount of ptRNA cleaved at a time point *t*;

A is a maximum amount of the pre-tRNA that could be cleaved (limit).

$\boldsymbol{k_{obs}}$ is an observed rate constant

3.7 Software

An open source PyMol software provided by DeLano Scientific LLC was applied for molecular visualization. The program produces high-quality 3-D images of biomolecules. Original files could be downloaded from databases (PDB, ExPASy etc.). Software allows showing single residues of nucleic acids and proteins of particular interest and, moreover, to measure precisely the distance between individual atoms.

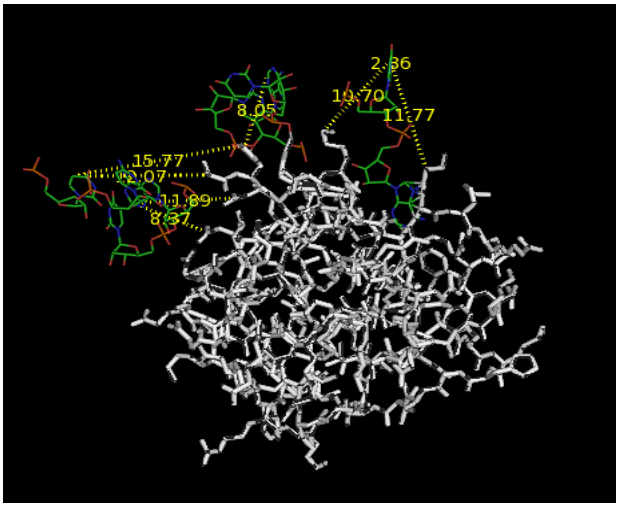

Figure 2.2. Detailed RNA -protein interactions in the hybrid RNase P holoenzyme (*B. stearothermophilus* P RNA and *B. subtilis* P protein). Figure created using PyMol software.

RNA -protein interactions in the hybrid RNase P holoenzyme detailed analysis was conducted using PyMol software. Until recently RNase P holoenzyme crystal structure of any species was not available. Therefore a hybrid holoenzyme model was designed by combining available crystal structures of *B. stearothermophilus* P RNA and *B. subtilis* P protein (Buck et al. 2006). Distances between all uridine and lysine residues were measured. Only uridines in close proximity (≤ 10 Å) to lysines were replaced by modified residues bearing an aldehyde group for further cross-linking studies.

3.8 Cloning experiments

Since chemical synthesis of full-length *Bacillus stearothermophilus* RNase P RNA (414 nt) bearing a single modified nucleotide is not possible (see Results and Discussion), we purchased a strategy where a chemically synthesized ribooligonucleotide carrying a site-specific modification is covalently ligated (or optionally annealed) to an enzymatically synthesized fragment representing the major portion of *B. stearothermophilus* RNase P RNA.

All P RNAs used in this work were produced by run-off transcription with T7 RNA polymerase (see 3.4.1).

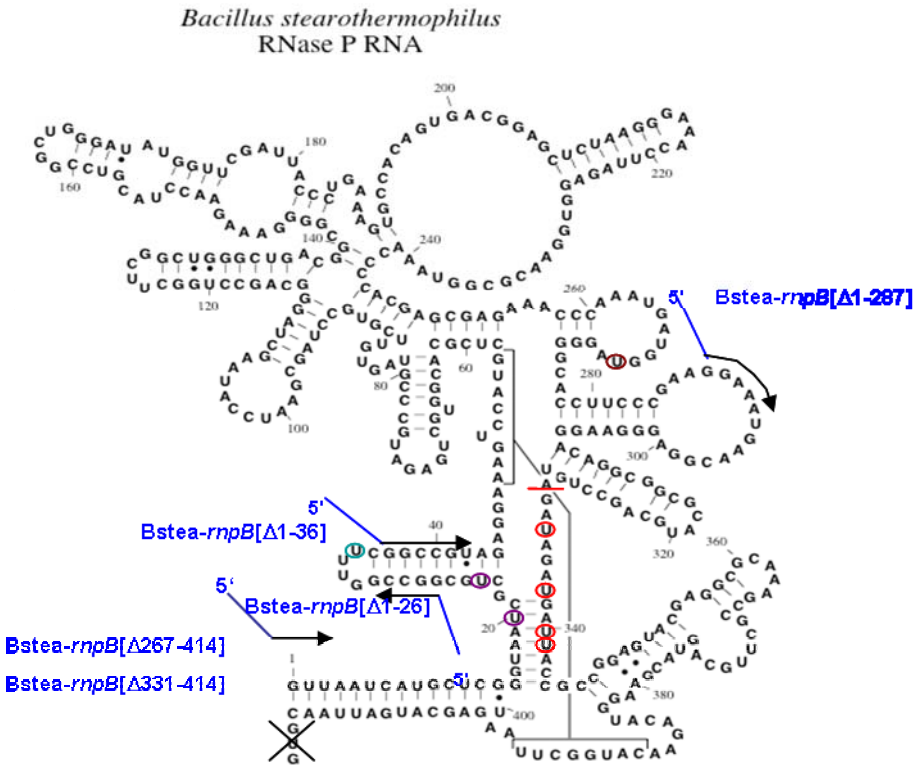

Figure 2.3. *Bacillus stearothermophilus* P RNA cloning scheme. 5'-termini of the P RNA fragments pBstea-*rnpB*[Δ1-26], pBstea-*rnpB*[Δ1-36], pBstea-*rnpB*[Δ267-414] and pBstea-*rnpB*[Δ331-414] are indicated by the arrows on the left. 5'- termini of the construct pBstea-*rnpB*[Δ1-287] is shown on the right. On the secondary structure of *B. stearothermophilus* P RNA, uridine 20 (U20) and uridine 24 (U24) are indicated by purple circle; uridine 35 (U35) is marked by green circle; uridine 270 (U 270) is marked by magenta circle; uridines 333, 337, 340 and 341 (U333, U 337, U 340 and U 341) are marked by red circle. Selected according to the *B. stearothermophilus* holoenzyme model that residues should be substituted by the 2'-aldehyde derivatives. For more details see the Results and Discussion chapter.

Construction of plasmid pSP64pBstea-*rnpB*[Δ1-26]

Plasmid pBstea-*rnpB*[Δ1-26] was prepared according to standard cloning and PCR procedure as described (see 3.3.6). Bstea-*rnpB*[Δ1-26], a 388 nt fragment of *rnpB* gene lacking the 5´-terminal 26 nucleotides , was amplified from a pUC19 derivative containing the *Bacillus stearothermophilus rnpB* gene) using primers: 1-ML: (5'-GAA AGC TTA ATA CGA CTC ACT ATA GGC CGG TTT CGG CCG TAG AGG AAA G-3') and 3-ML: (5'-GAG GAT CCG TTA ATC ATG CTC TAT AAG CCA TGT TCT GTA CC-3'). Digested with HindIII

and BamHl and cloned in pSP64 digested with the same enzymes. The resulting plasmid pBstea-*rnpB*[Δ1-26] was transformed into *E. coli* DH5α cells to be used as a template for T7 *in vitro* transcription (run-off transcription with BamH I-linearized plasmid) of Bstea-*rnpB*[Δ1-26].

Construction of plasmid pSP64pBstea-*rnpB*[Δ1-36]

Plasmid pBstea-*rnpB*[Δ1-36] was prepared according to standard cloning and PCR procedure as described (see 3.3.6). Bstea-*rnpB*[Δ1-36], a 378 nt fragment of *rnpB* gene lacking the 5´-terminal 36 nucleotides, was amplified from a pUC19 derivative containing the *Bacillus stearothermophilus rnpB* gene using primers: 2-ML: (5'- GAA AGC TTA ATA CGA CTC ACT ATA GGC CGT AGA GGA AAG TCC ATG CTC G -3') and 3-ML: (5'-GAG GAT CCG TTA ATC ATG CTC TAT AAG CCA TGT TCT GTA CC-3'). Digested with Hindlll and BamHl and cloned in pSP64 digested with the same enzymes. The resulting plasmid pBstea-*rnpB*[Δ1-26] was transformed into *E. coli* DH5α cells to be used as a template for T7 *in vitro* transcription (run-off transcription with BamH I-linearized plasmid) of Bstea-*rnpB*[Δ1-36].

Construction of plasmid pSP64pBstea-*rnpB*[Δ1-287]

Plasmid pBstea-*rnpB*[Δ1-287] was prepared according to standard cloning and PCR procedure as described (see 3.3.6). Bstea-*rnpB*[Δ1-287], a 127 nt fragment of *rnpB* gene lacking the 5´-terminal 287 nucleotides, was amplified from a pUC19 derivative containing the *Bacillus stearothermophilus rnpB* gene using primers: 6-ML: (5'- GAA AGC TTA ATA CGA CTC ACT ATA GGA AAT GAA CGG AGG GAA GGA CAG G -3') and 3-ML: (5'-GAG GAT CCG TTA ATC ATG CTC TAT AAG CCA TGT TCT GTA CC -3'). Digested with Hindlll and BamHl and cloned in pSP64 digested with the same enzymes. The resulting plasmid pBstea-*rnpB*[Δ1-287] was transformed into *E. coli* DH5α cells to be used as a template for T7 *in vitro* transcription (run-off transcription with BamH I-linearized plasmid) of Bstea-*rnpB*[Δ1-287].

Construction of plasmid pSP64pBstea-*rnpB*[Δ267-414]

Plasmid pBstea-*rnpB*[Δ267-414] was prepared according to standard cloning and PCR procedure as described (see 3.3.6., 3.4.3). Bstea-*rnpB*[Δ267-414], a 266 nt fragment of *rnpB*

gene lacking the 3´-terminal 148 nucleotides , was amplified from a pUC19 derivative containing the *Bacillus stearothermophilus rnpB* gene using primers: 4-ML: (5'- GTG AAT TCG TAA TAC GAC TCA CTA TAG GTT AAT CAT GCT CGG GTA ATC -3') and 5-ML: (5'- AGA TGC CAT GCC GAC CCT CAT TTG GGT TTC TCG CTC GTG GGG TTT AC -3'). An overlapping PCR fragment was amplified from a pUC19-Aae-6S-HDV containing HDV ribozyme sequence using primers: 8-ML: (5'- CGA GCG AGA AAC CCA AAT GAG GGT CGG CAT GGC ATC TCC ACC TCC TCG -3') and 9-ML: (5'- GAG GAT CCT TCT CCC TTA GCC TAC CGA AGT AGC CCA GGT C -3'). Overlapping PCR reaction with primers: 4-ML: (5'- GTG AAT TCG TAA TAC GAC TCA CTA TAG GTT AAT CAT GCT CGG GTA ATC -3') and 9-ML: (5'- GAG GAT CCT TCT CCC TTA GCC TAC CGA AGT AGC CCA GGT C -3') was performed.

The PCR product coding an HDV-sequence was digested with EcoRl and BamHl and cloned in pSP64 digested with the same enzymes. The resulting plasmid pBstea-*rnpB*[Δ267-414] was transformed into *E. coli* DH5α cells to be used as a template for T7 *in vitro* transcription (run-off transcription with BamH I-linearized plasmid) of Bstea-*rnpB*[Δ267-414].

Construction of plasmid pSP64pBstea-*rnpB*[Δ331-414]

Plasmid pBstea-*rnpB*[Δ331-414] was prepared according to standard cloning and PCR procedure as described (see 3.3.6., 3.4.3). Bstea-*rnpB*[Δ331-414], a 330 nt fragment of *rnpB* gene lacking the 3´-terminal 84 nucleotides, was amplified from a pUC19 derivative containing the *Bacillus stearothermophilus rnpB* gene using primers: 4-ML: (5'- GTG AAT TCG TAA TAC GAC TCA CTA TAG GTT AAT CAT GCT CGG GTA ATC -3') and 7-ML: (5'- TGG AGA TGC CAT GCC GAC CCT ACA GGC TGC ATG CGC CGC CTG TCC TTC C -3'). An overlapping PCR fragment was amplified from a pUC19-Aae-6S-HDV containing HDV ribozyme sequence using primers: 10-ML: (5'- CAG GCG GCG CAT GCA GCC TGT AGG GTC GGC ATG GCA TCT CCA CCT CCT CG -3') and 9-ML: (5'- GAG GAT CCT TCT CCC TTA GCC TAC CGA AGT AGC CCA GGT C -3'). Overlapping PCR reaction with primers: 4-ML: (5'- GTG AAT TCG TAA TAC GAC TCA CTA TAG GTT AAT CAT GCT CGG GTA ATC -3') and 9-ML: (5'- GAG GAT CCT TCT CCC TTA GCC TAC CGA AGT AGC CCA GGT C -3') was performed. The PCR product bearing an HDV-sequence was digested with EcoRl and BamHl and cloned in pSP64 digested with the same enzymes. The resulting plasmid pBstea-*rnpB*[Δ331-414] was transformed into *E. coli* DH5α

cells to be used as a template for T7 *in vitro* transcription (run-off transcription with BamH I-linearized plasmid) of Bstea-*rnpB*[Δ331-414].

DNA sequencing of the recombinant plasmids was performed by MWG-BIOTECH AG, Germany. pUC19 and pUC19-Aae-6S-HDV plasmids were provided by Dr. Dagmar Willkomm, Philipps University Marburg, Germany.

4. Results and Discussion

This section is a summary of results and discussion obtained in publications 1-3. For more detailed information concerning the results, see the respective publication.

4.1 Crosslinking studies of the bacterial RNase P holoenzyme

4.1.1 Analysis of RNA-protein interactions by crosslinking

There exist several biochemical methods that are used to investigate RNA-protein and protein-protein interactions. Among them, crosslinking techniques occupy an important place. The introduction of a reactive group into a predetermined position of the RNA oligonucleotide strand allows the probing of contact points between different domains of biomolecules, whereas variations of the chemical nature of the active group enable selective crosslinking to different types of amino acids in RNA-protein complexes. So far, crosslinking approaches to study the binding interfaces in RNA-protein complexes have utilized photoreactive base analogs (Harris et al., 1997; Kazantsev et al., 1998; Kalani et al., 1999) or long-range crooslinkers (Niranjanakumari et al., 2002; Rinke et al., 2004) attached to the phosphate. Short-range photoreactive groups at the 2'-ribose position have not yet been explored for RNA. The development of short-range ribose 2'-functionalities for crosslinking would extend the repertoire of tools to identify contacts at RNA-protein binding interfaces and would improve the resolution of the determined RNA-protein distance maps. The introduction of reactive groups into the sugar-phosphate backbone of RNA is the most promising approach (Zatsepin et al., 2005; Dolinnaya et al., 2009; Khomykova et al., 2010), while modification of heterocyclic bases can disturb complementary interactions of RNA as well as base-specific contacts to the protein moiety within RNA-protein complexes.

Identification of RNA-protein binding sites requires the analysis of RNA-protein heteroconjugates derived by proteolysis of the crosslinked protein moiety. When a proteolytic enzyme (ex. proteinase K) is used for protein degradation, the resulting reaction products are well defined and homogeneous. Nowadays, mass spectrometry is the analytical method of choice for the exact determination and direct identification of crosslinked amino acids. A number of different analytical strategies have been devised to facilitate the analysis of peptide-ribooligonucleotide heteroconjugates. In general, crosslinked RNA-protein complexes

are purified on the gel and the band of cross-linked RNA-protein heteroconjugate is cut out. After proteolytic degradation of the protein moiety, a peptide-oligonucleotide hybrid is obtained, which is analysed using mass spectrometry. MALDI-TOF mass spectrometry is well suited for the analysis of heteroconjugates produced by crosslinking of proteins to nucleic acids (Fig. 4.1.1).

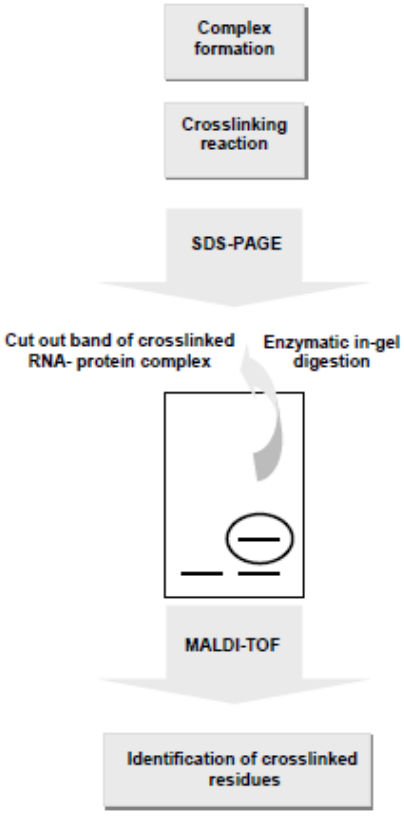

Figure 4.1.1. The general analytical strategy to analyze crosslinked RNA - protein complexes.

4.1.2 *Bacillus stearothermophilus* RNase P holoenzyme as a model system for crosslinking studies

In these studies, biochemically well-characterized bacterial RNase P served as a model system to test the validity of the results obtained and to establish the crosslinking methodology. Albeit the composition of the bacterial RNAse P is relatively simple – one catalytic RNA subunit (P RNA; ~ 130 kDa) and a small single protein (P protein; ~ 13 kDa), only recently the first crystal structure of the holoenzyme comlex was resolved (Reiter et al., 2010). Several bacterial RNase P holoenzyme models were proposed before the first holoenzyme crystal structure was resolved. *E. coli* (Buck et al., 2005), *B. subtilis* (Tsai et al., 2003;

Niranjanakumari et al., 2007) and *B. stearothermophilus* (Buck et al., 2005) holoenzyme models are based on the footprinting experiments, crosslinking studies and individual three-dimensional structures.

In our studies, started before the first bacterial RNAse P crystal structure was reported, we considered as a model system for our crosslinking studies the hybrid holoenzyme model of *Bacillus stearothermophilus* RNase P composed of *B. stearothermophilus* P RNA and *B. subtilis* P protein (Buck et al., 2005). The model is grounded on the crystal structure of *B. stearothermophilus* RNase P RNA (Kazantsev et al., 2005) and comparative footprinting studies of *E. coli*, *B. subtilis (*Stams et al., 1998) and *T. maritima* (Kazantsev et al., 2003) RNase P proteins (Buck et al., 2005).

4.1.3 2'-modified ribooligonucleotides for crosslinking studies

This project was conducted to establish a chemical crosslinking technique for RNA-protein complexes utilizing RNA with 2'-aldehyde reactive group. For 2'-aldehyde RNA derivatives, phosphoroamidite building blocks with 2'-*cis*-diol functionalities were synthesized in the group of Prof. Oretskaya (Chemistry Department and A. N. Belozersky Institute of Physico-Chemical Biology, Lomonosov Moscow State University, Russia) (Fig. 4.1.2).

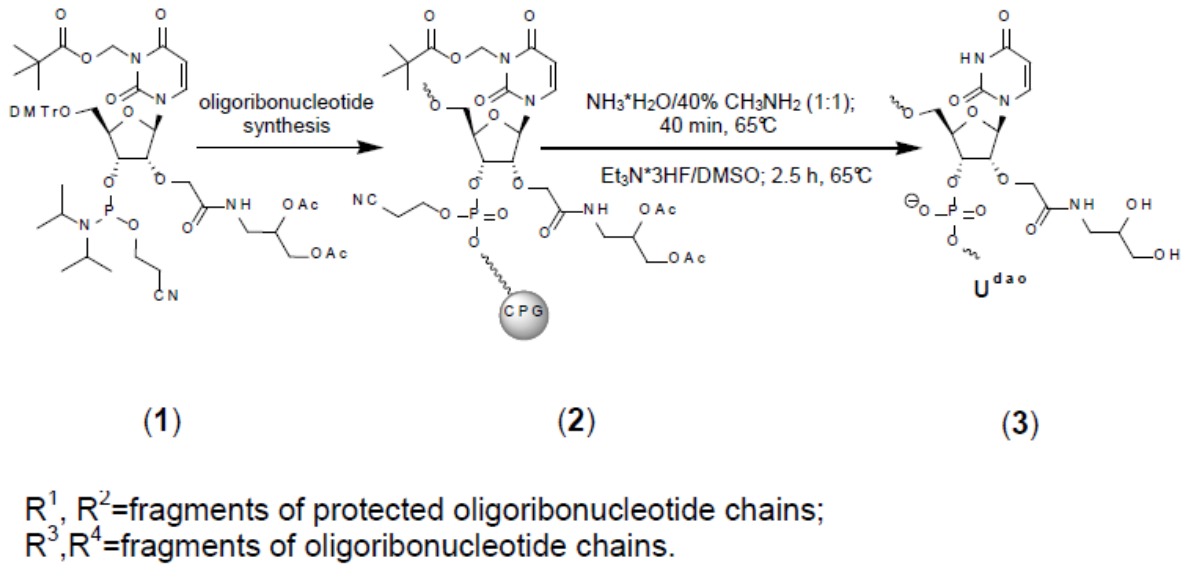

Figure 4.1.2. Synthesis of modified oligoribonucleotides bearing 2'-O-[2-(2,3-dihydroxypropyl)amino-2-oxoethyl]uridine (U^{dao}) residues (scheme reproduced from Sud'ina et al., 2005).

Such phosphoroamidite building blocks were incorporated site-specifically into ribooligonucleotides by solid-phase RNA synthesis, then physico-chemical properties of the 2'-modified ribooligonucleotides were scrutinized (Khomykova et al., 2012). Thermal stability studies of RNA-RNA and RNA-DNA duplexes formed by 2'-modified oligonucleotides have shown that melting temperature of respective duplexes did not change. Circular dichroism spectroscopy (CD) data revealed that a single modified residue $\mathbf{U}^{\mathbf{dao}}$ did not influence significantly the CD spectra of RNA-RNA and RNA-DNA duplexes.

For crosslinking investigations, ribooligonucleotides bearing modified uridines with 2'-*cis*-diol functionalities ($\mathbf{U}^{\mathbf{dap}}$) were activated by periodate oxidation. The interaction of ε-amino group of lysine residue with 2'-aldehyde group in modified RNA leads to the formation of a Schiff base followed by reduction to secondary amine by sodium cyanoborohydride (Fig.4.1.3).

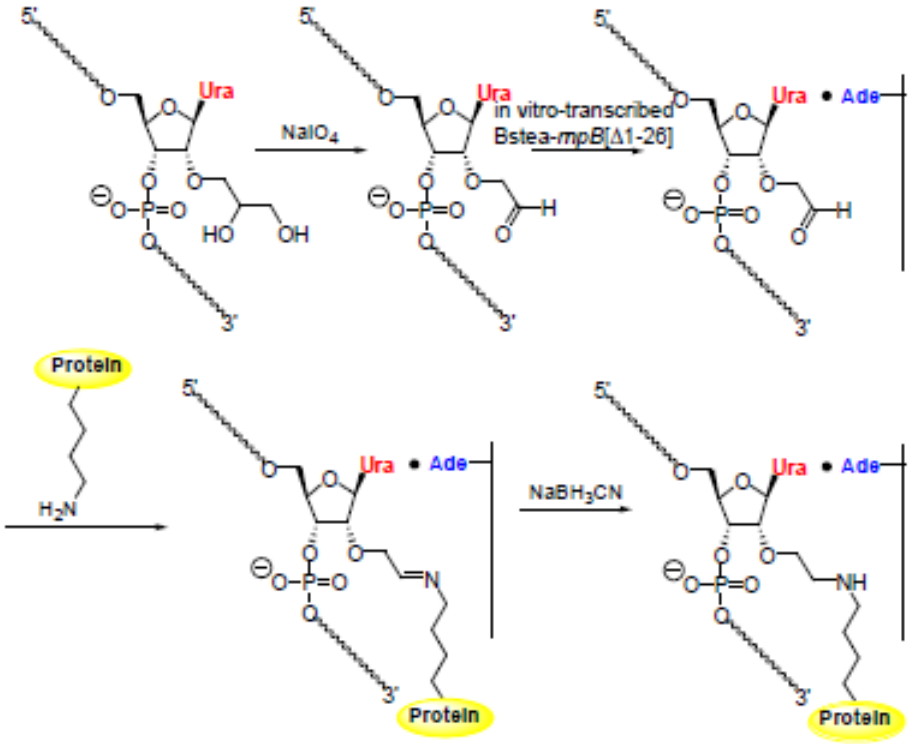

Figure 4.1.3. Crosslinking reaction: P RNA bearing 2'-O-[2-(2, 5-dioxo-3-azapenthyl)uridine (U^{dap}) binds to the lysine of P protein . The ε-amino group of lysine residue interacts with 2'-aldehyde group in modified RNA, leading to formation of a Schiff base followed by reduction to secondary amine by sodium cyanoborohydride.

Single uridine positions in the *B. stearothermophilus* P RNA sequence to be substituted by 2'-modified derivatives were selected according to the hybrid RNase P holoenzyme model. Applying PyMol software (DeLano Scientific LLC), distances between uridines of *B. stearothermophilus* P RNA and lysine amino acids of *B.subtilis* P protein were measured on

the holoenzyme model (distance limit was 10 Å). As candidates for being located at the RNA-protein binding interface several uridine residues were selected - U20, U 24, U35, U270, U333, U337, U340 and U341.

4.1.4 P RNA reconstitution

Currently, the efficiency of chemical RNA synthesis is such that high-quality RNA molecules up to 80 nucleotides long can be obtained from commercial sources. RNA oligonucleotides containing modified nucleotides are frequently utilized in the construction of a long chimeric RNA molecule. In such cases, the RNA oligonucleotides are ligated to other RNA molecules, which are often produced by *in vitro* transcription reactions. This combination provides a way to modify functional groups in virtually any position in a given RNA molecule.

Since chemical synthesis of full-length RNase P RNA (414 nt) bearing a single modified nucleotide is not possible, we purchased a strategy where a chemically synthesized ribooligonucleotide carrying a site-specific modification is covalently ligated (or optionally annealed) to a T7 transcript representing the major portion of RNase P RNA.

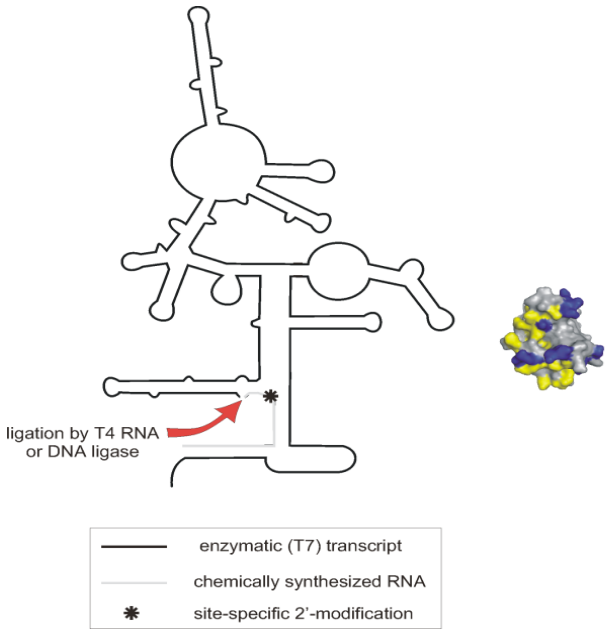

Figure 4.1.4. Schematic representation of a bacterial RNase P RNA (left) assembled from an enzymatically synthesized RNA fragment (black line) and a synthetic RNA oligonucleotide (gray line) carrying a site-specific 2'-functionality (black asterisk). The site of ligation is indicated by the red arrow, the B. subtilis RNase P protein on the right is shown with natural Lys residues in blue (Niranjanakumari et al., 2007).

First, to establish the ligation procedure and initial crosslinking reaction, we focused on the

tailoring of P RNAs bearing modified uridines in positions 20 and 24.

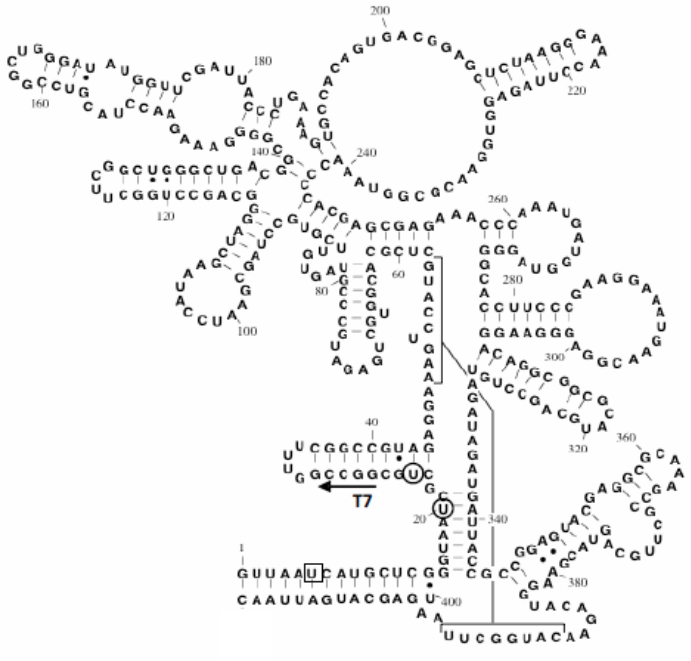

Figure 4.1.5. The secondary structure of *B. stearothermophilus* P RNA. According to the holoenzyme model (Buck et al., 2006), $\mathbf{U^{dap}}$ residues 20 and 24 are in close proximity to lysines of P protein (marked by the circle (○)) and $\mathbf{U^{dap}}$ residue 6 does not contact any lysine residue (indicated by the square (□)).

Two techniques were compared for P RNA reconstitution bearing a single 2'-modification: ligation and annealing of *in vitro*-transcribed P RNA fragment omitting 26 nucleotides at the 5'- termini (Bstea-*rnpB*[Δ1-26]) to chemically synthesized 2'-modified 26-mer ribooligonucleotide. During these studies, we found out that the ligation of long RNA molecules (approximately 400 nt) can be challenging. Direct ligation of chemically synthesized modified ribooligonucleotide and enzymatically sythesized RNA utilizing T4 RNA ligase resulted in low reaction yield.

Using the novel protocol, two RNA fragments were ligated on the bridging DNA splint oligonucleotide utilizing T4 DNA ligase.

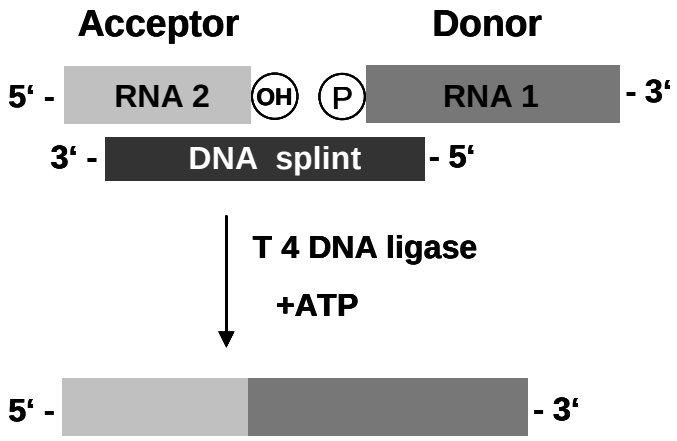

Figure 4.1.6. The principle of the RNA ligation with T4 DNA ligase. DNA splint oligonucleotide (black) hybridizes with two RNA molecules (light-grey and dark-white) and forms a double-helical structure. Ligation requires 3'-OH and 5'-monophosphate on acceptor and donor molecules, respectively. A gap in the double-stranded helix structure, or unpaired nucleotides at the junction (such as n+1 products resulting from T7 transcription) will inhibit the ligation.

The length of the DNA splint was optimized, as well as several reaction conditions. Product formation mainly depends on incubation time, temperature and buffer conditions. A maximum yield of 20% for full-length *B. stearothermophilus* P RNA was achieved during overnight incubation in the presence of RNase inhibitor and DTT without a pre-incubation step. The ratio of synthetic oligoribonucleotide: DNA splint: in vitro-transcribed Bstea-*rnpB*[Δ1-26] was 3:2:1 respectively (Fig.4.1.7). For detailed protocol see the Methods section.

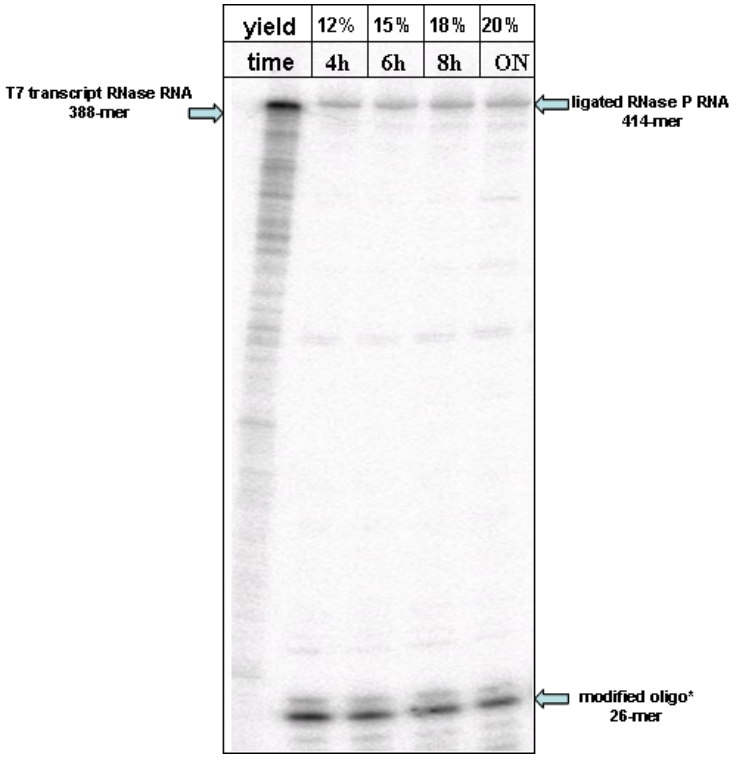

Figure 4.1.7. Efficiency of ligation reaction of ^{32}P-labeled 26-mer oligoribonucleotide and *in vitro* – transcribed Bstea-rnpB[Δ1-26] on the DNA splint at different time points. Lane Con - ^{32}P-labeled Bstea-*rnpB*[Δ1-26]. Ligated species were resolved on 8% denaturing polyacrylamide gel. Ligation assay: 1 µM T7 transcript (388 nt, Bstea-*rnpB*[Δ1-26]), 3µM RNA 26-mer , trace amounts of 5'-^{32}P-labeled 26-mer ribooligonucleotide, 2µM 52-mer DNA splint, 10 mM DTT, 1 mM ATP, 1x ligation buffer (Thermo Fisher Scientific), 40 U RNase Inhibitor (Thermo Fishe Scientific), 7.5 U T4 DNA ligase (Thermo Fisher Scientific) were incubated at 28 °C for indicated periods. 10% denaturing polyacrylamide gel.

We had explored in reconstitution experiments that the chemically synthesized RNA 26-mer and enzymatically synthesized RNA moiety Bstea-*rnpB*[Δ1-26]) were annealed to yield a full-length RNase P RNA molecule (Fig. 4.1.8).

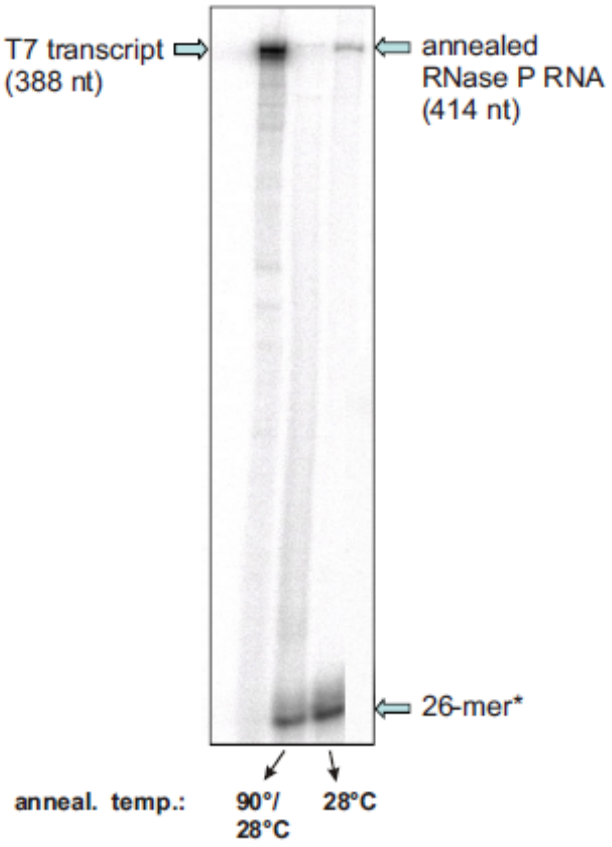

Figure 4.1.8. Annealing of chemically synthesized RNA 26-mer and enzymatically synthesized RNA moiety Bstea-rnpB[Δ1-26]). Annealing assay: 1 µM T7transcript (388 nt, Bstea-*rnpB*[Δ1-26]), 3µM RNA 26-mer, trace amounts of 5'-^{32}P-labeled 26-mer, 1x ligation buffer (Thermo Fisher Scientific); annealing reactions were incubated at 28°C with or without a preincubation step at 90°C.

4.1.5 Single turnover kinetic experiments with ligated and annealed *Bacillus stearothermophilus* P RNAs

In the next step, we tested the ability of ligated and annealed *B. stearothermophilus* P RNAs to promote cleavage of the bacterial precursor $tRNA^{Gly}$ substrate. *B. subtilis* P protein was incubated with ligated *in vitro*-transcribed Bstea-*rnpB*[Δ1-26] and unmodified oligoribonucleotide (**XIV**), ligated *in vitro*-transcribed Bstea-*rnpB*[Δ1-26] and modified oligoribonucleotide (**IX**), annealed *in vitro*-transcribed Bstea-*rnpB*[Δ1-26] and unmodified oligoribonucleotide (**XIV**) and annealed *in vitro*-transcribed Bstea-*rnpB*[Δ1-26] and modified oligoribonucleotide (**IX**). For P RNA reconstitution *in vitro*-transcribed Bstea-*rnpB*[Δ1-26] was added to modified oligoribonucleotide (**IX**) or its unmodified analog (**XIV**) at a ratio of 20:1 respectively. ^{32}P-labeled pre-$tRNA^{Gly}$ was added to the pre-incubated at 37°C ribonucleoprotein complex.

Table 4.1.1. Rate constants of pre-$tRNA^{Gly}$ 5'-processing by ligated and annealed *B. stearothermophilus* P RNA and RNase P holoenzyme.

P RNA *B. stearothermophilus*	P protein *B. subtilis*	k_{obs}, (min^{-1})
wild type *B. stearothermophilus* P RNA	+	4.23±0.51
	-	2.33±0.25
ligated *in vitro*-transcribed Bstea-*rnpB*[Δ1-26] and unmodified oligoribonucleotide (**XIV**)	+	3.88±0.30
	-	2.25±0.15
ligated *in vitro*-transcribed Bstea-*rnpB*[Δ1-26] and modified oligoribonucleotide (**IX**)	+	3.89±0.81
	-	2.28±0.24
annealed *in vitro*-transcribed Bstea-*rnpB*[Δ1-26] and unmodified oligoribonucleotide (**XIV**)	+	2.94±0.17
	-	1.99±0.13
annealed *in vitro*-transcribed Bstea-*rnpB*[Δ1-26] and modified oligoribonucleotide (**IX**)	+	2.68±0.47
	-	1.29±0.22

Enzymatic efficiency of the ligated bacterial RNase P holoenzyme with modified oligoribonucleotide (**IX**) or unmodified oligoribonucleotide (**XIV**) was slightly lower than enzymatic activity of the wild type RNase P. In contrast, enzymatic capacity of the annealed RNase P holoenzyme bearing unmodified oligoribonucleotide (**XIV**) or modified oligoribonucleotide (**IX**) was only 1.5-fold lower than enzymatic activity of wild type *B. stearothermophilus* RNase P. Therefore, *B. stearothermophilus* RNase P holoenzyme bearing

either ligated or annealed P RNA bearing either modified (**IX**) or unmodified (**XIV**) oligoribonucleotide promoted 5'- processing of precursor $tRNA^{Gly}$ at near wild-type levels.

Consequently, the *B. stearothermophilus* RNase P holoenzyme activity is independent from reconstitution approach and the introduction of a single modified residue U^{dap} into *B. stearothermophilus* P RNA does not affect RNase P cleavage efficiency. Obviously, the *B. stearothermophilus* holoenzyme complex with annealed P RNA shows activity comparable to the wild type RNase P holoenzyme. Due to these facts, for the cross-linking experiments *B. stearothermophilus* P RNA was reconstituted by annealing, while this approach makes the identification of crosslinked amino acids easier in the subsequently planned MALDI-TOF analysis.

4.1.6 Crosslinking experiments

All crosslinking experiments were done under conditions favourable for thermodynamic stability of the periodate-oxidized 2'-modified ribooligonucleotide.

Oxidation of the 2'-modified RNA oligonucleotides (**XIV**) and (**XV**) (2 pmol each) bearing 2'-*cis*-diol group was carried out in 15µl 0.4 M sodium acetate (pH 4.0–5.0) and 15 µl 0.23 M $NaIO_4$, while the reaction mixture was incubated for 30 min at 25°C in the dark. In control experiments we observed slight decomposition of the periodateoxidized 2'-modified RNA oligonucleotides (**XIV**) and (**XV**) during gel electrophoresis (data not shown).

The RNA oligonucleotides bearing the 2'-*cis*-diol group react primarily with proximal lysine residues with formation of the Schiff base according to Figure 4.1.3. The second reaction step is reduction of the RNA - protein heteroconjugate with sodium cyanoborohydride.

Cross-linking of *B. subtilis* P protein to *B. stearothermophilus* P RNA was performed under conditions favourable for complex formation. *In vitro*-transcribed Bstea-*rnpB*[Δ1-26] and preliminary oxidized 26-mer ribooligonucleotide, at a ratio of 20:1 respectively, were annealed to formed full-length *B. stearothermophilus* P RNA (Fig.4.1.8). 5'-^{32}P-labeled oligonucleotides (**XIV**), (**XV**) and (**XVI**) (2 pmol) were incubated with *in vitro*-transcribed Bstea-*rnpB*[Δ1-26] (40 pmol) in 50mM HEPES-KOH, pH 7. 4, 4.5mM $MgCl_2$, 150mM NH_4OAc, 4mM β-mercaptoethanol 5 min for 55°C and for 30 min at 37°C. Reconstituted full-length *B. stearothermophilus* P RNA was incubated with *B. subtilis* P protein (from 20 to 200 pmol) for 10 min at 37°C. Then 275 mM sodium cyanoborohydride was added to the reaction mixture to a final concentration of 50mM and incubated for 1 hour at 37°C. To destroy noncovalent RNA-protein complexes, the reaction mixtures were treated for 5

minutes at 95°C in denaturing buffer [50 Mm Tris-HCl (pH 6.8), 2% glycerol, 1% SDS, 0.05% β-mercaptoethanol and 0.1% Bromophenol Blue]. Reaction products were separated from the unbound P RNA and P protein on 4%/13 % SDS-PAGE (Schägger-Jagow protocol).

To find optimal conditions for crosslinking, unmodified RNA 26-mer (**XV**) (Table 4) was selected for the crosslinking reaction optimization of *B. subtilis* P protein to *B. stearothermophilus* P RNA. First, to increase the yield of the covalent complex, P protein concentration was varied. The highest reaction yield was obtained at a ratio of 1:100 of oligoribonucleotide to protein. No crosslinking occurred with the non-oxidized RNA oligonucleotide.

Table 4.1.2 summarizes the *B. subtilis* P protein to *B. stearothermophilus* P RNA crosslinking results under optimal reaction conditions.

There is no remarkable difference in the crosslinking behaviour of *B. stearothermophilus* P RNA to *B. subtilis* P protein depending on the reactive 2'- aldehyde group location. The highest yield was observed with *B. stearothermophilus* RNase P holoenzyme bearing oligonucleotides (**XIV**) and (**XVI**) (crosslinking capacity was approximately 9%). RNase P containing ribooligonucleotide (**XV**) was successfully crosslinked to P protein with 8% efficiency, though somewhat less efficiently than oligos (**XIV**) (9%). No covalent attachment of the P protein to P RNA bearing non-oxidized RNA oligonucleotide was detected. One can see that the crosslinking yield of 2'- modified oligonucleotides (**XIV**), (**XV**) and (**XVI**) alone to P protein was only 1.5 – fold lower then those for P RNA bearing respective 2'-modified oligonucleotides (Fig.4.1.9).

Remarkably, RNA oligonucleotide (**XVI**) bears a modified uridine in position 6 (does not have predicted contacts with P protein on the holoenzyme model), nevertheless, it was crosslinked at 9% efficiency to *B. subtilis* P protein.

Table 4.1.2. Cross-linking efficiency of DNA-duplexes and oligoribonucleotides with B.subtilis P protein in presence (+) or in omission (-) of in vitro-transcribed Bstea-*rnpB*[Δ1-26]

RNA oligo	**Bstea-*rnpB*[Δ1-26]**	**Oligoribonucleotide (5'→3') or DNA-duplex (5'→3'/3'→5')**	**Cross-linking efficiency*, %**
(XIV)	+	r(GUUAAUCAUGCUCGGGUAA**U**^{dap}CGCUG)dC	**9**
(XIV)	-	r(GUUAAUCAUGCUCGGGUAA**U**^{dap}CGCUG)dC	**6**
(XV)	+	r(GUUAAUCAUGCUCGGGUAAUCGC**U**^{dap}G)dC	**8**

(XV)	-	r(GUUAAUCAUGCUCGGGUAAUCGC**U**^{dap}G)dC	**6**
(XVI)	+	r(GUUAA**U**^{dap}CAUGCUCGGGUAAUCGCUG)dC	**9**
(XVI)	-	r(GUUAA**U**^{dap}CAUGCUCGGGUAAUCGCUG)dC	**5**
E		d(GCACCTCGGAA**U**^{dap}GTCCCCTCT) d(GAGCCTTT--CAGGGGAGATG)	**15**
F		d(ATCAAAACAGGACAAAT**U**^{dap}GTCCTAAAACCAA) d(TAGTTTTGTCCTGTTTAA--CAGGATTTTGGTT)	**10**

*The average values of no less than three independent experiments are given. The experimental error was no more than 15%.

These data imply a non-specific covalent attachment of *B. subtilis* P protein to 2'-modified RNA oligonucleotides.

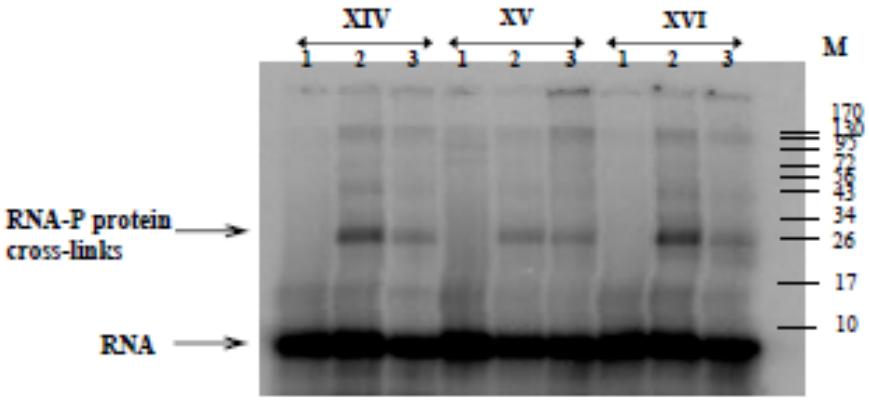

Figure 4.1.9. Crosslinks of *B. subtilis* P protein to modified *B. stearothermophilus* P RNA (*in vitro*-transcribed Bstea-*rnpB*[Δ1-26] was annealed with ribooligonucleotides (XIV), beaing U^{dap} in position 20; with ribooligonucleotides **(XV),** beaing U^{dap} in position 24 and with ribooligonucleotides (XVI), beaing U^{dap} in position 6. Lanes 1 contain respective ribooligonucleotide and *in vitro*-transcribed Bstea-*rnpB*[Δ1-26] only; Lanes 2 contain respective oligo, *in vitro*-transcribed Bstea-*rnpB*[Δ1-26] and P protein; Lanes 3 contain P protein and respective ribooligonucleotide. M indicates protein markers, molecular masses are shown in kDa on the right side.

Additionally, in NMR studies of *Staphylococcus aureus* RNase P protein it was observed that P protein has a strong preference for RNA oligonucleotides over DNA oligonucleotides as well as an ability to bind uncharged nucleosides, which can be accounted for by the stronger hydrogen bonding capability of RNA (Spitzfaden et al., 2000). According to these results, DNA duplexes **F** and **E** bearing randomly inserted 2'-modified uridines were crosslinked to *B. subtilis* P protein under respective reaction conditions. Eventually, it was observed that

DNA duplexes **F** and **E** were also crosslinked to P protein at 10 and 15% efficiency respectively (Fig. 4.1.10).

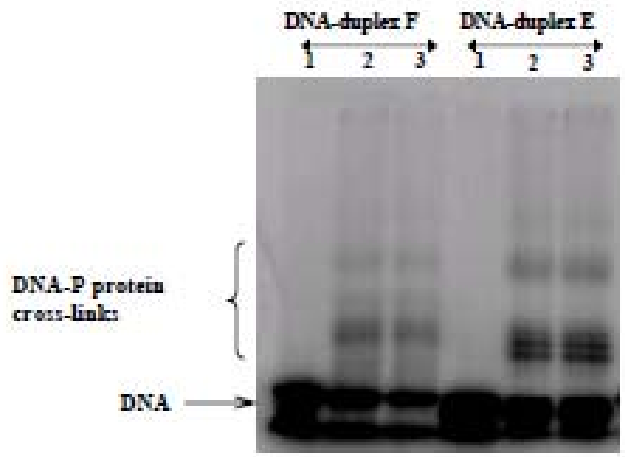

Figure 4.1.10. Crosslinks of *B. subtilis* P protein to modified DNA duplexes E and F. Lanes 1 contain – DNA duplexes **E** and **F** only. In lanes *2,* DNA duplex (**F)** - P protein concentration ratio is 100:1, and in lanes 3, DNA duplex (**E)** - P protein concentration ratio is 200:1.

Furthermore, we investigated the effect of periodate oxidation on the integrity of modified RNA oligonucleotides (data not shown). These experiments revealed oligonucleotide damage (supported by kinetic data), indicating that unwanted side reactions occur at the internal 2'-*cis*-diols.

In conclusion, according to the established protocol for DNA-protein interactions (Sud'ina et al., 2005) using the 2'-aldehyde approach resulted in multiple crosslinks to the RNase P protein regardless of the presence of the T7 RNA transcript contributing the major part of RNase P RNA. We attribute this to a high reactivity and limited specificity of internal 2'-aldehyde groups combined with the capability of the bacterial RNase P protein to bind to single-stranded RNA and DNA oligonucleotides at high concentrations. Nevertheless, 2'-aldehyde ribooligonucleotides could potentially be used for conjugation with low-molecular weight compounds, peptides and proteins for further target cell delivery of siRNAs (Jeong et al., 2009).

4.1.7 UV-crosslinking approach to investigate the bacterial RNase P holoenzyme

To explore another persepective for our crosslinking studies, we also pursued a UV-crosslinking approach using 5-iodopyrimidine-modified oligoribonucleotides instead of 2'-

aldehyde modifications. With 5-iodopyrimidine modifications, nucleobase-specific contacts to amino acid side chains can be captured *in situ* as "zero-length crosslinks" upon irradiation with long wavelength UV light. The fact that crosslinking is inducible raises the likelihood that obtained crosslinks reflect specific contacts. Preferential targets are phenylalanine, tyrosine, tryptophan, histidine and methionine amino acids.

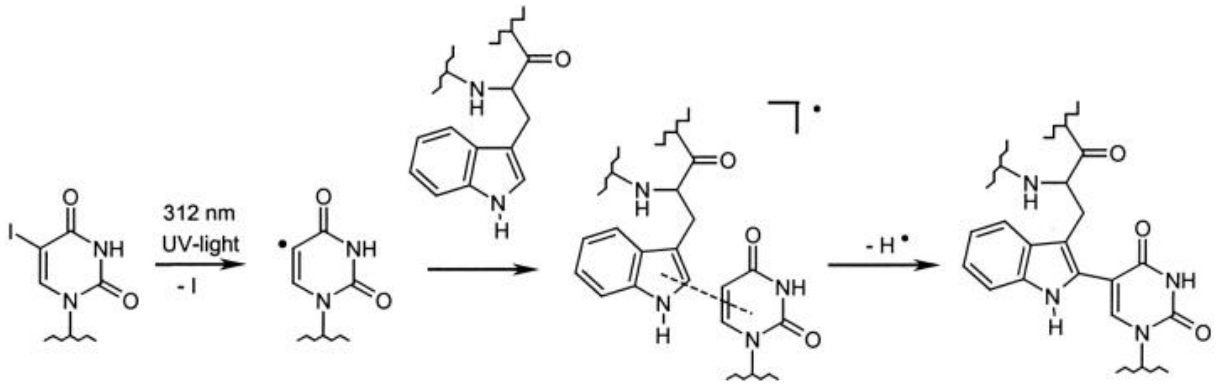

Figure 4.1.11. Suggested reaction mechanism for the crosslinking of 5-iodouracil to tryptophan (scheme reproduced from Norris et al., 2006).

Applying PyMol software (DeLano Scientific LLC), distances between uridines and cytosines of *B. stearothermophilus* P RNA and Phe, Tyr, Trp, His and Met residues of *B.subtilis* P protein were measured on the holoenzyme model (distance limit was from 0 to 10 Å). As candidates for being located at the RNA-protein binding interface, uridine residues U20 and U 24, as well as cytosine residues C21, C23 were selected.

A single 26-mer ribooligonucleotide containing four 5-iodomodified pyrimidines (U20, U24, C21 and C23) was synthesized (Noxxon Pharma AG) and ligated to the enzymatically synthesized remaining portion of RNase P RNA (*in vitro*-transcribed Bstea-*rnpB*[Δ1-26] (388 nt). Due to the fact that 5-iodopyrimidine modifications are photosensitive, all manipulations with the modified ribooligonucleotide and the ligated product containing 5-iodopyrimidine-modified ribooligonucleotide were performed in the dark. Ligation assays were conducted under conditions established at the initial stage of the crosslinking project for P RNA ligation with 2'-modified derivatives. Ligation mixture containing 1 μM *in vitro*-transcribed Bstea-*rnpB*[Δ1-26] (388 nt), 3μM 5-iodouracil containing ribooligonucleotide (26-mer), trace amounts of 5'-^{32}P-labeled 26-mer ribooligonucleotide, 2μM 52-mer DNA splint, 10 mM DTT, 1 mM ATP, 1x ligation buffer (Thermo Fisher Scientific), 40 U RNase Inhibitor (Thermo Fisher Scientific), 7.5 U T4 DNA ligase (Thermo Fisher Scientific) was incubated at 28 °C overnight. The ligated product was purified on the 10% denaturing polyacrylamide gel.

The ligated RNase P RNA product (lig5I20-24) was incubated with the 5'-^{32}P-labeled lig5I20-24 product and *B. subtilis* P protein in buffer LMS [50 Mm HEPES-KOH, pH 7.4, 150 mM NH_4OAc, 5 mM $MgCl_2$] and irradiated for 15 min at 0°C in the Eppendorf tubes with a HeCd-laser equipped with 312-nm bulbs.

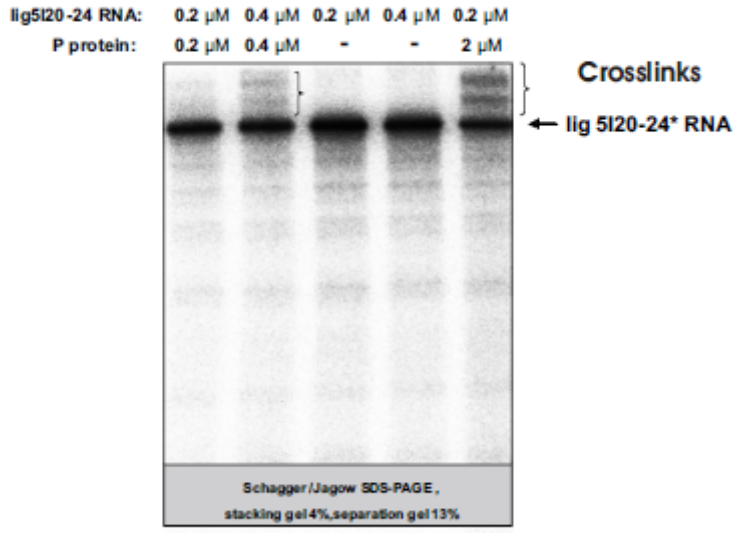

Figure 4.1.12. UV-crosslinking of *B. subtilis* P protein to *B. stearothermophilus* P RNA. Crosslinking assay: ligated P RNA product (lig5I20-24) was incubated for 5 min at 55°C and for 50 min at 37°C in the buffer LMS (50 Mm HEPES-KOH, pH 7.4, 150 mM NH_4OAc, 5 mM $MgCl_2$), then P protein in ratio 1:1 and 1:10 was added and the crosslinking mixture was incubated for 10 min at 37°C. Afterwards, the mixtures were irradiated for 15 min at 0°C with a HeCd-laser emitting at 312 nm. Then reaction mixtures were mixed with the 1x SDS-PAGE loading buffer and crosslinking products were purified on the SDS-PAGE gel (Schägger/Jagow system).

Photochemical crosslinking performed on a preparative scale revealed multiple crosslinks (indicated by brackets above), which may also, based on pronounced mobility differences, represent products involving more than one RNase P molecule. We were unable to detect any RNase P protein by Coomasie staining in the crosslinked material, thus precluding further MALDI-TOF-MS analysis. These experiences eventually led us to discontinue this project.

4.2 Functional characterisation of the novel protein-only RNase P from *Arabidopsis thaliana*

4.2.1 *Arabidopsis thaliana* RNase P

Essentially all tRNAs are transcribed as precursors with extra sequences at the 5'- and 3'-ends. The endonuclease RNase P removes the 5'-flanking sequences to generate the mature 5'-end of tRNA molecules. While the enzyme is generally a ribonucleoprotein particle (RNP) in Bacteria and Archaea (Hartmann et al., 2009), its evolution has diverged in Eukarya. In the latter domain, the nuclear enzyme is an RNP in mammals and yeast (Walker et al., 2010), but is a single polypeptide in the land plant *Arabidopsis thaliana* and trypanosomatids (Gutmann et al., 2012; Taschner et al., 2012). The absence of an RNA subunit seems to be even more widespread among eukaryotic organelles. While the distinct mitochondrial RNase P of yeast is an RNP, mitochondrial RNase P from human and trypanosomatids as well as that from mitochondria and chloroplasts of land plants is devoid of an RNA subunit (Taschner et al., 2012; Holzmann et al., 2008; Gobert et al., 2012; Rossmanith, 2012). These RNA-free RNase P activities have been termed PRORP for "Proteinaceous RNase P" (Gobert et al., 2012; Rossmanith, 2012). *A. thaliana* encodes three PRORP homologs, of which PRORP1 is confined to mitochondria and chloroplasts, while PRORP2 and 3 are found in the nucleus (Gutmann et al., 2012; Gobert et al., 2012). RNase P from spinach chloroplasts, an enzyme that was investigated in much detail by Peter Gegenheimer's group in the 1980 to 90s (, Wang et al., 1988; Thomas et al., 1995), likely belongs to the family of PRORP enzymes as well, although its identity has not been unraveled.

4.2.2 Effects of phosphorothioate modification on precursor tRNA processing by RNase Ps

Bacterial RNase P is composed of a catalytic RNA subunit (~ 130 kDa) and a small single protein (~ 13 kDa). *In vitro*, the RNA subunit alone is an efficient catalyst in the presence of unphysiologically high Mg^{2+} concentrations (Guerrier-Takada et al., 1983). The divalent metal ion-dependent cleavage mechanism of bacterial RNase P RNA (P RNA) was investigated by phosphorothioate modifications at the scissile phosphodiester. Sulfur

substitution of the non-bridging (*pro*-)*R*p oxygen (see Fig. 4.2.1) reduced the rate constant for cleavage under single turnover conditions by three orders of magnitude, but activity could be rescued by ~ two orders of magnitude when Mg^{2+} was replaced with the thiophilic transition metal ion Cd^{2+}, indicating that a direct metal ion coordination occurs to the (*pro*-)*R*p substituent in the transition state (Warnecke et al., 1996, 1999). Essentially the same observations were made when using a precursor tRNA (ptRNA) substrate with *R*p-phosphorothioate modifications 5' of each G residue including the canonical cleavage site (G +1), either in the RNA-alone reaction (Warnecke et al., 1996, 1999) or in the holoenzyme reaction (P RNA + P protein) at 10 mM Mg^{2+} (Warnecke et al., 1997). An *S*p-phosphorothioate modification at the canonical cleavage site (between nt -1/+1 of 5'-ptRNA; see Fig. 4.2.1) also essentially abolished hydrolysis at the canonical site in the presence of Mg^{2+}, but could not be rescued by thiophilic Cd^{2+} or Mn^{2+}. Instead, this modification induced weak aberrant cleavage at the neighbouring phosphodiester (nt –2/-1). Unlike the *R*p sulfur modification, an *S*p sulfur weakened substrate ground state binding about 30-fold (Warnecke et al., 1996), pointing to steric interference caused by a sulfur substitution at this location. Sulfur replacement of the 3'-bridging oxygen also abolished cleavage in the presence of Mg^{2+} as well as thiophilic metal ions, such as Mn^{2+} or Cd^{2+} (Warnecke et al., 2000).

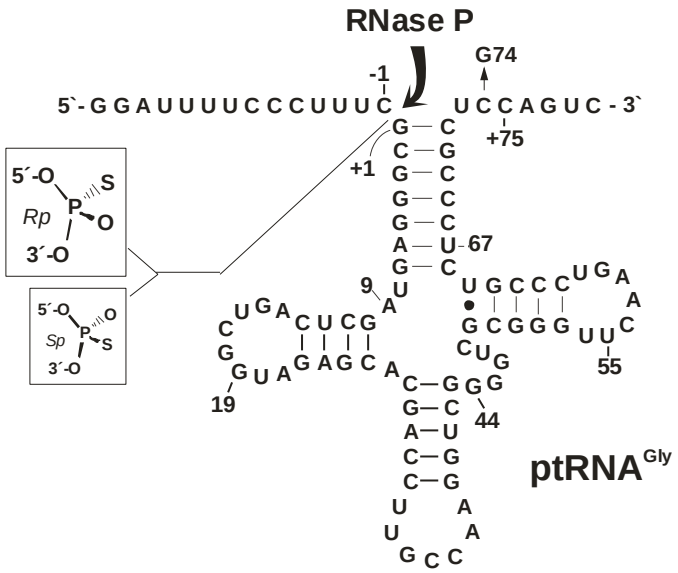

Figure 4.2.1. The bacterial ptRNA^{Gly} substrate obtained by T7 transcription. The substrate was transcribed in the presence of the normal four NTPs (control ptRNA^{Gly}) or under conditions where GTP was fully replaced with *S*p-GTPαS or *S*p-ITPαS, resulting in transcripts that carry an *R*p-phosphorothioate modification 5' of every G residue (ptRNA^{Gly}[GαS] or ptRNA^{Gly}[IαS]). In ptRNA^{Gly}[IαS], all guanosines were additionally replaced with inosine. Only the *R*p-phosphorothioate modification at the RNase P cleavage site, present in ptRNA^{Gly}[GαS] or

ptRNA^{Gly}[IαS], is depicted; the diastereoisomeric *S*p modification, although not analyzed here, is shown for comparison. The arrow indicates the canonical RNase P cleavage site between nt -1/+1. The G74 mutation disrupting the CCA interaction with the P15 loop of bacterial P RNAs (Wegscheid& Hartmann, 2006) is depicted as well.

A single *R*p or *S*p modification at the nt –1/+1 site had somewhat different effects in ptRNA processing reactions catalyzed by nuclear RNP RNase P enzymes from *Homo sapiens sapiens*, *Saccharomyces cerevisiae* and *Dictyostelium discoideum* (Pfeiffer et al., 2000), all three consisting of an RNA subunit plus multiple different protein components (Walker et al., 2010; Stamatopoulou et al., 2010). These enzymes were strongly inhibited by Cd^{2+} ions, and to some extent also by Mn^{2+} ions, even in the presence of an excess of Mg^{2+}, thus precluding the application of Cd^{2+} rescue strategies for thioate-modified substrates (Pfeiffer et al., 2000). However, all three enzymes were strongly inhibited by an *R*p or *S*p-phosphorothioate modification at the canonical RNase P cleavage site, in line with what has been observed for bacterial RNase P. At least for yeast nuclear RNase P, moderate Mn^{2+} rescue of cleavage at the *R*p-modified nt –1/+1 was consistent with direct metal ion coordination to the (*pro*)-*R*p substituent during catalysis as observed for bacterial RNase P enzymes (Pfeiffer et al., 2000).

For spinach chloroplast RNase P activity it was shown that the enzyme is permissive to an *R*p-phosphorothioate modification at the canonical cleavage site. The 5-fold reduced cleavage rate was attributed to the inherently slower chemistry of phosphorothioates versus phosphodiesters and was interpreted as arguing against a direct metal ion coordination to the (*pro*-)*R*p substituent in the transition state of this enzyme (Thomas et al., 2000).

4.2.3 PRORP enzymes acting on bacterial ptRNA^{Gly} - mapping of the cleavage site

A. thaliana PRORP1, 2 and 3, recombinantly expressed in *E. coli* and purified via C-terminal His tags, were tested for processing of bacterial precursor tRNA^{Gly} (ptRNA^{Gly}; Fig. 4.2.1). This substrate (Busch et al., 2000) was transcribed *in vitro* by T7 RNA polymerase, either in the presence of all natural four NTPs or by replacing GTP with the *S*p-GTPαS or *S*p-ITPαS analog. In the latter two cases, all transcripts carried an *R*p-phosphorothioate modification 5' of every G residue including the canonical RNase P cleavage site (nt –1/+1; see Fig. 4.2.1). In addition, all guanosines were replaced with inosines when *S*p-ITPαS was substituted for GTP during T7 transcription. Note that T7 RNA polymerase inverts the configuration at the phosphorus atom during polymerization, such that incorporation of *S*p-NTPαS analogs results

in *R*p-phosphorothioate modifications (Griffiths et al., 1987). The modified substrates are termed ptRNA^{Gly}[GαS] and ptRNA^{Gly}[IαS] in the following.

For mapping the cleavage site, we used ptRNA^{Gly}G74 carrying a 3'-GCA instead of 3'-CCA triplet, leading to substantial miscleavage at the nt –2/-1 position (Wegscheid& Hartmann, 2006). Analysis of unmodified ptRNA^{Gly} and ptRNA^{Gly}[GαS] revealed that cleavage of both substrates predominantly occurred at the canonical –1/+1 site in reactions catalyzed by PRORP1 and 3 using Mg^{2+} as the sole divalent metal ion (Fig. 4.2.2, lanes 4, 8, 10 and 14). PRORP2 was completely inactive in these assays performed at 37°C (Fig. 4.2.2, lanes 6 and 12). In a parallel study, we observed that PRORP2, in contrast to PRORP1 (Gobert et al., 2010), was only able to complement the *E. coli* RNase P mutant strain BW (Wegscheid& Hartmann, 2006) at 28°C, but not at 37°C (data not shown). This prompted us to test processing by PRORP2 *in vitro* at 28°C, where the enzyme indeed turned out to be active (see below).

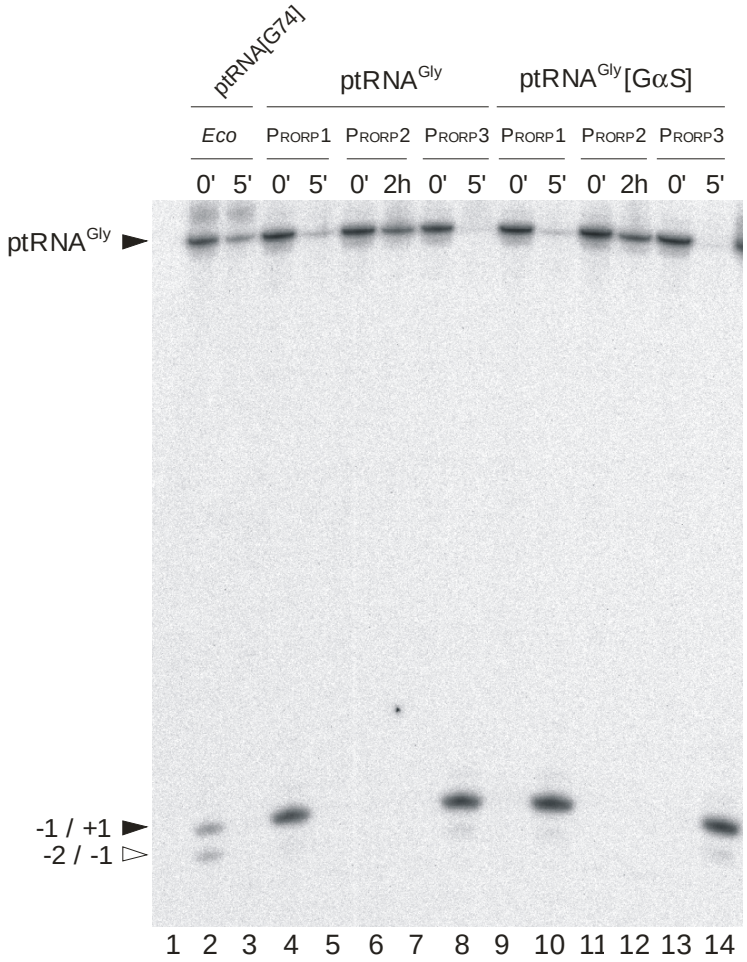

Figure 4.2.2. Cleavage site selection by PRORP enzymes. Processing of trace amounts of unmodified ptRNA^{Gly} (lanes 3-8) or ptRNA^{Gly}[GαS] (lanes 9-14) were incubated with *A. thaliana* PRORP1, 2 or 3 (2 µM) in buffer KN supplemented with 10 mM $Mg(OAc)_2$ at 37°C for the time period indicated above each lane. Note that

PRORP2 is completely inactive at 37°C. Cleavage of the mutant substrate ptRNA^{Gly}[G74] with a disrupted CCA interaction (Wegscheid & Hartmann, 2006) by *E. coli* RNase P (*Eco*) under the same conditions (lanes 1 and 2) enabled cleavage site assignment for products derived from processing by PRORP enzymes: *E. coli* RNase P considerably miscleaves the ptRNA^{Gly}[G74] substrate at the –2/-1 site, one nt upstream of the canonical –1/+1 site (see Fig. 4.2.1). Reactions were analyzed on 20% PAA/8 M urea gels. Bands corresponding to ptRNAs and 5'-cleavage products are indicated on the left.

Since recombinant PRORP proteins equipped with a C-terminal His tag were purified via Ni-NTA affinity chromatography from *E. coli* lysates there was the formal possibility that the enzyme preparations might contain traces of *E. coli* RNase P including its catalytic RNA subunit. RT-PCR analysis essentially ruled out that any of the basic results obtained here with PRORP enzymes had been influenced by contaminations with *E. coli* RNase P (see Fig. 4.2.3).

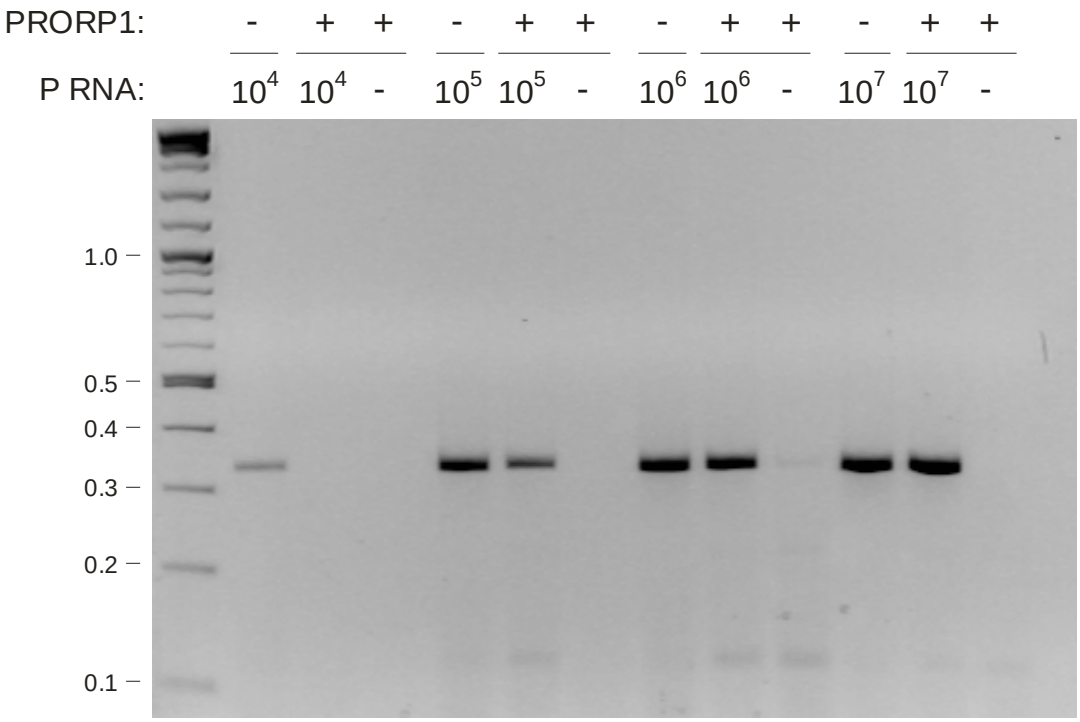

Figure. 4.2.3. *A. thaliana* PRORP1 purified by Ni-NTA affinity chromatography was analyzed for possible *E. coli* P RNA contaminations by RT-PCR. 90 pmol PRORP1 (corresponding to 4.5 µM, somewhat higher than the concentration of 2 µM used in our standard 20-µl reactions) was analyzed by RT-PCR with primers specific for *E. coli* P RNA. Additionally, the detection limit for *E. coli* P RNA was determined by adding defined quantities (10^4–10^7 molecules) of *in vitro* transcribed RNase P RNA to aliquots of the PRORP1 preparation. RT-PCR reactions were analyzed for the presence of the specific 330-bp amplification product on ethidium bromide-stained 2% agarose gels.

4.2.4 Single turnover kinetic analysis of ptRNA^{Gly} cleavage by *A. thaliana* PRORP1

To explore the catalytic capacity of PRORP1 we performed single turnover kinetics using trace amounts (< 1 nM) of ^{32}P-endlabeled ptRNA^{Gly} and varying excess amounts (0.01 – 7.0 µM) of PRORP1. The single turnover V_{max} (k_{react}) and K_m ($K_{(sto)}$) were determined as 4.3 min^{-1} and 1.4 µM, respectively, for processing of the bacterial ptRNA^{Gly} substrate in KN buffer containing 10 mM $Mg(OAc)_2$ (Fig. 4.2.4), a buffer we routinely use for bacterial RNase P holoenzymes to closely mimic physiological conditions (Wegscheid& Hartmann, 2006).

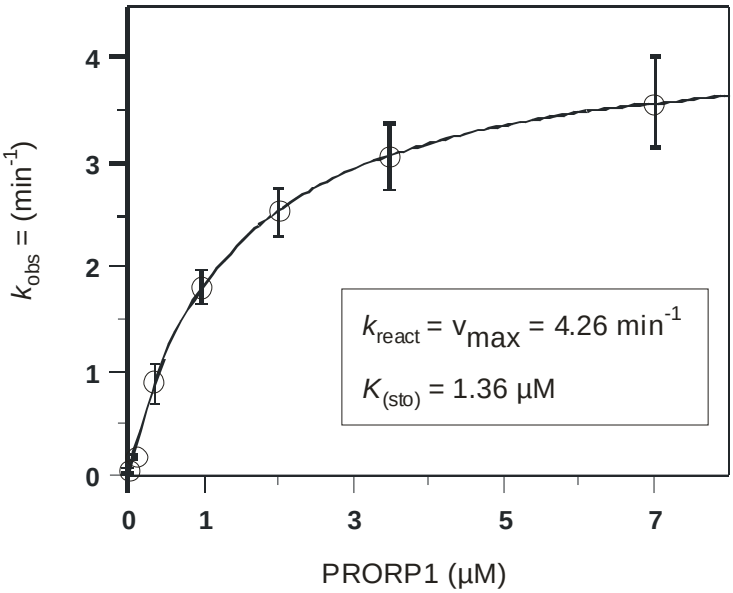

Figure 4.2.4. Single turnover kinetics of *A. thaliana* PRORP1 as a function of the PRORP1 concentration. Processing assays were performed at 37°C with trace amounts of unmodified ptRNA^{Gly} in buffer KN containing 10 mM $Mg(OAc)_2$. The k_{obs} values are mean values from at least three independent experiments, with error bars indicating the standard error of the mean. $K_{m(sto)}$ is the single turnover K_m (describes the enzyme concentration at which half the maximum rate under conditions of [E] >> [S] is achieved), and k_{react} is the single turnover V_{max}.

Based on the data in Table 4.2.1, the V_{max} values for PRORP2 and 3 may even exceed that for PRORP1 (Table 4.2.1, k_{obs} = 4.9 ± 2.0 and 7.7 ± 4.6 min^{-1} for PRORP2 and 3, respectively, at 2 µM enzyme conctration). A V_{max} of 4.3 min^{-1} is similar to that measured for *E. coli* RNase P (Tallsjö & Kirsebom, 1993), but roughly one order of magnitude lower than the V_{max} values measured for several other RNA-containing RNase P holoenzymes (Kurz et al., 1998; Feltens et al., 2003; Cho et al., 2010; Xiao et al., 2006) under similar conditions albeit with different

substrates. The corresponding K_m values for these previously characterized RNase P enzymes varied roughly between 20 and 250 nM (Tallsjö & Kirsebom, 1993; Kurz et al., 1998; Cho et al., 2010; Xiao et al., 2006). In conclusion, the catalytic efficiency of *A. thaliana* PRORP1 measured *in vitro* seems to be within the lower normal range of RNase P activities, although this statement should be considered with caution owing to the differences in kinetic assay conditions and substrates used in the various activity studies.

4.2.5 *E. coli* RNase P sensitivity to an *R*p-phosphorothioate modification at the cleavage site and metal ion rescue

Single turnover cleavage of unmodified ptRNA^{Gly}, ptRNA^{Gly}[GαS] and ptRNA^{Gly}[IαS] by the *E. coli* RNase P holoenzyme yielded results in line with findings previously obtained for this P RNA in the absence (Warnecke et al., 1996, 1999) or presence (Warnecke et al. 1997) of the P protein: *E. coli* RNase P cleaved the unmodified ptRNA^{Gly} substrate in the presence of Mg^{2+} and/or Mn^{2+}, but not with the thiophilic Cd^{2+} as the sole metal ion cofactor (Fig. 4.2.5).

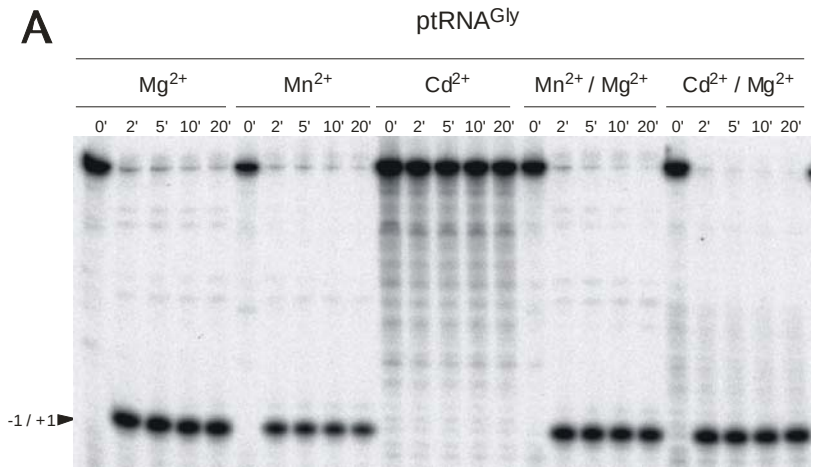

Figure 4.2.5. Processing of (A) unmodified ptRNA^{Gly} by *E. coli* RNase P in the presence of different divalent ion acetates. Trace amounts of substrate were incubated with 1 µM *E. coli* RNase P holoenzyme (1 µM P RNA plus 3 µM P protein) at 37°C in buffer KN containing either 10 mM Mg^{2+}, 10 mM Mn^{2+}, 10 mM Cd^{2+}, 7.5 mM Mg^{2+}/2.5 mM Mn^{2+} or 7.5 mM Mg^{2+}/2.5 mM Cd^{2+}. The time of incubation is specified above each lane. Products were analyzed by 20% PAGE in the presence of 8 M urea. The 5'-flank originating from cleavage at the canonical (-1/+1) site is indicated at the left margin in panels A and B. In panel C, co-electrophoresis of miscleaved 5'-cleavage products derived from ptRNA^{Gly}[G74] (see also Fig. 4.2.1) shows that cleavage of

ptRNA^{Gly}[IαS] by *E. coli* RNase P primarily occurs at the canonical –1/+1 site in the presence of Cd^{2+} and Mg^{2+}/Cd^{2+}.

Conversely, significant processing of substrates ptRNA^{Gly}[GαS] and ptRNA^{Gly}[IαS] (Fig. 4.2.6) was achieved only in the presence Cd^{2+}, and to a very minor extent with Mn^{2+} in case of ptRNA^{Gly}[GαS] (Fig. 4.2.6 B).

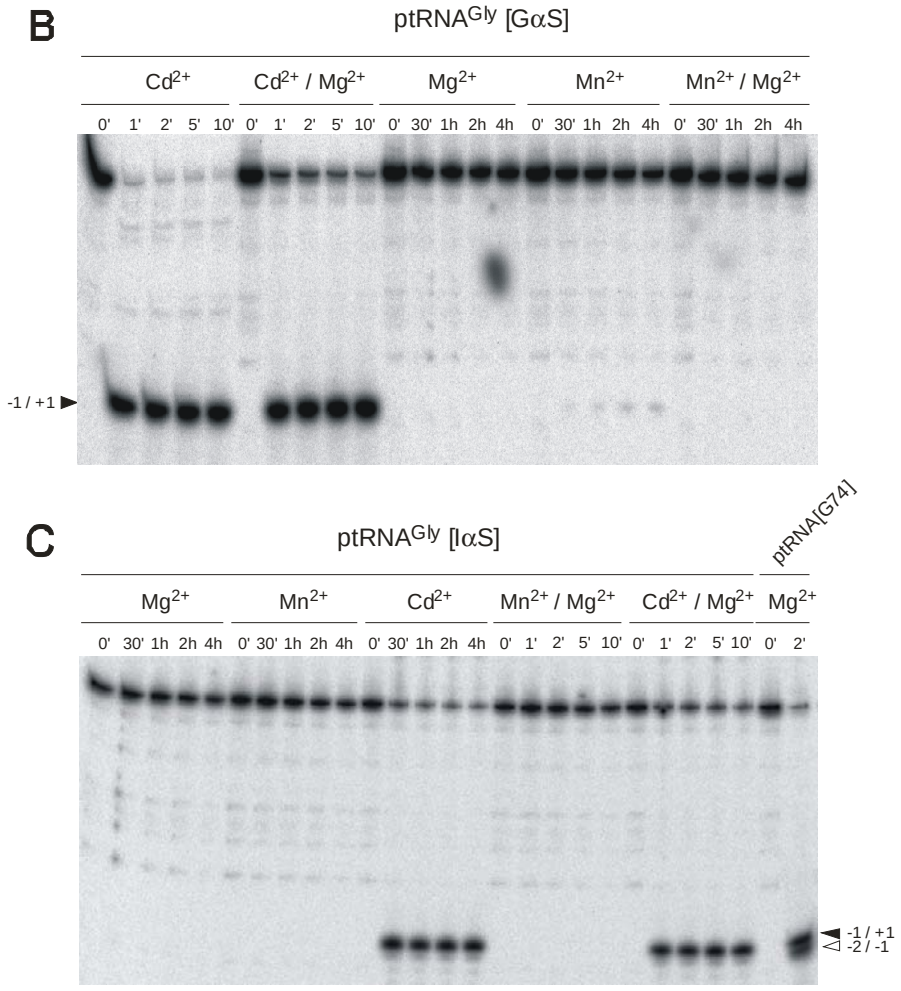

Figure 4.2.6: Processing of (B) ptRNA^{Gly}[GαS] and (C) ptRNA^{Gly}[IαS] by *E. coli* RNase P in the presence of different divalent ion acetates. Trace amounts of substrate were incubated with 1 µM *E. coli* RNase P holoenzyme (1 µM P RNA plus 3 µM P protein) at 37°C in buffer KN containing either 10 mM Mg^{2+}, 10 mM Mn^{2+}, 10 mM Cd^{2+}, 7.5 mM Mg^{2+}/2.5 mM Mn^{2+} or 7.5 mM Mg^{2+}/2.5 mM Cd^{2+}. The time of incubation is specified above each lane. Products were analyzed by 20% PAGE in the presence of 8 M urea. The 5'-flank originating from cleavage at the canonical (-1/+1) site is indicated at the left margin in panels A and B. In panel C, co-electrophoresis of miscleaved 5'-cleavage products derived from ptRNA^{Gly}[G74] (see also Fig. 4.2.1)

shows that cleavage of ptRNA^{Gly}[IαS] by *E. coli* RNase P primarily occurs at the canonical –1/+1 site in the presence of Cd^{2+} and Mg^{2+}/Cd^{2+}.

4.2.6 *A. thaliana* RNase P sensitivity to an *R*p-phosphorothioate modification at the cleavage site and metal ion rescue effect

When we tested *A. thaliana* PRORP1 with the same set of substrates under identical buffer conditions, we already observed a difference to *E. coli* RNase P in case of the unmodified ptRNA^{Gly} substrate: whereas *E. coli* RNase P cleaved this substrate quite efficiently in the presence of a mixture of 7.5 mM Mg^{2+}/2.5 mM Cd^{2+}, *A. thaliana* PRORP1 was strongly inhibited under these conditions, indicating that Cd^{2+} is highly deleterious to the activity of this protein-only RNase P (Fig. 5.2.7). Processing of ptRNA^{Gly}[GαS] and ptRNA^{Gly}[IαS] by *A. thaliana* PRORP1 proceeded with comparable efficiency in the presence of Mg^{2+} and/or Mn^{2+} (Fig. 5.2.8), in sharp contrast to inefficient cleavage of these substrates by *E. coli* RNase P with Mg^{2+} or Mn^{2+} as the metal cofactor (Fig. 5.2.8). The presence of Cd^{2+} failed to rescue cleavage of ptRNA^{Gly}[GαS] and ptRNA^{Gly}[IαS] by *A. thaliana* PRORP1, again contrasting the efficient Cd^{2+} rescue in the reaction catalyzed by *E. coli* RNase P.

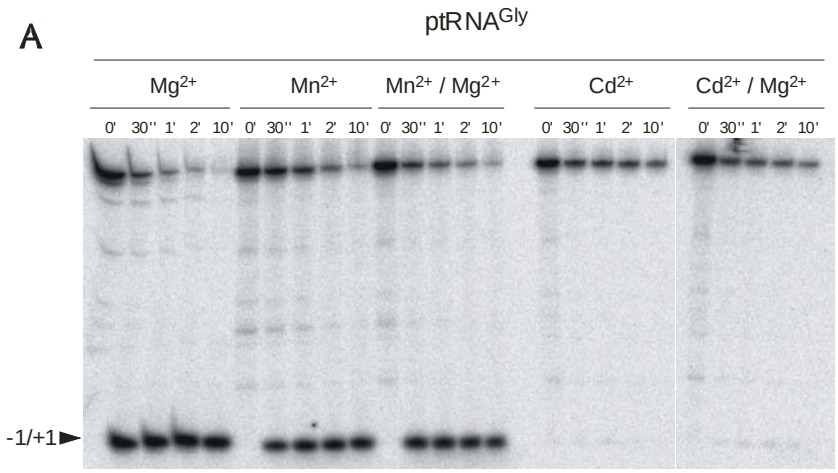

Figure. 4.2.7. Processing of (A) unmodified ptRNA^{Gly} by *A. thaliana* PRORP1 in the presence of different divalent ion acetates. Trace amounts of substrate were incubated with 2 µM *A. thaliana* PRORP1 at 37°C in buffer KN containing either 10 mM Mg^{2+}, 10 mM Mn^{2+}, 10 mM Cd^{2+}, 7.5 mM Mg^{2+}/2.5 mM Mn^{2+} or 7.5 mM Mg^{2+}/2.5 mM Cd^{2+}. The time of incubation is specified above each lane. For further details, see legend to Fig. 4. Con. a (panel B): ptRNA^{Gly}[G74] cleaved by *E. coli* RNase P for 1 min at 37°C as specified in Fig. 4; Con. b, c: cleavage of ptRNA^{Gly}[IαS] by PRORP1 for 10 min in buffer KN plus 10 mM Mg^{2+} or 7.5 mM Mg^{2+}/2.5 mM Mn^{2+}, respectively. The bands for the 5'-cleavage product migrated close to the bottom of the gels in all three

panels. To dispel potential doubts that there might be some additional smaller cleavage products derived from cleavage upstream of the –2 site, we have added an image of an exemplary gel with product bands that migrated less far (Fig. 4.2.9).

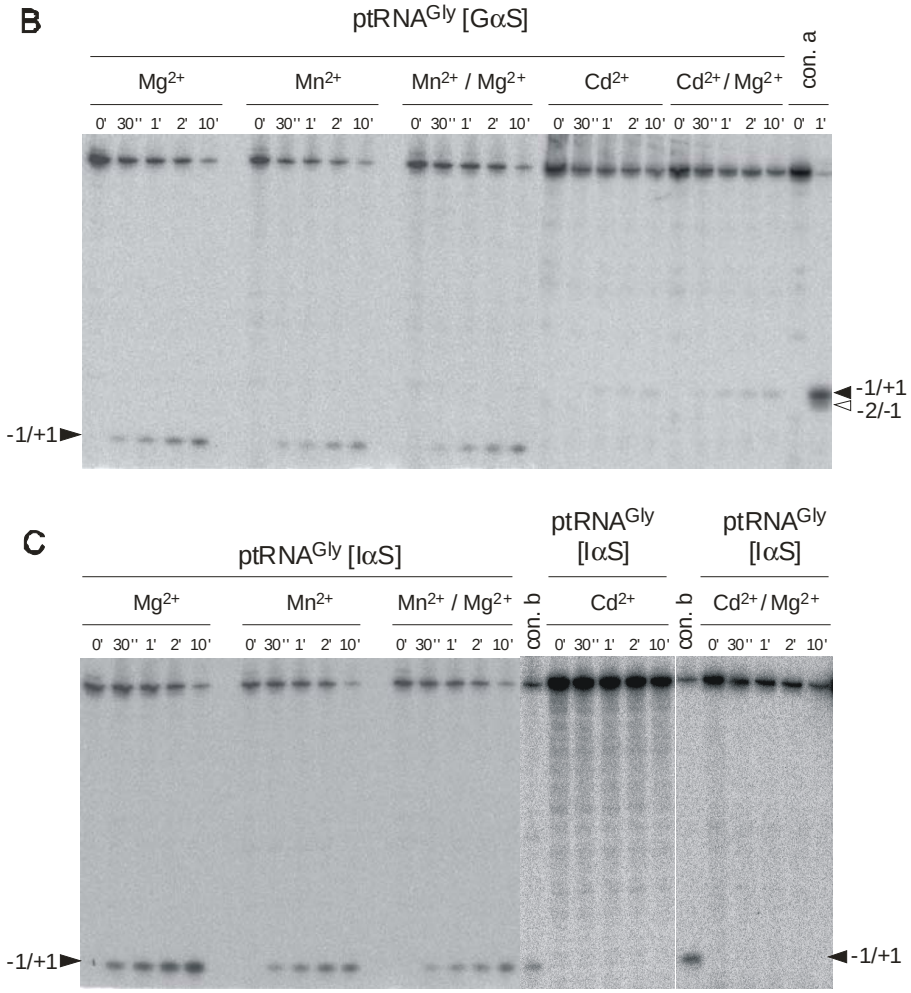

Figure. 4.2.8. Processing of (A) unmodified ptRNA^{Gly}, (B) ptRNAGly[GαS] and (C) ptRNAGly[IαS] by *A. thaliana* PRORP1 in the presence of different divalent ion acetates. Trace amounts of substrate were incubated with 2 µM *A. thaliana* PRORP1 at 37°C in buffer KN containing either 10 mM Mg^{2+}, 10 mM Mn^{2+}, 10 mM Cd^{2+}, 7.5 mM Mg^{2+}/2.5 mM Mn^{2+} or 7.5 mM Mg^{2+}/2.5 mM Cd^{2+}. The time of incubation is specified above each lane. For further details, see legend to Fig. 4. Con. a (panel B): ptRNA^{Gly}[G74] cleaved by *E. coli* RNase P for 1 min at 37°C as specified in Fig. 4; Con. b, c: cleavage of ptRNA^{Gly}[IαS] by PRORP1 for 10 min in buffer KN plus 10 mM Mg^{2+} or 7.5 mM Mg^{2+}/2.5 mM Mn^{2+}, respectively. The bands for the 5'-cleavage product migrated close to the bottom of the gels in all three panels. To dispel potential doubts that there might be some additional smaller cleavage products derived from cleavage upstream of the –2 site, we have added an image of an exemplary gel with product bands that migrated less far (Fig. 4.2.9).

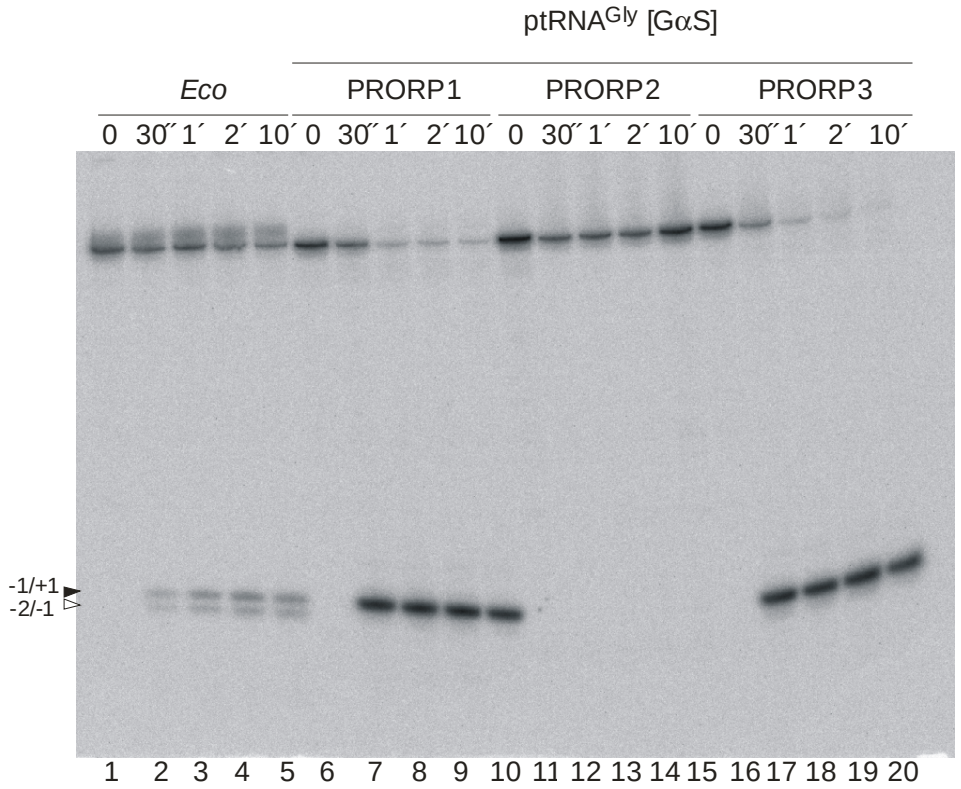

Figure 4.2.9. Processing of ptRNA^{Gly}[GαS] by *A. thaliana* PRORP1 and 3 at 10 mM Mg^{2+} at 37°C. Lanes 1-5: trace amounts (< 1 nM) of 5'-[^{32}P]-endlabeled ptRNA^{Gly}[G74] were incubated with 1 µM *E. coli* RNase P holoenzyme at 37°C in a final reaction volume of 20 µl of buffer A containing 10 mM $Mg(OAc)_2$.; lanes 6-20: trace amounts (< 1 nM) of 5'-[^{32}P]-endlabeled ptRNA^{Gly}[GαS] were incubated with 2 µM *A. thaliana* PRORP1 (lanes 6-10), PRORP2 (lanes 11-15) or PRORP3 (lanes 16-20) at 37°C in a final reaction volume of 20 µl of buffer A containing 10 mM $Mg(OAc)_2$. The time of incubation is specified above each lane. Products were analyzed by 20% PAGE in the presence of 8 M urea. 5'-cleavage products originating from cleavage at the canonical (-1/+1) site or at the aberrant –2/-1 site (lanes 2-5) are indicated at the left.

4.2.7 Single turnover kinetic analysis of ptRNA^{Gly}, ptRNA^{Gly}[GαS] and ptRNA^{Gly}[IαS] cleavage by *A. thaliana* PRORP enzymes and *E. coli* RNase P

Determination of single turnover rate constants (k_{obs} [min^{-1}]) for tRNA 5'-end maturation (Table 4.2.1) substantiated that *A. thaliana* PRORP1 acts on all three tested substrates ptRNA^{Gly}, ptRNA^{Gly}[GαS] and ptRNA^{Gly}[IαS] with similar efficiency in the presence of Mg^{2+} or Mn^{2+}.

Table 4.1: Single turnover rate constants (k_{obs} [min^{-1}]) for processing of trace amounts (< 1 nM) unmodified ptRNA^{Gly}, ptRNA^{Gly} [GαS] or ptRNA^{Gly} [IαS] by 1 µM *E. coli* (*Eco*) RNase P or 2 µM PRORP1-3 in the presence of different divalent ion acetates.

Me^{2+}	ptRNA^{Gly}, k_{obs}				ptRNA^{Gly} [GαS], k_{obs}				ptRNA^{Gly} [IαS], k_{obs}	
	Eco RNase P	PRORP1	PRORP2 (at 28¡C)	PRORP3	*Eco* RNase P	PRORP1	PRORP2 (at 28¡C)	PRORP3	*Eco* RNase P	PRORP1
Mg	2.6 ± 1.0	2.3 ± 1.1	4.9 ± 2.0	7.7 ± 4.6	² 10^{-4}	0.5 ± 0.3	0.9 ± 0.3	1.7 ± 1.3	n.d.	0.31 ± 0.06
Mn	3.9 ± 1.9	0.94 ± 0.25	1.04 ± 0.15		² 6×10^{-4}	1.0 ± 0.5	1.0 ± 0.1		² 8×10^{-4}	0.21 ± 0.08
Mg/Mn	2.2 ± 0.4	1.4 ± 0.7			$(1 \pm 0.5) \times 10^{-3}$	0.16 ± 0.03	.		² 3×10^{-4}	0.8 ± 0.5
Cd	n.d.	n.d.			3.35 ± 1.3	n.d.			1.8 ± 0.6	n.d.
Mg/Cd	3.9 ± 2.4	n.d.			2.1 ± 0.9	n.d.			1.7 ± 0.6	n.d.

n.d.: not detectable; *k*obs values are given with standard deviations; assays were conducted at 37°, except for PRORP2 (28°C).

At 10 mM Mg^{2+}, k_{rel} ($k_{obs(PO)}/k_{obs(PS)}$,Table 4.2.2) for ptRNA^{Gly} relative to ptRNA^{Gly}[GαS] was roughly 5 for PRORP1, but ≥ 26000 for *E. coli* RNase P. At 10 mM Mn^{2+}, the corresponding k_{rel} values were roughly 1 versus ≥ 6500 (Table 4.2.2).

Table 4.2: Relative cleavage rates for ptRNA^{Gly} and ptRNAGly[GαS].

Me^{2+}	k_{rel} [$k_{obs(PO)}$ / $k_{obs(PS)}$]			
	E. coli	PRORP 1	PRORP 2	PRORP 3
Mg^{2+}	≥ 26000	4.6	5.4	4.5
Mn^{2+}	≥ 6500	0.9	1.0	n.a.

n.a.: not analyzed

Rate constants for PRORP1 acting on ptRNA^{Gly}[IαS] tended to be somewhat lower than with ptRNA^{Gly}[GαS], which can be attributed to a general tRNA destabilization effect owing to replacement of the many guanosines with inosine in ptRNA^{Gly}[IαS]. *A. thaliana* PRORP1 localizes to mitochondria and chloroplasts, while *A. thaliana* PRORP2 and 3 are confined to the nucleus (Gobert et al., 2010), which may entail functional differences between PRORP1 versus 2 and 3. When we tested PRORP2 with ptRNA^{Gly} or ptRNA^{Gly}[GαS] as substrate, assays were conducted at 28°C because *A. thaliana* PRORP2 was inactive at 37°C (see Fig. 4.2.1). As observed for the organellar homolog, PRORP2 cleaved both substrates at the

canonical site and with similar efficiency in the presence of Mg^{2+} or Mn^{2+} (Fig. 4.2.10), the individual rate constant not differing by more than ~5-fold (Tables 4.2.1 and 4.2.2).

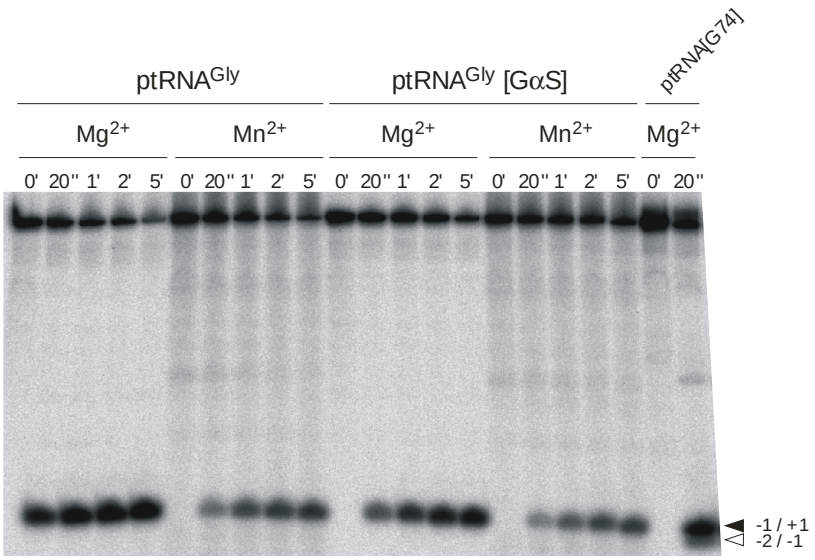

Figure 4.2.10. Processing of unmodified ptRNA^{Gly} and ptRNA^{Gly}[GαS] by *A. thaliana* PRORP2. Trace amounts of substrate were incubated with 2 µM *A. thaliana* PRORP2 at 28°C in buffer KN containing either 10 mM $Mg(OAc)_2$ or 10 mM $Mn(OAc)_2$. The time of incubation is specified above each lane. Last two lanes on the right: processing of ptRNA^{Gly}[G74] by *E. coli* RNase P (for details, see legend to Fig. 4.2.2).

Finally, we also analyzed PRORP3 for cleavage of ptRNA^{Gly} or ptRNA^{Gly}[GαS] in the presence of Mg^{2+}. Again, the difference in k_{obs} did not exceed a factor of 5 (Table 4.2.1). Our results support the notion that all three *A. thaliana* PRORP enzymes are mechanistically closely related.

4.2.8 Catalysis by proteinaceous RNase P - effect of an *R*p-phosphorothioate substitution at the scissile phosphodiester

Here we have shown that *A. thaliana* PRORP1 acts on a bacterial ptRNA substrate with a catalytic efficiency that is roughly within the lower normal range of RNA-based RNase P activities characterized so far at the standard assay temperature of 37°C. This is consistent with our previous finding that *A. thaliana* PRORP1 can replace the endogenous *E. coli* RNase P *in vivo* to provide the essential tRNA 5'-end maturation activity in this bacterium (Gobert et al., 2010). Since plants do not sustain thermal homeostasis and taking into account that *A. thaliana* P optimally grows at 23-25°C, the activity at 37°C may provide only a partial picture

of the catalytic capacity of *A. thaliana* PRORP enzymes. Conceivably, these plant PRORP enzymes may have adapted to being effective over a broad temperature range and particularly at lower temperatures, a hypothesis testable in future studies and in line with our finding that *A. thaliana* PRORP2 is very active at 28°C, but inactive at 37°C.

The K_m 1.4 µM determined for processing of bacterial ptRNAGly is somewhat higher than the submicromolar K_m values reported for RNA-containing RNase P enzymes (see Results section). Since PRORP1 is able to sustain all essential tRNA 5'-end maturation functions in an *E. coli* RNase P mutant strain (Gobert et al., 2010), we conclude that its selectivity for and affinity to ptRNA substrates is sufficient even in the bacterial context. The bacterial P protein increases the affinity for ptRNA relative to mature tRNA by interacting with the 5'-precursor segment (Kurz et al., 1998). This facilitates product release and may contribute to preventing inhibition of bacterial RNase P by the cellular excess of mature tRNAs. It will be intriguing to see if PRORP enzymes bind ptRNAs and mature tRNAs also with differential affinity. If not, higher substrate dissociation rate constants, and thus increased K_m values, may make PRORP-ptRNA interactions more transient, thus counteracting potential product inhibition effects.

With respect to substrate recognition, we found that substituting a sulfur for the (*pro*-)*R*p oxygen at all 26 G residues of our ptRNA substrate (Fig. 4.2.1), including the canonical cleavage site, had little effect on processing efficiency. Even additional inosine replacements at these positions were largely tolerated. First of all, this indicates that productive PRORP-ptRNA interaction is accomplished without substantial contributions from any of the affected (*pro*-) *R*p oxygens or exocyclic 2-amino groups, the latter missing in inosines relative to guanosines.

In reactions catalyzed by the three *A. thaliana* PRORP enzymes, an *R*p-phosphorothioate modification at the canonical –1/+1 site neither increased the frequency of miscleavage nor reduced the rate constant of cleavage at 10 mM Mg^{2+} or 10 mM Mn^{2+} more than 5-fold. In contrast, the same modification caused miscleavage and a drastic rate reduction by three orders of magnitude with *E. coli* RNase P tested under the same conditions. The mild *R*p-thioate effect seen with the PRORP enzymes is reminiscent of what was reported for partially purified RNase P from spinach chloroplasts by Thomas et al. (Thomas et al., 2000). They also observed cleavage of a ptRNA carrying an *R*p-sulfur at the canonical site, and, very similar to our results, measured a 5-fold slower reaction of the *R*p-modified substrate relative to one with a normal phosphodiester. This coincidence makes it very likely that the partially enriched RNase P activity from spinach chloroplasts was indeed the organellar PRORP of *Spinacia oleracea*.

Mechanistically, tolerance to an *R*p-phosphorothioate modification at the scissile phosphodiester with Mg^{2+} as the sole metal ion cofactor essentially rules out that the catalysis involves an inner-sphere coordination to the (*pro*-)*R*p substituent (Pearson, 1963). The 5-fold rate reduction can be attributed to the lower intrinsic reactivity (4- to 11-fold reduction) of phosphorothioate versus phosphate diesters (Herschlag et al., 1991). Thus, it is evident that the mechanistic strategies employed by PRORP enzymes versus ribonucleoprotein RNase P enzymes are different in a fundamental aspect, although both types of enzyme generate the same products (5'-phosphates and 3'-hydroxyls). It will be interesting to analyze the effect of an *S*p-phosphorothioate modification at the scissile phosphodiester. If inhibitory it will yet be difficult to prove a potential inner-sphere coordination of the (*pro*-)*S*p substituent because the PRORP polypeptides have been found to be strongly inhibited by Cd^{2+} ions, even if an excess of Mg^{2+} ions is present (7.5 mM Mg^{2+}/2.5 mM Cd^{2+}, Fig. 5). A similar problem in related studies of eukaryotic nuclear ribonucleoprotein RNase P enzymes precluded the demonstration of persuasive metal ion rescue effects for the *R*p-thioate at the processing site (Pfeiffer et al., 2000).

A. thaliana PRORP1 and 2 were previously identified in bioinformatic screens as members of the so-called NYN domain group of proteins with predicted RNase activity (Anantharaman & Aravind, 2006). The MRPP3/PRORP subunit of human mitochondrial RNase P was the first NYN protein for which endonuclease activity was demonstrated experimentally (Holzmann et al., 2008). The NYN family members are also related to proteins harbouring a PIN nuclease domain as well as to exonucleases and endonucleases of the FLAP superfamily, including RNase H of bacteriophage T4 (Anantharaman & Aravind, 2006). The NYN metallonuclease domain harbors five conserved Asp and two conserved His residues (Rossmanith, 2012), which includes the two consecutive aspartate residues which we showed by mutation to be essential for catalytic activity of *A. thaliana* PRORP1 (Gobert et al., 2010). Proteins with an NYN domain were predicted to expose four conserved aspartates to provide a ligand sphere for a single catalytic metal ion, whereas members of the FLAP superfamily, such as T4 RNase H, were proposed to have evolved a second metal ion binding site through fusion of their nuclease domain to a helix-hairpin-helix domain (Anantharaman & Aravind, 2006). Whether PRORP enzymes engage one or two catalytic metal ions is as yet unclear.

Although the catalytic mechanism of PRORP enzymes is still speculative at present, it is worth mentioning some similarities between PRORP RNases and RNase H enzymes, apart from the fact that both types of nuclease generate 5'-phosphate and 3'-OH termini. RNase H enzymes expose 4-5 acidic amino acid side chains in their active site that are proposed to

provide the ligand sphere for two catalytic metal ions (Nowotny & Yang, 2006; Tadokoro & Kanaya, 2009). The currently favored two-metal-ion catalytic mechanism for RNase H enzymes, mainly based on the identification of two active site metal ions in RNase H crystal structures (Nowotny & Yang, 2006), predicts that both metal ions directly coordinate to the (*pro*-)*S*p oxygen at the scissile phosphodiester, and one metal ion activates the water nucleophile, while the second stabilizes the oxyanion leaving group in the transition state (Tadokoro & Kanaya, 2009). *Thermus thermophilus* Argonaute (Ago) harbors a PIWI domain that adopts an RNase H fold (Wang et al., 2009). An *S*p-phosphorothioate modification at the cleavage site in a target DNA substrate for *T. thermophilus* Ago completely blocked cleavage, whereas an *R*p-phosphorothioate modification was permissive particularly in the presence of Mn^{2+} ions (Wang et al., 2009). Insensitivity to an *R*p-sulfur modification is a feature also observed for the PRORP enzymes studied here. It will thus be instructive to analyse the effect of *S*p sulfur at the RNase P cleavage site in reactions catalyzed by PRORP, notwithstanding the potential difficulties with thiophilic metal ion rescue experiments (see above).

5. Summary

Ribonuclease P (RNase P) is the ubiquitous processing enzyme that generates the mature 5'-termini of tRNA molecules. In Bacteria and Archaea the enzyme is a ribonucleoprotein, whereas in some Eukarya the RNAse P is exclusively proteinaceous. This work is focused on two topics: (i) crosslinking studies of bacterial RNase P holoenzyme utilizing novel 2'-ribooligonucleotides and (ii) functional investigations to the catalytical mechanism of recently discovered protein-only RNase P from *Arabidopsis thaliana.*

Crosslinking studies of RNase P holoenzyme

The composition of the bacterial RNAse P is relatively simple – one catalytic RNA subunit (P RNA; ~ 130 kDa) and a small single protein (P protein; ~ 13 kDa). Nevertheless, the first crystal structure of the holoenzyme complex was resolved only recently (Reiter et al., 2010). There exist several biochemical methods that are used to investigate RNA-protein and protein-protein interactions, among which crosslinking techniques occupy an important place. The introduction of a reactive group into a predetermined position of the RNA oligonucleotide strand allows the probing of contact points between different domains of ribonucleoprotein. Variations of the chemical nature of the active group enable selective cross-linking to different types of amino acids in RNA-protein complexes. The introduction of reactive groups into the sugar-phosphate backbone of RNA is the most promising approach, while modification of heterocyclic bases can disturb complementary interactions of RNA as well as base-specific contacts to the protein moiety within RNA-protein complexes. This project was conducted to establish chemical crosslinking technique for RNA-protein complexes utilizing RNA with 2'-aldehyde reactive group. In these studies the bacterial RNase P served as a relatively simple RNA - protein complex.

In our investigations, ribooligonucleotides bearing modified uridines with 2'-*cis*-diol functionalities were activated by periodate oxidation to 2'-aldehyde groups. The interaction of ε-amino group of lysine residue with 2'-aldehyde group in modified RNA leads to the formation of a Schiff base followed by reduction to secondary amine by sodium cyanoborohydride.

Single uridine positions in the P RNA sequence to be substituted by 2'-modified derivatives were selected according to the hybrid RNase P holoenzyme model (*Bacillus*

stearothermophilus P RNA and *Bacillus subtilis* P protein, the individual crystal structures of which are available; Buck et al., 2006).

Two techniques were compared for P RNA reconstitution bearing a single 2'-modification: ligation and annealing of *in vitro* transcribed P RNA fragment to chemically synthesized 2'-modified ribooligonucleotide.

To compare the enzymatic activity of P RNAs, single turnover kinetic experiments with ligated and annealed *B. stearothermophilus* P RNAs were peformed. RNase P bearing either ligated or annealed P RNA promoted 5'- processing of precursor tRNA (ptRNA) at near wild-type levels. Therefore, the holoenzyme activity is independent from the P RNA reconstitution approach and the introduction of a single modified residue into RNA derivative does not affect RNase P cleavage efficiency. Due to these reasons, for the cross-linking experiments P RNA was reconstituted by annealing, while this approach makes the identification of crosslinked amino acids easier in the subsequently planned MALDI-TOF analysis.

Crosslinking studies have shown that P RNA as well as a modified ribooligonucleotide alone were crosslinked to P protein with the same yield (approximate crosslinking efficiency: 9% with reconstituted P RNA, 6% with chemically synthezised oligoribonucleotid). Control experiments with randomly 2'-modified single stranded RNA- and double stranded DNA-oligonucleotides revealed between 10 and 15% crosslinking yield respectively.

In conclusion, the 2'-aldehyde approach resulted in multiple crosslinks to the RNase P protein regardless of the presence of the T7 RNA transcript contributing the major part of RNase P RNA. We attribute this to a high reactivity and limited specificity of internal 2'-aldehyde groups combined with the capability of the bacterial RNase P protein to bind to single-stranded RNA and DNA oligonucleotides at high concentrations. Nevertheless, 2'-aldehyde ribooligonucleotides could potentially be used for conjugation with low-molecular weight compounds, peptides and proteins for further target cell delivery of siRNAs (Jeong et al., 2009).

Functional characterisation of the novel protein-only RNase P from *Arabidopsis thaliana*

The land plant *Arabidopsis thaliana* encodes three single-polypetide PRORP (standing for "proteinaceous" RNase P) homologs. PRORP1 was identified in mitochondria and chloroplasts, while PRORP2 and 3 are found exclusively in the nucleus.

In the present studies, the catalytic efficiency of bacterial ptRNA^{Gly} substrate cleavage by *A. thaliana* PRORP1 was investigated. The single turnover V_{max} and K_m were determined as

4.3 min^{-1} and 1.4 µM, respectively, at under physiological Mg^{2+} and pH-conditions. The catalytic capacity of the enzyme appears to be within the lower normal range of RNase P enzymes with a catalytic RNA subunit activities characterized so far. We show that PRORP 1, PRORP2 and PRORP3 cleave the bacterial ptRNA at the canonical –1/+1 site.

In order to elucidate the catalytic mechanism of PRORP enzymes, a chemogenetic approach was applied. The divalent metal ion-dependent cleavage mechanism of bacterial RNase P RNA (P RNA) was investigated by phosphorothioate modifications at the scissile phosphodiester. Sulfur substitution of the non-bridging (*pro*-)*R*p oxygen reduced the rate constant for cleavage under single turnover conditions by three orders of magnitude, but activity could be rescued by ~ two orders of magnitude when Mg^{2+} was replaced with the thiophilic transition metal ion Cd^{2+}, indicating that a direct metal ion coordination occurs to the (*pro*-)*R*p substituent in the transition state (Warnecke et al., 1996, 1999). All three PRORP variants were tested, along with the *E. coli* RNase P holoenzyme, for cleavage of $ptRNA^{Gly}$ carrying an *R*p-phosphorothioate modification at all guanosine/inosine residues including the cleavage site.

Fundamentally different sensitivity of PRORP enzymes and bacterial ribonucleoprotein RNase P to an *R*p-phosphorothioate modification at the canonical cleavage site in a 5'-precursor tRNA substrate (ptRNA) was observed. Whereas processing by bacterial RNase P is inhibited by three orders of magnitude in the presence of this sulfur substitution and Mg^{2+} as the metal ion cofactor, the PRORP enzymes are affected by not more than a factor of 5 under the same conditions, without any evidence for increased miscleavage. The presence of Cd^{2+} is strongly deleterious for the PRORP enzymes. Conversely, significant processing of all- *R*p-$ptRNA^{Gly}$ by the *E.coli* RNase P was achieved in the presence of Cd^{2+}.

Consequently, *R*p-phosphorothioate modification at all G residues of the tRNA body had only minor effects on processing by PRORP. These findings indicate that the catalyic mechanism utilized by proteinaceous RNase P is different from that of RNA-based bacterial RNase P, taking place without a direct metal ion coordination to the (*pro*-)*R*p substituent. To conclude, productive PRORP-substrate interaction is not critically dependent on any of the affected *pro-R*p - oxygens or guanosine 2-amino groups.

6. Outlook

Our work opened the door for a variety of follow-up studies. First of all, chemical crosslinking experiments can be conducted due to big demand of such techniques applied for RNA-protein systems. Our collaborators (Prof.Tatjana Oretskaya, Lomonosov Moscow State University, Russia) have synthesized phosphoramidite nucleotide building blocks with 2'-iodoacetamido functions for crosslinking to cysteine residues. These analogs modified at the ribose moiety can be incorporated into RNA during chemical synthesis, as was done in previous studies. Bacterial RNase P proteins are basic and thus include numerous lysines. In a former study, several amino acid residues in the *E. coli* RNase P protein were replaced with cysteines without functional consequences. Such Cys variants of the protein will be used for crosslinking experiments involving the 2'-iodoacetamido modification.

Photoactivated cross-linking approach is the most established for RNA-protein interaction studies, though it often has the disadvantage of being non-specific. Besides, activation demands UV irradiation that leads to the destruction of biopolymers. Numerous UV-crosslinking studies have been conducted for RNase P RNA and P protein as well as for the holoenzyme - ptRNA complex. Here, we propose to study proteinaceous RNase P PRORP1, PRORP2 and PRORP3 and their substrate using this technique. So far, no individual crystal structure of PRORP has been resolved. UV-sensible 5-iodo-pyrimidine modified ptRNA could be cross-linked to one of the proteins. That can help to identify individual contacts between protein and substrate and build up the PRORP-ptRNA model, as well as to reveal the active site involved in protein-only RNase P cleavage.

PRORP2 and PRORP3 are localized exclusively in *A. thaliana* nucleus. Consequently, they may act cooperatively. Because most protein interactions are transient events, the crosslinking technique is an important approach to capture and stabilize them so that they can be analyzed. Heterobifunctional crosslinkers, usually photo-activated, could be used for studies of PRORP2 – PRORP3 interactions.

To explain the catalytic chemistry of proteinaceous RNase P enzymes, it is useful to compare it to other protein enzymes that catalyse phosphodiester bond hydrolysis, generating products with 3’-hydroxyl and 5’-phosphoryl groups and for which phophorothioate sensitivity is known. They belong to either Rp-specific class (ex. RNase lll, RNase H1, *Eco*RV) or Sp-specific class (ex. Zn^{2+} -dependent endonucleases) of enzymes. No comparison can be made between these nucleases and PRORP proteins, thus Sp-phosphorothioate sensitivity could be studied.

Structural and biochemical data suggest that the monomeric homing endonuclease PI – *Sce*I harbors two catalytical centers. UV-crosslinking studies revealed several aspartates involved in the active sites' architecture and served as ligands for Mg^{2+}, which can be replaced by Mn^{2+} *in vitro*. Mutation of these residues into alanines or asparagines resulted in loss of DNA cleavage in the presence of oxophilic Mg^{2+}, thus indicating that these amino acids are crucial for substrate cleavage. Mutants were more active in the presence of thiophilic Mn^{2+}, concluding that aspartates are principal ligands for Mg^{2+} (Schöttler *et al.,* 2000). PRORP enzymes were reported to have two aspartates conserved in the C-terminal domain and responsible for the endonucleolytic activity of the enzymes. Mutation of these residues into alanines resulted in loss of activity for PRORP1, PRORP2 and PRORP3 (Gobert *et al.,* 2010; Gutmann *et al.,* 2012). On the basis of the experiments of Schöttler *et al.*, mutated PRORP enzymes' activity could be tested in the presence of Mn^{2+} to study cofactor binding. Obtained information could be helpful in building a model of the catalytic center of the PRORP enzymes.

7. Zusammenfassung

Ribonuklease P (RNase P) ist ein ubiquitär vorkommendes Enzym, welches die maturen 5´-Enden von tRNA-Molekülen generiert. Während das Enzym in Bakterien und Archaeen ausschliesslich ein Ribonukleoprotein mit einer katalytischen RNA-Untereinheit ist, so existieren in einigen Eukaryoten auch Formen, die nur aus Protein(en) bestehen.
Im Fokus der vorliegenden Arbeit sind die beiden Themen: (i) *Crosslinking* (Quervernetzungs)-Studien an bakteriellem RNase P Holoenzym unter Verwendung neu entwickelter 2´-Oligoribonukleotide und (ii) funktionelle Untersuchungen zum Katalyse-Mechanismus der erst kürzlich entdeckten Protein-Enzyme der RNase P aus *Arabidopsis thaliana*.

***Crosslinking*-Studien an bakteriellem RNase P Holoenzym**

Die Zusammensetzung bakterieller RNase P ist relativ einfach. Sie besteht aus einer katalytischen RNA-Untereinheit (P RNA; ~130 kDa) und einer kleinen Proteinuntereinheit (P Protein; ~13 kDa). Trotz intensiver Bemühungen gelang die Aufklärung der Kristallstruktur des bakteriellen Holoenzym-Komplexes erst kürzlich (Reiter et al., 2010). Es existieren verschiedene biochemische Methoden zur Untersuchung von RNA-Protein- und Protein-Protein-Interaktionen, worunter *Crosslinking*-Techniken einen wichtigen Stellenwert einnehmen. Das Einführen einer reaktiven Gruppe in eine vorbestimmte Position des RNA-Oligonukleotidstrangs ermöglicht die Identifizierung von Kontaktstellen zwischen verschiedenen Struktur-Domänen in Ribonukleoproteinen. Durch Variation der chemischen Identität der aktiven Gruppe kann ein selektives Quervernetzen an bestimmte Aminosäureseitenketten in RNA-Protein-Komplexen erreicht werden. Die Einführung reaktiver Gruppen in das Zucker-Phosphat-Rückgrat des RNA-Strangs ist der vielversprechendste Ansatz, wohingegen die Modifizierung von heterozyklischen Basen sowohl komplementäre Interaktionen innerhalb der RNA als auch basenspezifische Wechselwirkungen mit Aminosäureseitenketten im RNA-Protein-Komplex stören kann. Das vorliegende Projekt hatte zum Ziel chemische *Crosslinking*-Techniken für RNA-Protein-Komplexe zu etablieren. Für die Studien wurde, stellvertretend für einen RNA-Protein-Komplex, bakterielles RNase P-Holoenzym als relativ einfaches Modellsystem ausgewählt. Bei der verwendeten RNA waren einzelne Ribosereste der Nukleotide mit reaktiven 2´-Aldehydgruppen modifiziert. Die Interaktion zwischen der aktivierten 2´-Aldehydgruppe der

modifizierten RNA mit einer ε-Aminogruppe einer Lysinseitenkette des Proteins führt zur Bildung eines Imins, welches in der Folge mittels Natriumcyanoborhydrid zu einem sekundären Amin reduziert werden kann. Zu Beginn der Arbeit war nur die Kristallstruktur einzelner Komponenten des RNase P Holoenzyms bekannt (P RNA von *Bacillus stearothermophilus*, P Protein von *Bacillus subtilis*), aus denen das Strukturmodell eines Hybrid-Komplexes erstellt wurde (Buck et al., 2006). Anhand dieses Modells wurden einzelne Uridinnukleotid-Positionen in der P RNA-Sequenz bestimmt, die sich in der Nähe bestimmter Aminosäureseitenketten der Proteinuntereinheit befinden und folglich durch 2´-modifizierte Derivate ersetzt werden sollten. Zur Herstellung einer P RNA mit einzelnen 2´-modifizierten Nukleotidderivaten wurden zwei Strategien gewählt und miteinander verglichen: Rekonstitution *in vitro*-transkribierter P RNA-Fragmente mit 5´- oder 3´- Deletion durch (i) Ligation und (ii) Hybridisierung (komplementäre Anlagerung) an chemisch synthetisierte Oligoribonukleotide mit singulärer 2´-Modifikation. Die enzymatische Aktivität von ligierter und hybridisierter P RNA-Variante von *B. stearothermophilus* wurde in *single-turnover* Kinetikexperimenten ([Substrat] >> [Enzym]) miteinander verglichen. Dabei stellte sich heraus, dass sowohl die ligierte als auch hybridisierte P RNA-Variante nahezu die gleiche Aktivität bei der 5´-Prozessierung von Vorläufer-tRNAs (prä-tRNAs) aufweist wie native *B. stearothermophilus* P RNA. Bei den entsprechenden Holoenzym-Komplexen mit *B. subtilis* P Protein konnte ebenfalls kein signifikanter Aktivitätsunterschied festgestellt werden. Folglich hat weder die Methode der Rekonstitution noch die Nukleotidmodifikation einen wesentlichen Einfluss auf die enzymatische RNase P-Aktivität. Anhand der erzielten Ergebnisse wurde für die *Crosslinking*-Experimente die Hybridisierungsmethode zur Rekonstitution der P RNA gewählt, da in diesem Fall die aufwendige Ligationsprozedur entfällt und die Identifizierung quervernetzter Aminosäuren bei der im Anschluss geplanten MALDI-TOF-Analyse vereinfacht ist. Im weiteren Verlauf der Studien hat sich allerdings herausgestellt, dass die *Crosslinking*-Reaktion teilweise unspezifisch ist. So wurde während der Reaktion neben rekonstituierter P RNA auch das synthetische Oligoribonukleotid allein in einem Kontrollansatz mit vergleichbarer Effizienz mit dem P Protein quervernetzt (Quervernetzungseffizienz: 9% mit rekonstituierter P RNA, 6 % mit synthetischem Oligoribonukleotid). Zusätzliche Kontrollexperimente mit randomisiert 2´-modifizierten Einzelstrang-RNA- und Doppelstrang-DNA-Oligonukleotiden ergab eine Quervernetzungseffizienz von 10% bzw. 15%.

Zusammenfassend wurde festgestellt, dass die hier analysierte *Crosslinking*-Reaktion zwischen 2´-Aldehyd-modifizierter P RNA und Aminosäureseitenketten des P Protein im

RNase P Holoenzym einen unspezifischen Charakter besitzt. Denkbar wäre allerdings eine Verwendung der 2´-Aldehyd-modifizierten Oligoribonukleotide im Zusammenhang mit dem zellspezifischem Einbringen von siRNAs. Hierbei könnten modifizierte siRNAs mit niedermolekularen Verbindungen, Peptiden und Proteinen konjugiert werden.

Funktionelle Untersuchungen zum Katalyse-Mechanismus der kürzlich entdeckten Protein-Enzyme der RNase P von *Arabidopsis thaliana*

Das Genom der Landpflanze *Arabidopsis thaliana* kodiert für drei verschiedene Varianten des aus einem monomeren Protein bestehenden RNase P-Enzyms PRORP (*proteinaceous* RNase P). Das Isoenzym PRORP1 wurde in Mitochondrien und Chloroplasten identifiziert, die Isoenzyme PRORP2 und PRORP3 ausschliesslich im Nukleus.
In der vorliegenden Studie wurde die katalytische Effizienz von *A. thaliana* PRORP1 anhand der 5´-Prozessierung bakterieller Glycin-prä-tRNA (prä-RNA^{Gly}) Substrate untersucht. Die kinetischen Konstanten von *single-turnover* ([Substrat] >> [Enzym]) Enzymreaktionen wurden unter physiologischen Mg^{2+}- und pH-Bedingungen ermittelt (v_{max} = 4,3 min^{-1} und K_m = 1,4 µM). Die katalytische Effizienz des Enzyms liegt demnach im normalen unteren Bereich von RNase P-Enzymen mit katalytischer RNA-Untereinheit. Zudem konnte gezeigt werden, dass alle drei Enzyme (PRORP1, PRORP2 und PRORP3) das bakterielle prä-tRNA^{Gly}-Substrat spezifisch an der kanonischen Position (–1/+1) endonukleolytisch spalten. Ungewöhnlich war das Ergebnis, dass PRORP2 bei 28°C eine katalytische Aktivität aufweist, bei 37°C hingegen katalytisch inaktiv ist. Von bakteriellen RNase P-Enzymen mit katalytischer RNA-Komponente war bekannt, dass eine *Rp*-Phosphorothioatmodifikation an der Spaltstelle im Substrat in Gegenwart von Mg^{2+}-Ionen zu einer Blockierung der endonukleolytischen Spaltung führt, die durch Zugabe thiophiler Metallionen wie Cd^{2+} oder Mn^{2+} aufgehoben werden kann (Warnecke et al., 1996, 1999). Die Ergebnisse legten eine direkte Koordination von Metallionen an den (*pro*-)*Rp*-Substituenten nahe. Zur Aufklärung des katalytischen Mechanismus wurde die Prozessierungseffizienz der PRORP-Enzyme in Gegenwart von prä-tRNA^{Gly}-Substraten mit *Rp*-Phosphorothioatmodifikationen an den Guanosinnukleotiden, einschliesslich an der kanonischen Spaltstelle (G_{+1}), untersucht. Parallel dazu wurde auch ein prä-tRNA^{Gly}-Substrat getestet, bei dem alle Guanosinnukleotide gegen *Rp*-Phosphorothioat-modifizierte Inosinnukleotide ausgetauscht waren. Die durchgeführten kinetischen Untersuchungen zeigten, dass die PRORP-Enzyme eine unterschiedliche Sensitivität gegenüber *Rp*-Phosphorothioatmodifikationen im Substrat

aufweisen, als das Ribonukleoprotein-Enzym aus *Escherichia coli*. In Gegenwart von Mg^{2+}-Ionen wurde die Prozessierungsaktivität der bakteriellen RNase P durch die Schwefelsubstitution um den Faktor ~2600 inhibiert, die von PRORP aus Arabidopsis hingegen nur um den Faktor ~5. Zudem wurden in Reaktionen mit *E. coli* RNase P durch die Phosphorothioatmodifikation an der Spaltstelle Fehlspaltungen verursacht, in Reaktionen mit den jeweiligen PRORP-Enzymen hingegen konnte keine erhöhte Frequenz an Fehlspaltung festgestellt werden. Ein deutlicher Unterschied zwischen den beiden RNase P-Enzymen aus *E. coli* und Arabidopsis war auch bei der katalytischen Aktivität in Gegenwart von Cd^{2+}-Ionen erkennbar. So waren alle drei PRORP-Enzyme unter diesen Bedingungen im Gegensatz zu bakterieller RNase P sowohl in Gegenwart von modifiziertem als auch unmodifiziertem Substrat vollständig inhibiert. Folglich kann aus den kinetischen Untersuchungen mit *Rp*-Phosphorothioatmodifizierten Substraten geschlossen werden, dass sich die Protein-katalysierte Reaktion von PRORP aus *Arabidopsis* und die RNA-katalysierte Reaktion von RNase P aus Bakterien mechanistisch unterscheiden. Auch erscheint eine direkte Koordinierung eines Metallions durch den (*pro*-)*Rp*-Substituenten an der Spaltstelle, wie sie im Falle der RNA-katalysierten Reaktion erfolgt, bei den PRORP-Enzymen unwahrscheinlich. Da *Rp*-Phosphorothioat- und Inosinmodifizierungen an allen 26 Guanosinnukleotiden im verwendeten tRNA-Substrat nur geringe Effekte auf die Prozessierung zeigten, kann daraus abgeleitet werden, dass die betroffenen (*pro*-)*Rp*-Sauerstoffatome oder Guanosin-2-Aminogruppen keine entscheidende Funktion bei der PRORP-Substrat-Interaktion ausüben.

8. Appendix

8.1 Chemicals

Acrylamide M-Bis (50% stock solution 24:1)	Gerbu
Agar Agar	Serva
Agarose	Roth
Ampicillin	Gerbu
Ammonium acetate	Fluka
Ammoniumperoxodisulfate	Roth
BioRad Reagent Dye Concentrate	BioRad
Boric acid	Roth
Bromophenol blue (BPB)	Merck
Cadmium acetate	Roth
Chloroform	Merck
Glucose monohydrate	Roth
Coomassie Blue	Roth
Crystal violet	Fluka
Deoxynucleosidtriphosphates (dNTPs)	Boehringer
Disodiumhydrogenphosphate	Merck
Dithiothreitol (DTT)	Gerbu
Ethanol p.a. 99.8 %	Roth
Ethidiumbromide	Roth
Fluoresceine-5-thiosemicarbazide	Fluka
Ethylendiamine tetraacetate (EDTA)	Gerbu
Glucose monohydrate	Roth
Glycerol	Gerbu
Glycine	Roth
Guanisine-5-monophosphate	Sigma
Glycogen	Roche
HEPES	Gerbu
Isopropanol	Acros
Kalium acetate	Roth
Imidazol	Roth
Isopropanol	Roth
Magnesium acetate	Roth
Magnesium chloride	Roth
Magnesium sulphate	Roth
Methanol	Roth
Manganese acetate	Roth
β-Mercaptoethanol	Serva
Propanol	Roth
Potassiumdihydrogenphosphate	Fluka
Propanol	Roth
RothSafe®	Roth
Sodiumacetate	Merck
Sodium borohydrate	Sigma

Sodium meta periodate	Roth
Sephadex G-25	Sigma
SYBRGold	Invitrogene
Nucleosidtriphosphates (NTPs)	Roche
Peptone	Roth
Phenol	Roth
Sodium chloride	Roth
Bovine serum albumin (BSA)	Sigma
Skim milk powder (blotting grade)	Roth
N,N,N‘,N‘-Tetraethylmethylenediamin (TEMED)	Serva
Tris-(hydroxymethyl)aminomethane	Gerbu
Tryptone	Roth
Xylenecyanol blue (XCB)	Serva
Urea	Gerbu
Yeast extract	Gerbu

All chemicals listed above have a purity grade “pro analysis”.

8.2 Radioisotopes

[γ-^{32}P] ATP	Hartmann Analytic
[5’-^{32}P] pCp	Hartmann Analytic

8.3 Size markers

1 kb DNA ladder	Thermo Scientific
10 bp DNA ladder	Thermo Scientific
2 Log DNA ladder	Thermo Scientific
100 bp DNA ladder GeneRuler Plus	Thermo Scientific
100-1000 bp low range RNA ladder	Thermo Scientific
Spectra Milticolor broad range protein ladder	Thermo Scientific
PageRuler™ Prestained protein ladder	Thermo Scientific

8.4 Enzymes and enzyme inhibitors

Alkaline Phosphatase	Thermo Scientific
Pfu-Polymerase	Prof.Hartmann lab, Philipps University Marburg
Pyrophosphatase	Roche
Proteinase inhibitor cocktail P8849	Sigma
RNase Inhibitor	Thermo Scientific
Restriction endonucleases	Thermo Scientific and New England Biolabs
Taq polymerase	Thermo Scientific and Prof.Hartmann lab
T4 DNA ligase 30 Weiss U/µl	Thermo Scientific
T4 Polynucleotide kinase	Thermo Scientific
T4 RNA ligase	New England Biolab

T4 RNA ligase 2	New England Biolab
T7 RNA polymerase	Thermo Scientific
T7 RNA polymerase (Y639F)	Prof.Hartmann lab, Philipps University Marburg

8.5 Antibodies

Primary antibodies

Anti-*B. subtilis* RnpA-Antiserum from rabbits (P.ab syra 6)	C. A. Fierke, University of California, U.S.A.
Anti-*E. coli* RnpA-Antiserum from rabbits	A. Vioque, University of Sevilla, Spain (Pascual and Vioque, 1996)

Secondary antibodies

Anti-Rabbit IgG made in goat (affinity purified), conjugated with alkaline phosphatase	Roche Diagnostics

8.6 Kits

Wizard® SV Gel and PCR Clen-Up System	Promega
GenJET® Plasmide Miniprep Kit	Thermo Scientific
Plasmide DNA Purification Nucleobond® PC500	Macherey-Nagel
Silver stain kit	Thermo Scientific
TranscriptAid® T7 High Yield Transcription Kit	Thermo Scientific

8.7 Equipment

Agarose gel chamber	Biorad, Mini Sub Cell
Autoclave	Systec V95
Blotting device	Schleicher & Schuell, SammyDry
Electroporator	Biorad, Gene Pulser Xcell, PC- and CE- module
FPLC	Amersham, ÄktaBasic
Gel documentation system	Cybertech, CS1 with Mitsubishi Video Copy Processor; Biostep, GelSystem MINI
Gel dryer	Biorad, Model 483 SLAB Dryer
Hand-monitor	Berthold, LB 1210 B
Heating blocks	Techne, Dri-Block DB-3D; Biometra, TB1
Incubator	Memmert BE400
Imager cassettes	Fuji Film, Bas cassette 4043, Rego, 35,6x43,2cm
Magnetic stirrers	Heidolph, MR 2002
Power supply	Pharmacia, EPS 3500; Bio Rad, Power Supply160/1.6 (Power Pac 3000); Apelex, PS 9009T
PAA-gel chamber	Custom-made, University of Lübeck
PCR cycler	Biometra, TGradient Thermocycler
pH-Meter	WTW, pH Level 1
Phosphoimager	Raytest, Bio-Imaging Analyser BAS 1000 (Fujifilm); FLA 3000, (Fujifilm)

Pipettes	Gilson-Pipetman, P20, P200, P1000 Abimed 0.1-2µl
Protein Gel chamber	Mini Protean 3 cell, Biorad
Quartz cuvette	Hellma 104-QS, 105.202, 115B-QS, 105
Mixer	IKA, Vibrax-VXR; Eppendorf, Thermomixer 5436, Thermomixer comfort
Shaking incubator	GFL 3033
Spectrophotometer	Hewlett Packard, Photometer 8453; Varian, Cary 50 Conc; Thermo Spectronic, Biomate 3
Software	PCBas/Aida Image Analyser v.3.45, Corel Graphics Suite; GraFit 3.0; Microsoft Office; Pymol, Delano, W.L. 2002 Vector NTI®, Invitrogen
Speedvac	Heto vacuum centrifuge
Scintillation counters	Perkin Elmer, Wallac WINSPECTRAL a/b 1414 Liquid Scintillation Counter; Packard, Tricarb 2000CA
Centrifuges	Heraeus, Biofuge pico, Heraeus Biofuge fresco; Sigma, Typ 112; Eppendorf, centrifuge 5810R, minispin plus Stratagene, PicoFuge
Vacuum dryer	Biorad Slab dryer model 483

8.8 Synthetic DNA oligonucleotides

DNA oligonucleotides were ordered from Metabion International AG. The sequence of DNA oligonucleotides is given in the 5' to 3' direction. Nucleotides in **bold** letters indicate T7 promoter sequence. Underlined sequences indicate either restriction enzyme recognition sites; *rnpB* sequence is marked by *italic* letters; HDV sequence is indicated by *underlined italic* letters.

N	Name	Used for	5'→ 3' sequence
1	DNA_20-24	DNA splint Bstea-*rnpB*[Δ1-26]	GACTTTCCTCTACGGCCGAAACCGGC CGCAGCGATTACCCGAGCATGATTAAC
2	DNA_35	DNA splint Bstea-*rnpB*[Δ1-36]	CAGCACCGTGCGAGCATGGACTTTCCT CTACGGCCGAAACCGGCCGCAGCGAT TACCCGAGCATGATTAAC
3	DNA_270	DNA splint Bstea-*rnpB*[Δ1-287]	CGCCGCCTGTCCTTCCCTCCGTTCATT TCCTTCGGGAAGGTGCCCCTACCATCAT

		and Bstea-*rnpB*[Δ267-414]	TTGGGTTTCTCGCTCGTGGGGTTTAC
4	DNA_3XX	DNA splint Bstea-*rnpB*[Δ331-414]	TGTACCTTCGTACTGCAAGCGGCTTTGCGCCT CGTACTCCGGCGGTAATCATCTATCTACAGGC TGCATGCGCCGCCTGTC
5	DNA_20-24	truncated DNA splint Bstea-*rnpB*[Δ1-26]	CCT TCG TAC TGC AAG CGG CTT TGC GCC TCG TAG
6	1-ML	5'-primer for *rnpB* (construct Bstea-*rnpB*[Δ1-26])	GAA AGC T**TA ATA CGA CTC ACT ATA** GGC CGG TTT CGG CCG TAG AGG
7	2-ML	5'-primer for *rnpB* (Bstea-*rnpB*[Δ1-36])	GAA AGC T**TA ATA CGA CTC ACT ATA** GGC CGT AGA GGA AAG TCC ATG
8	3-ML	3'-primer for *rnpB* (construct Bstea-*rnpB*[Δ1-26], Bstea-*rnpB*[Δ1-36], Bstea-*rnpB*[Δ1-287])	GAG GAT CCG TTA ATC ATGG CTC TAT AAG CCA TGT TCT GTA CC
9	4-ML	5'-primer for *rnpB* (Bstea-*rnpB*[Δ267-414], Bstea-*rnpB*[Δ331-414])	GTGG AAT TCG **TAA TAC GAC TCA CTA TA**G GTT AAT CAT GAT CGG GTA ATC G
10	5-ML	3'-primer for *rnpB* (construct Bstea-*rnpB*[Δ267-414])	*TGG AGA TGC CAT GCC GAC CC***T CAT TTG GGT TTC TCG CTC GTG GGG TTT AC**
11	6-ML	5'-primer for *rnpB* (construct	GAA AGC T**TA ATA CGA CTC ACT ATA** GGA AAT GAA CGG AGG GAA GGA CAG G

		Bstea-*rnpB*[Δ1-287])	
12	7-ML	3'-primer for *rnpB* (construct Bstea-*rnpB*[Δ331-414])	*TGG AGA TGC CAT GCC GAC CC***T ACA GGC TGC ATG CGC CGC CTG TCC TTC C**
13	8-ML	5'-primer for HDV (construct Bstea-*rnpB*[Δ267-414])	*CGA GCG AGA AAC CCA AAT GA***G GGT CGG CAT GGC ATC TCC ACC TCC TCG**
14	9-ML	3'-primer for HDV (construct Bstea-*rnpB*[Δ267-414], Bstea-*rnpB*[Δ331-414])	**GAG GAT CCT TCT CCC TTA GCC TAC CGA AGT AGC CCA GGT C**
15	10-ML	5'-primer for HDV (construct Bstea-*rnpB*[Δ331-414])	*CAG GCG GCG CAT GCA GCC TGT A***GG GTC GGC ATG GCA TCT CC ACCT CCT CG**

8.9 Synthetic RNA oligonucleotides

RNA oligonucleotides bearing 2'- modified uridines U^{dap} (marked as ***U***) were synthesized by Dr. Elena Khomykova in the lab of Prof.Dr. Sabine Müller (Ersnt Moritz Arndt University Greifswald) as described (Khomykova et al., 2012). The sequence is given in the 5' to 3' direction. Modified nucleotides are marked in bold italic.

No	Name	Used for	5'→ 3' sequence
1	Oligo U 20 / (**XIV**)	Ligation to T7 transcript Bstea-*rnpB*[Δ1-26]	GUU AAU CAU GCU CGG GUA A***U***C GCU GC
2	Oligo U 24 / (**XV**)	Ligation to T7 transcript Bstea-*rnpB*[Δ1-26]	GUU AAU CAU GCU CGG GUA AUC GC***U*** GC
3	Oligo U 35	Ligation to T7 transcript	GUU AAU CAU GCU CGG GUA AUC GCU GCG GCC

		Bstea-*rnpB*[Δ1-36]	GGU U***U***C
4	Oligo U 270	Ligation to T7 transcript Bstea-*rnpB*[Δ267-414] and Bstea-*rnpB*[Δ1-287]	UGG UAG GGG CAC CUU CCC GAA
5	Oligo U 333	Ligation to T7 transcript Bstea-*rnpB*[Δ331-414]	GA***U*** AGA UGA UUA CCG CCG GAG UAC GAG GCG CA
6	Oligo U 337	Ligation to T7 transcript Bstea-*rnpB*[Δ331-414]	GAU AGA ***U***GA UUA CCG CCG GAG UAC GAG GCG CA
7	Oligo U 340	Ligation to T7 transcript Bstea-*rnpB*[Δ331-414]	GAU AGA UGA ***U***UA CCG CCG GAG UAC GAG GCG CA
8	Oligo U 341	Ligation to T7 transcript Bstea-*rnpB*[Δ331-414]	GAU AGA UGA U***U***A CCG CCG GAG UAC GAG GCG CA
9	Oligo 3XX-3'-end unmodified	Ligation to T7 transcript Bstea-*rnpB*[Δ331-414]	AAG CCG CUU GCA GUA CGA AGG UAC AGA ACA UGG CUU AUA GAG CAU GAU UAA C
10	Oligo 20-24 unmodified	Ligation to T7 transcript Bstea-*rnpB*[Δ1-26]	GUU AAU CAU GCU CGG GUA AUC GCU GC
11	Oligo 3XX unmodified	Ligation to T7 transcript Bstea-*rnpB*[Δ331-414]	GAU AGA UGA UUA CCG CCG GAG UAC GAG GCG CA
12	Oligo U 6 / (**XVI**)	Ligation to T7 transcript Bstea-*rnpB*[Δ1-26]	GUU AA***U*** CAU GCU CGG GUA AUC GCU GC

8. 10 Bacterial strains

Strain	Relevant Genotype	Reference
E. coli DH5α	*supE*44 delta*lacU*169 (phi80 *lacZ* deltaM15) *hsdR*17 *recA*1 *endA*1 *gyrA*96 *thi*-1 *relA*1	Sambrook *et al.*, 1989
BL21(DE3)	*fhuA2 [lon] ompT gal (λ DE3) [dcm] ΔhsdS λ DE3 = λ sBamHIo ΔEcoRI-B int::(lacI::PlacUV5::T7 gene1) i21 Δnin5*	New England Biolabs

8.11 Plasmide vectors

Vector	Relevant Genotype	Reference
pSP64	ori pMB1 Amp^r	Promega
pET28b(+)	f1pBR322 P_{T7} MCSHisTaglacI Kan^r	Novagen
pUC19-Aae-6S-HDV	ori pMB1 Amp^r lacZlacIHDV virus	Willkomm D., Hartmann lab

PUC19	ori pMB1 Amp^r lacZlacI	Yanisch-Peron *et al*., 1985

8.12 Plasmide vectors for T7 transcription

Vector	Genotype	Reference	Linearised with
pSBpt3'HH	$ptRNA^{Gly}$ from *Thermus thermophilus* with 14mer flank	Busch *et al.*, 2000	*Bam* HI

8.13 Abbreviations and Units

A_{260}	absorption at 260 nm
A	Adenosine
aa	amino acid(s)
ad	adjust
Amp	Ampicillin
AP	Alkaline Phosphatase
APS	Ammonium peroxodisulfat
bp	base pair(s)
BPB	Bromophenol blue
ca.	capproximataly
BSA	Bovine serum albumine
Bq	Becquerel
°C	centigrade
C	cytosine
C5	protein subunit of E. coli RNase P
c_{End}	end concentration
c_{Stock}	stock concentration
Ci	Curie
CIAP	calf intestinal alkaline phosphatase
cm	centimetre
cpm	counts per minute
Da	dalton
DNA	deoxyribonucleic acid
DNase	deoxyribonuclease
dNTP	deoxynucleoside triphosphates
DTT	dithiothreitol
E	extinction
ε	molar extinction coefficient
EDTA	Ethylenediamine tetraacedic acid
e.g.	example gratia (for example)
et al.	et alii (and others)
Fig.	Figure
g	Gram
g	acceleration of gravity
G	guanosine

h	hour(s)
HEPES	N-2-Hydroxyethylpiperazin-N'-2-ethane sulfonic acid
His	histidine
IPTG	Isopropyl-β-D-thiogalactopyranosid
kan	Kanamycin
kb	kilo bases
kDa	kilodalton
l	Liter
LB	Luria-Bertani
µg	microgram
µl	microliter
µM	micromolar
M	molar [mol/l]
mA	milliampere
MBq	Megabecquerel
mg	Milligram
min(s)	Minute
ml	Milliliter
mmol	Millimole
mM	Millimilar
mRNA	messenger RNA
MW	Molecular weight
N	any nucleotide
NAP	
NBT	p-Nitroblue-tetrazolium chloride
ng	Nanogram
Ni-NTA	nickel-nitrilotriacetic acid
nm	Nanometer
nM	Nanomolar
nt(s)	Nucleotide(s)
NTP	Ribonucleosidtriphosphate
OD_{600}	optical density at 600 nm
p.a.	pro analysis
PAA	Polyacrylamide
PAGE	Polyacrylamid gel elektrophoresis
PCR	Polymerase chain reaction
pmol	Picomol
PMSF	phenylmethylsulfonyl fluoride
P Protein	Protein subunit of RNase P
P RNA	RNA subunit of RNase P
RNA	ribonucleic acid
RNase	ribonuclease
rpm	rounds per minute
SAP	shrimp alkaline phosphatese
SOC	super optimal broth
SDS	natriumdodecylsulfat
s/sec	second(-s)

T	Thymine
TB	Terrific Broth
TBE	Tris-Borat-EDTA Buffer
Tm	melting temperature
Tris	Tris-hydroxymethylaminomethan
(p)tRNA	(precursor) transfer RNA
U	Unit(s) (unit for enzyme activity)
U	Uridine
v/v	volume per volume
w/v	weight per volume
wt	wild-type
XCB	Xylene cyanol blue

8.14 List of figures

8.15 List of tables

8.16 Index of buffers and solutions

Bibliography

Alifano, P.; Rivellini, F.; Piscitelli, C.; Arraiano, C. M.; Bruni, C. B.; Carlomagno, M. S., Ribonuclease E provides substrates for ribonuclease P-dependent processing of a polycistronic mRNA. *Genes Dev* **1994,** *8* (24), 3021-31.

Altman, S.; Robertson, H. D., RNA precursor molecules and ribonucleases in E. coli. *Mol Cell Biochem* **1973,** *1* (1), 83-93.

Altman, S.; Wesolowski, D.; Guerrier-Takada, C.; Li, Y., RNase P cleaves transient structures in some riboswitches. *Proc Natl Acad Sci U S A* **2005,** *102* (32), 11284-9.

Anantharaman, V.; Aravind, L., The NYN domains: novel predicted RNAses with a PIN domain-like fold. *RNA Biol* **2006,** *3* (1), 18-27.

Auletta, G., Colage, I., Cook, G., D'Ambrosio, P., Ramon, M.,. Functional equivalence between plant PRORP1 and bacterial RNase P Ribonucleic acid (RNA) raises questions on control and recognition mechanisms. *Journal of Computational Biology and Bioinformatics Research* **2011,** 3 (5), 63-64

Baum, M.; Cordier, A.; Schön, A., RNase P from a photosynthetic organelle contains an RNA homologous to the cyanobacterial counterpart. *J Mol Biol* **1996,** *257* (1), 43-52.

Birnboim, H. C., A rapid alkaline extraction method for the isolation of plasmid DNA. *Methods Enzymol* **1983,** *100*, 243-55.

Bothwell, A. L.; Stark, B. C.; Altman, S., Ribonuclease P substrate specificity: cleavage of a bacteriophage phi80-induced RNA. *Proc Natl Acad Sci U S A* **1976,** *73* (6), 1912-6.

Bradford, M. M., A rapid and sensitive method for the quantitation of microgram quantities of protein utilizing the principle of protein-dye binding. *Anal Biochem* **1976,** *72*, 248-54.

Buck, A. H.; Kazantsev, A. V.; Dalby, A. B.; Pace, N. R., Structural perspective on the activation of RNAse P RNA by protein. *Nat Struct Mol Biol* **2005,** *12* (11), 958-64.

Busch, S.; Kirsebom, L. A.; Notbohm, H.; Hartmann, R. K., Differential role of the intermolecular base-pairs G292-C(75) and G293-C(74) in the reaction catalyzed by Escherichia coli RNase P RNA. *J Mol Biol* **2000,** *299* (4), 941-51.

Cho, I. M.; Lai, L. B.; Susanti, D.; Mukhopadhyay, B.; Gopalan, V., Ribosomal protein L7Ae is a subunit of archaeal RNase P. *Proc Natl Acad Sci U S A* **2010,** *107* (33), 14573-8.

Christ, F.; Schoettler, S.; Wende, W.; Steuer, S.; Pingoud, A.; Pingoud, V., The monomeric homing endonuclease PI-SceI has two catalytic centres for cleavage of the two strands of its DNA substrate. *EMBO J* **1999,** *18* (24), 6908-16.

Collins, L. J.; Moulton, V.; Penny, D., Use of RNA secondary structure for studying the evolution of RNase P and RNase MRP. *J Mol Evol* **2000,** *51* (3), 194-204.

Cordier, A.; Schön, A., Cyanelle RNase P: RNA structure analysis and holoenzyme properties

of an organellar ribonucleoprotein enzyme. *J Mol Biol* **1999,** *289* (1), 9-20.

DeLano, W.L. The PyMOL Molecular Graphics System (2002) on World Wide Web. http://www.pymol.org

Dinos, G.; Wilson, D. N.; Teraoka, Y.; Szaflarski, W.; Fucini, P.; Kalpaxis, D.; Nierhaus, K. H., Dissecting the ribosomal inhibition mechanisms of edeine and pactamycin: the universally conserved residues G693 and C795 regulate P-site RNA binding. *Mol Cell* **2004,** *13* (1), 113-24.

Dunn, M. J.; Bradd, S. J., Separation and analysis of membrane proteins by SDS-polyacrylamide gel electrophoresis. *Methods Mol Biol* **1993,** *19*, 203-10.

England, T. E.; Uhlenbeck, O. C., Enzymatic oligoribonucleotide synthesis with T4 RNA ligase. *Biochemistry* **1978,** *17* (11), 2069-76.

Frederiksen, J. K.; Piccirilli, J. A., Identification of catalytic metal ion ligands in ribozymes. *Methods* **2009,** *49* (2), 148-66.

Freier, S. M.; Altmann, K. H., The ups and downs of nucleic acid duplex stability: structure-stability studies on chemically-modified DNA:RNA duplexes. *Nucleic Acids Res* **1997,** *25* (22), 4429-43.

Gegenheimer, P., Enzyme nomenclature: functional or structural? *RNA* **2000,** *6* (12), 1695-7.

Gobert, A.; Gutmann, B.; Taschner, A.; Gössringer, M.; Holzmann, J.; Hartmann, R. K.; Rossmanith, W.; Giegé, P., A single Arabidopsis organellar protein has RNase P activity. *Nat Struct Mol Biol* **2010,** *17* (6), 740-4.

Griffiths, A. D.; Potter, B. V.; Eperon, I. C., Stereospecificity of nucleases towards phosphorothioate-substituted RNA: stereochemistry of transcription by T7 RNA polymerase. *Nucleic Acids Res* **1987,** *15* (10), 4145-62.

Guerrier-Takada, C.; Altman, S., M1 RNA with large terminal deletions retains its catalytic activity. *Cell* **1986,** *45* (2), 177-83.

Guerrier-Takada, C.; Gardiner, K.; Marsh, T.; Pace, N.; Altman, S., The RNA moiety of ribonuclease P is the catalytic subunit of the enzyme. *Cell* **1983,** *35* (3 Pt 2), 849-57.

Gutmann, B.; Gobert, A.; Giegé, P., PRORP proteins support RNase P activity in both organelles and the nucleus in Arabidopsis. *Genes Dev* **2012**.

Gyi, J. I.; Conn, G. L.; Lane, A. N.; Brown, T., Comparison of the thermodynamic stabilities and solution conformations of DNA.RNA hybrids containing purine-rich and pyrimidine-rich strands with DNA and RNA duplexes. *Biochemistry* **1996,** *35* (38), 12538-48.

Handbook of RNA Biochemistry. 2nd Edition (eds.R.K.Harmann, A.Bindereif, A.Schön, E.Westhof), WILLY-VCH, Weinheim, Germany. Year of publication: 2012

Hardt, W. D.; Warnecke, J. M.; Erdmann, V. A.; Hartmann, R. K., Rp-phosphorothioate modifications in RNase P RNA that interfere with tRNA binding. *EMBO J* **1995,** *14* (12),

2935-44.

Harris, M. E.; Kazantsev, A. V.; Chen, J. L.; Pace, N. R., Analysis of the tertiary structure of the ribonuclease P ribozyme-substrate complex by site-specific photoaffinity crosslinking. *RNA* **1997,** *3* (6), 561-76.

Hartmann, E.; Hartmann, R. K., The enigma of ribonuclease P evolution. *Trends Genet* **2003,** *19* (10), 561-9.

Hartmann, R. K.; Gössringer, M.; Späth, B.; Fischer, S.; Marchfelder, A., The making of tRNAs and more - RNase P and tRNase Z. *Prog Mol Biol Transl Sci* **2009,** *85*, 319-68.

Hartmann, R. K.; Heinrich, J.; Schlegl, J.; Schuster, H., Precursor of C4 antisense RNA of bacteriophages P1 and P7 is a substrate for RNase P of Escherichia coli. *Proc Natl Acad Sci U S A* **1995,** *92* (13), 5822-6.

Herschlag, D.; Piccirilli, J. A.; Cech, T. R., Ribozyme-catalyzed and nonenzymatic reactions of phosphate diesters: rate effects upon substitution of sulfur for a nonbridging phosphoryl oxygen atom. *Biochemistry* **1991,** *30* (20), 4844-54.

Hsieh, J.; Koutmou, K. S.; Rueda, D.; Koutmos, M.; Walter, N. G.; Fierke, C. A., A divalent cation stabilizes the active conformation of the B. subtilis RNase P x pre-tRNA complex: a role for an inner-sphere metal ion in RNase P. *J Mol Biol* **2010,** *400* (1), 38-51.

Jackman, J. E.; Montange, R. K.; Malik, H. S.; Phizicky, E. M., Identification of the yeast gene encoding the tRNA m1G methyltransferase responsible for modification at position 9. *RNA* **2003,** *9* (5), 574-85.

Jeong, J. H.; Mok, H.; Oh, Y. K.; Park, T. G., siRNA conjugate delivery systems. *Bioconjug Chem* **2009,** *20* (1), 5-14.

Kachalova, A. V.; Zatsepin, T. S.; Romanova, E. A.; Stetsenko, D. A.; Gait, M. J.; Oretskaya, T. S., Synthesis of modified nucleotide building blocks containing electrophilic groups in the 2'-position. *Nucleosides Nucleotides Nucleic Acids* **2000,** *19* (10-12), 1693-707.

Kazantsev, A. V.; Pace, N. R., Identification by modification-interference of purine N-7 and ribose 2'-OH groups critical for catalysis by bacterial ribonuclease P. *RNA* **1998,** *4* (8), 937-47.

Kazantsev, A. V.; Krivenko, A. A.; Harrington, D. J.; Carter, R. J.; Holbrook, S. R.; Adams, P. D.; Pace, N. R., High-resolution structure of RNase P protein from Thermotoga maritima. *Proc Natl Acad Sci U S A* **2003,** *100* (13), 7497-502.

Kazantsev, A. V.; Krivenko, A. A.; Harrington, D. J.; Holbrook, S. R.; Adams, P. D.; Pace, N. R., Crystal structure of a bacterial ribonuclease P RNA. *Proc Natl Acad Sci U S A* **2005,** *102* (38), 13392-7.

Kazantsev, A. V.; Pace, N. R., Bacterial RNase P: a new view of an ancient enzyme. *Nat Rev Microbiol* **2006,** *4* (10), 729-40.

Kilani, A. F.; Liu, F., UV cross-link mapping of the substrate-binding site of an RNase P

ribozyme to a target mRNA sequence. *RNA* **1999,** *5* (9), 1235-47.

Komine, Y.; Kitabatake, M.; Yokogawa, T.; Nishikawa, K.; Inokuchi, H., A tRNA-like structure is present in 10Sa RNA, a small stable RNA from Escherichia coli. *Proc Natl Acad Sci U S A* **1994,** *91* (20), 9223-7.

Kurz, J. C.; Niranjanakumari, S.; Fierke, C. A., Protein component of Bacillus subtilis RNase P specifically enhances the affinity for precursor-tRNAAsp. *Biochemistry* **1998,** *37* (8), 2393-400.

Laemmli, U. K., Cleavage of structural proteins during the assembly of the head of bacteriophage T4. *Nature* **1970,** *227* (5259), 680-5.

Lai, L. B.; Bernal-Bayard, P.; Mohannath, G.; Lai, S. M.; Gopalan, V.; Vioque, A., A functional RNase P protein subunit of bacterial origin in some eukaryotes. *Mol Genet Genomics* **2011**.

Li, Y.; Altman, S., A specific endoribonuclease, RNase P, affects gene expression of polycistronic operon mRNAs. *Proc Natl Acad Sci U S A* **2003,** *100* (23), 13213-8.

Lurin, C.; Andrés, C.; Aubourg, S.; Bellaoui, M.; Bitton, F.; Bruyère, C.; Caboche, M.; Debast, C.; Gualberto, J.; Hoffmann, B.; Lecharny, A.; Le Ret, M.; Martin-Magniette, M. L.; Mireau, H.; Peeters, N.; Renou, J. P.; Szurek, B.; Taconnat, L.; Small, I., Genome-wide analysis of Arabidopsis pentatricopeptide repeat proteins reveals their essential role in organelle biogenesis. *Plant Cell* **2004,** *16* (8), 2089-103.

Mans, R. M.; Guerrier-Takada, C.; Altman, S.; Pleij, C. W., Interaction of RNase P from Escherichia coli with pseudoknotted structures in viral RNAs. *Nucleic Acids Res* **1990,** *18* (12), 3479-87.

Massire, C.; Jaeger, L.; Westhof, E., Derivation of the three-dimensional architecture of bacterial ribonuclease P RNAs from comparative sequence analysis. *J Mol Biol* **1998,** *279* (4), 773-93.

Moore, M. J.; Sharp, P. A., Site-specific modification of pre-mRNA: the 2'-hydroxyl groups at the splice sites. *Science* **1992,** *256* (5059), 992-7.

Morse, D. P.; Schmidt, F. J., Sequences encoding the protein and RNA components of ribonuclease P from Streptomyces bikiniensis var. zorbonensis. *Gene* **1992,** *117* (1), 61-6.

Niranjanakumari, S.; Day-Storms, J. J.; Ahmed, M.; Hsieh, J.; Zahler, N. H.; Venters, R. A.; Fierke, C. A., Probing the architecture of the B. subtilis RNase P holoenzyme active site by cross-linking and affinity cleavage. *RNA* **2007,** *13* (4), 521-35.

Niranjanakumari, S.; Lasda, E.; Brazas, R.; Garcia-Blanco, M. A., Reversible cross-linking combined with immunoprecipitation to study RNA-protein interactions in vivo. *Methods* **2002,** *26* (2), 182-90.

Niranjanakumari, S.; Stams, T.; Crary, S. M.; Christianson, D. W.; Fierke, C. A., Protein component of the ribozyme ribonuclease P alters substrate recognition by directly contacting

precursor tRNA. *Proc Natl Acad Sci U S A* **1998,** *95* (26), 15212-7.

Nowotny, M.; Yang, W., Stepwise analyses of metal ions in RNase H catalysis from substrate destabilization to product release. *EMBO J* **2006,** *25* (9), 1924-33.

Pace, C. N.; Vajdos, F.; Fee, L.; Grimsley, G.; Gray, T., How to measure and predict the molar absorption coefficient of a protein. *Protein Sci* **1995,** *4* (11), 2411-23.

Pannucci, J. A.; Haas, E. S.; Hall, T. A.; Harris, J. K.; Brown, J. W., RNase P RNAs from some Archaea are catalytically active. *Proc Natl Acad Sci U S A* **1999,** *96* (14), 7803-8.

Pascual, A.; Vioque, A., Cloning, purification and characterization of the protein subunit of ribonuclease P from the cyanobacterium Synechocystis sp. PCC 6803. *Eur J Biochem* **1996,** *241* (1), 17-24.

Peracchi, A.; Beigelman, L.; Scott, E. C.; Uhlenbeck, O. C.; Herschlag, D., Involvement of a specific metal ion in the transition of the hammerhead ribozyme to its catalytic conformation. *J Biol Chem* **1997,** *272* (43), 26822-6.

Persson, T.; Cuzic, S.; Hartmann, R. K., Catalysis by RNase P RNA: unique features and unprecedented active site plasticity. *J Biol Chem* **2003,** *278* (44), 43394-401.

Pfander, S.; Fiammengo, R.; Kirin, S. I.; Metzler-Nolte, N.; Jäschke, A., Reversible site-specific tagging of enzymatically synthesized RNAs using aldehyde-hydrazine chemistry and protease-cleavable linkers. *Nucleic Acids Res* **2007,** *35* (4), e25.

Pfeiffer, T.; Tekos, A.; Warnecke, J. M.; Drainas, D.; Engelke, D. R.; Séraphin, B.; Hartmann, R. K., Effects of phosphorothioate modifications on precursor tRNA processing by eukaryotic RNase P enzymes. *J Mol Biol* **2000,** *298* (4), 559-65.

Placido, A.; Sieber, F.; Gobert, A.; Gallerani, R.; Giege, P.; Marechal-Drouard, L., Plant mitochondria use two pathways for the biogenesis of tRNAHis. *Nucleic Acids Res* **2010,** *38* (21), 7711-7.

Randau, L.; Schröder, I.; Söll, D., Life without RNase P. *Nature* **2008,** *453* (7191), 120-3.

Reiner, H.; Plankensteiner, K.; Fitz, D.; Rode, B. M., The possible influence of L-histidine on the origin of the first peptides on the primordial Earth. *Chem Biodivers* **2006,** *3* (6), 611-21.

Reiner, R.; Ben-Asouli, Y.; Krilovetzky, I.; Jarrous, N., A role for the catalytic ribonucleoprotein RNase P in RNA polymerase III transcription. *Genes Dev* **2006,** *20* (12), 1621-35.

Reiter, N. J.; Osterman, A.; Torres-Larios, A.; Swinger, K. K.; Pan, T.; Mondragón, A., Structure of a bacterial ribonuclease P holoenzyme in complex with tRNA. *Nature* **2010,** *468* (7325), 784-9.

Rinke, J.; Meinke, M.; Brimacombe, R.; Fink, G.; Rommel, W.; Fasold, H., The use of azidoarylimidoesters in RNA-protein cross-linking studies with Escherichia coli ribosomes. *J Mol Biol* **1980,** *137* (3), 301-4.

Rivera-León, R.; Green, C. J.; Vold, B. S., High-level expression of soluble recombinant RNase P protein from Escherichia coli. *J Bacteriol* **1995,** *177* (9), 2564-6.

Robertson, H. D.; Altman, S.; Smith, J. D., Purification and properties of a specific Escherichia coli ribonuclease which cleaves a tyrosine transfer ribonucleic acid presursor. *J Biol Chem* **1972,** *247* (16), 5243-51.

Romanenkov, A. S.; Ustyugov, A. A.; Zatsepin, T. S.; Nikulova, A. A.; Kolesnikov, I. V.; Metelev, V. G.; Oretskaya, T. S.; Kubareva, E. A., Analysis of DNA-protein interactions in complexes of transcription factor NF-kappaB with DNA. *Biochemistry (Mosc)* **2005,** *70* (11), 1212-22.

Rossmanith, W., Of P and Z: Mitochondrial tRNA processing enzymes. *Biochim Biophys Acta* **2011**.

Rossmanith, W.; Karwan, R. M., Characterization of human mitochondrial RNase P: novel aspects in tRNA processing. *Biochem Biophys Res Commun* **1998,** *247* (2), 234-41.

Rossmanith, W.; Tullo, A.; Potuschak, T.; Karwan, R.; Sbisà, E., Human mitochondrial tRNA processing. *J Biol Chem* **1995,** *270* (21), 12885-91.

Salavati, R.; Panigrahi, A. K.; Stuart, K. D., Mitochondrial ribonuclease P activity of Trypanosoma brucei. *Mol Biochem Parasitol* **2001,** *115* (1), 109-17.

Sambrook, J., Fritsch, E.F. and Maniatis, T.E. 1989. Molecular cloning. A laboratory manual. Cold spring Harbor Laboratory, Cold Spring Harbor, N.Y.

Schägger, H.; von Jagow, G., Tricine-sodium dodecyl sulfate-polyacrylamide gel electrophoresis for the separation of proteins in the range from 1 to 100 kDa. *Anal Biochem* **1987,** *166* (2), 368-79.

Schön, A., Ribonuclease P: the diversity of a ubiquitous RNA processing enzyme. *FEMS Microbiol Rev* **1999,** *23* (3), 391-406.

Schöttler, S.; Wende, W.; Pingoud, V.; Pingoud, A., Identification of Asp218 and Asp326 as the principal Mg2+ binding ligands of the homing endonuclease PI-SceI. *Biochemistry* **2000,** *39* (51), 15895-900.

Smith, D.; Burgin, A. B.; Haas, E. S.; Pace, N. R., Influence of metal ions on the ribonuclease P reaction. Distinguishing substrate binding from catalysis. *J Biol Chem* **1992,** *267* (4), 2429-36.

Smith, D.; Pace, N. R., Multiple magnesium ions in the ribonuclease P reaction mechanism. *Biochemistry* **1993,** *32* (20), 5273-81.

Spitzfaden, C.; Nicholson, N.; Jones, J. J.; Guth, S.; Lehr, R.; Prescott, C. D.; Hegg, L. A.; Eggleston, D. S., The structure of ribonuclease P protein from Staphylococcus aureus reveals a unique binding site for single-stranded RNA. *J Mol Biol* **2000,** *295* (1), 105-15.

Stamatopoulou, V.; Toumpeki, C.; Tzakos, A.; Vourekas, A.; Drainas, D., Domain architecture of the DRpp29 protein and its interaction with the RNA subunit of Dictyostelium

discoideum RNase P. *Biochemistry* **2010,** *49* (50), 10714-27.

Stams, T.; Niranjanakumari, S.; Fierke, C. A.; Christianson, D. W., Ribonuclease P protein structure: evolutionary origins in the translational apparatus. *Science* **1998,** *280* (5364), 752-5.

Steinberg, T. H.; Jones, L. J.; Haugland, R. P.; Singer, V. L., SYPRO orange and SYPRO red protein gel stains: one-step fluorescent staining of denaturing gels for detection of nanogram levels of protein. In *Anal Biochem*, United States, 1996; Vol. 239, pp 223-37.

Steitz, T. A.; Steitz, J. A., A general two-metal-ion mechanism for catalytic RNA. *Proc Natl Acad Sci U S A* **1993,** *90* (14), 6498-502.

Sud'ina, A. E.; Zatsepin, T. S.; Pingoud, V.; Pingoud, A.; Oretskaya, T. S.; Kubareva, E. A., Affinity modification of the restriction endonuclease SsoII by 2'-aldehyde-containing double stranded DNAs. *Biochemistry (Mosc)* **2005,** *70* (8), 941-7.

Tadokoro, T.; Kanaya, S., Ribonuclease H: molecular diversities, substrate binding domains, and catalytic mechanism of the prokaryotic enzymes. *FEBS J* **2009,** *276* (6), 1482-93.

Tallsjö, A.; Kirsebom, L. A., Product release is a rate-limiting step during cleavage by the catalytic RNA subunit of Escherichia coli RNase P. *Nucleic Acids Res* **1993,** *21* (1), 51-7.

The RNA Worlds: From Life's Origins to Diversity in Gene Regulation.3d edition (editor: Gesteland R.), Cold Spring Harbor. Year of publication: 2005

Thomas, B. C.; Gao, L.; Stomp, D.; Li, X.; Gegenheimer, P. A., Spinach chloroplast RNase P: a putative protein enzyme. *Nucleic Acids Symp Ser* **1995,** (33), 95-8.

Thomas, B. C.; Li, X.; Gegenheimer, P., Chloroplast ribonuclease P does not utilize the ribozyme-type pre-tRNA cleavage mechanism. *RNA* **2000,** *6* (4), 545-53.

Tsai, H. Y.; Masquida, B.; Biswas, R.; Westhof, E.; Gopalan, V., Molecular modeling of the three-dimensional structure of the bacterial RNase P holoenzyme. *J Mol Biol* **2003,** *325* (4), 661-75.

Tuma, R. S.; Beaudet, M. P.; Jin, X.; Jones, L. J.; Cheung, C. Y.; Yue, S.; Singer, V. L., Characterization of SYBR Gold nucleic acid gel stain: a dye optimized for use with 300-nm ultraviolet transilluminators. *Anal Biochem* **1999,** *268* (2), 278-88.

Turmel, M.; Lemieux, C.; Burger, G.; Lang, B. F.; Otis, C.; Plante, I.; Gray, M. W., The complete mitochondrial DNA sequences of Nephroselmis olivacea and Pedinomonas minor. Two radically different evolutionary patterns within green algae. *Plant Cell* **1999,** *11* (9), 1717-30.

Turmel, M.; Otis, C.; Lemieux, C., The complete chloroplast DNA sequence of the green alga Nephroselmis olivacea: insights into the architecture of ancestral chloroplast genomes. *Proc Natl Acad Sci U S A* **1999,** *96* (18), 10248-53.

Walker, S. C.; Engelke, D. R., A protein-only RNase P in human mitochondria. *Cell* **2008,** *135* (3), 412-4.

Wang, M. J.; Davis, N. W.; Gegenheimer, P., Novel mechanisms for maturation of chloroplast transfer RNA precursors. *EMBO J* **1988,** *7* (6), 1567-74.

Wang, Y.; Juranek, S.; Li, H.; Sheng, G.; Wardle, G. S.; Tuschl, T.; Patel, D. J., Nucleation, propagation and cleavage of target RNAs in Ago silencing complexes. *Nature* **2009,** *461* (7265), 754-61.

Warnecke, J. M.; Fürste, J. P.; Hardt, W. D.; Erdmann, V. A.; Hartmann, R. K., Ribonuclease P (RNase P) RNA is converted to a Cd(2+)-ribozyme by a single Rp-phosphorothioate modification in the precursor tRNA at the RNase P cleavage site. *Proc Natl Acad Sci U S A* **1996,** *93* (17), 8924-8.

Warnecke, J. M.; Held, R.; Busch, S.; Hartmann, R. K., Role of metal ions in the hydrolysis reaction catalyzed by RNase P RNA from Bacillus subtilis. *J Mol Biol* **1999,** *290* (2), 433-45.

Warnecke, J. M.; Sontheimer, E. J.; Piccirilli, J. A.; Hartmann, R. K., Active site constraints in the hydrolysis reaction catalyzed by bacterial RNase P: analysis of precursor tRNAs with a single 3'-S-phosphorothiolate internucleotide linkage. *Nucleic Acids Res* **2000,** *28* (3), 720-7.

Wegscheid, B.; Hartmann, R. K., The precursor tRNA 3'-CCA interaction with Escherichia coli RNase P RNA is essential for catalysis by RNase P in vivo. *RNA* **2006,** *12* (12), 2135-48.

Wegscheid, B.; Hartmann, R. K., In vivo and in vitro investigation of bacterial type B RNase P interaction with tRNA 3'-CCA. *Nucleic Acids Res* **2007,** *35* (6), 2060-73.

Xiao, S.; Hsieh, J.; Nugent, R. L.; Coughlin, D. J.; Fierke, C. A.; Engelke, D. R., Functional characterization of the conserved amino acids in Pop1p, the largest common protein subunit of yeast RNases P and MRP. *RNA* **2006,** *12* (6), 1023-37.

Xu, Y. Z.; Liu, W. Y., Effects of the active aldehyde group generated by RNA N-glycosidase in the sarcin/ricin domain of rat 28S ribosomal RNA on peptide elongation. *Biol Chem* **2000,** *381* (2), 113-9.

Yanish-Peron, C., Viera, J., Messing, J.1985. Improved M13 phage cloning vectors and host strains: nucleotide sequences of the M13mp18 and pUC19 vectors.*Gene*.**33(1):**103-19.

Zatsepin, T. S.; Gait, M. J.; Oretskaya, T. S., 2'-Functionalized nucleic acids as structural tools in molecular biology. *IUBMB Life* **2004,** *56* (4), 209-14.

Zatsepin, T. S.; Romanova, E. A.; Stetsenko, D. A.; Gait, M. J.; Oretskaya, T. S., Synthesis of 2'-modified oligonucleotides containing aldehyde or ethylenediamine groups. *Nucleosides Nucleotides Nucleic Acids* **2003,** *22* (5-8), 1383-5.

Zatsepin, T. S.; Stetsenko, D. A.; Arzumanov, A. A.; Romanova, E. A.; Gait, M. J.; Oretskaya, T. S., Synthesis of peptide-oligonucleotide conjugates with single and multiple peptides attached to 2'-aldehydes through thiazolidine, oxime, and hydrazine linkages. *Bioconjug Chem* **2002,** *13* (4), 822-30.

Zubin, E. M.; Stetsenko, D. A.; Zatsepin, T. S.; Gait, M. J.; Oretskaya, T. S., Oligonucleotides containing 2'-O-[2-(2,3-dihydroxypropyl)amino-2-oxoethyl]uridine as suitable precursors of 2'-aldehyde oligonucleotides for chemoselective ligation. *Bioorg Med Chem* **2005,** *13* (16),

4912-20.

Zuleeg, T.; Hartmann, R. K.; Kreutzer, R.; Limmer, S., NMR spectroscopic evidence for Mn(2+)(Mg(2+)) binding to a precursor-tRNA microhelix near the potential RNase P cleavage site. *J Mol Biol* **2001,** *305* (2), 181-9.

Acknowledgements

I would like to thank…

… Prof. Dr. Roland K. Hartmann for giving me the opportunity to work in his lab and for his support during my PhD research.

… Prof. Dr. Peter Friedhoff for serving as the second examiner at thesis defence.

… Prof. Dr. Michael Keusgen, Prof. Dr. Maike Petersen for participation in the examination committee.

… International Reasearch Training Group “Enzymes and multienzyme complexes acting on nucleic acids” for research funding.

… Dr. Markus Gößringer for introducing me to the basics of molecular biology, helpful discussions and proofreading of my dissertation.

… Dominick Helmecke for exellent technical support in the lab.

… Katja Hütte and Dr.Anja Drescher for helping me to manage bureucracy.

… all of my colleagues in Marburg and collaborators in Moscow and Vienna for cooperativeness, helpfulness and especially for the friendly atmosphere in- and outside the lab.

… Christine and Bill Andreopoulos, Karen Köhler for proofreading of this manuscript.

… моих маму, папу, брата, кто все это время поддерживал и верил в меня.Спасибо!

… my husband for infinite love, encouragement and support.

Publications arising from this work

Articles

Turunen J.J., Pavlova L.V., Hengesbach M., Helm M., Hartmann R.K., Frilander M.J. Enzymatic RNA ligation. In:Handbook of RNA Biochemistry, 2nd Edition (eds.R.K.Harmann, A.Bindereif, A.Schön, E.Westhof), WILLY-VCH, Weinheim, Germany. Year of publication: 2012

Khomykova E.I., Zubin E.M., Pavlova L.V., Kazanova E.V., Smirnov I.P., Pozmogova G.E., Müller S., Dolinnaya N.G., Kubareva E.A., Hartmann R.K., Oretskaya T.S. 2'-modified oligoribonucleotides, containing 1, 2 - diol and aldehyde groups. Synthesis and properties. Russian Journal of Bioorganic Chemistry, 2012, 5: 1-14.

Pavlova L.V., Gößringer M., Weber C., Buzet A., Rossmanith W. and Hartmann R.K. Catalysis by proteinaceous RNase P - effect of an *R*p-phosphorothioate substitution at the scissile phosphodiester (submitted to Nucleic Acid Research; NAR-01534-2012)

Poster presentations

• 1st GGL Conference in Natural and Life Sciences, 30 September -1 October 2008, Giessen, Germany
• Minisymposium of the IRTG 1384, 27 November 2009, Moscow, Russia
• Workshop "Enzymes and multienzyme complexes acting on nucleic acids"of the IRTG 1384, 16-19 May 2010 Vilnius, Latvia
• Off-spring-Meeting of the IRTG 1384 "Enzymes and multienzyme complexes acting on nucleic acids", 16-20 Juni 2010, Moscow, Russia
• On-site evaluation of the IRTG 1384 "Enzymes and multienzyme complexes acting on nucleic acids", 26 September 2010, Giessen, Germany
• 6th Meeting of the German Society for Biochemistry and Molecular Biology (GBM) Study Section "RNA Biochemistry", October 2010, Hohenwart, Pforzheim, 30 September-3 October 2010
• 62.Mosbacher Kolloquium of the German Society for Biochemistry and Molecular Biology (GBM) "Mechanisms of RNA-mediated regulation", 06-09 April 2011, Mosbach, Germany
• Tag der Wissenschaft 2012, Graduiertenzentrum Lebens- und Naturwissenschaften, Philipps University Marburg, 15 January 2012, Marburg, Germany

Oral presentations

• Minisymposium "Small RNAs in Bacteria, Archaea and Eukarya", 21-25 March 2009, Hirschegg, Austria
• Minisymposium "Snow RNAs: biogenesis, structure, function and evolution", 3-7 April 2010, Hirschegg, Austria
• Minisymposium "Non-coding RNAs", 13-17 March 2011, Hirschegg, Austria
• Symposium "Proteinaceous RNase P (PRORP) and tRNA:m1R9 methyltransferase " 15-18 September 2011, Wien, Austria

Curriculum vitae

Name	Liudmila V. Pavlova
Date of birth:	August 18th, 1984
Place of Birth:	Ardatov, Russia
Citizenship:	Russian Federation
Address:	Neue Kasseler Str.44, 35039, Marburg, Germany
Tel.:	+49 0 1577 370 22 53
Email :	pavloval@staff.uni-marburg.de

Education

2007-2012	Ph.D. studies, Institute of Pharmaceutical Chemistry, Philipps University Marburg, Germany
2006-2007	Post-graduate studies in Pharmaceutical Chemistry, Samara State Medical University, Russia
2001-2006	Studies in pharmacy (Diploma with honours), Samara State Medical University, Russia

Ph.D.thesis

Title: Crosslinking studies of the bacterial RNase P holoenzyme and functional characterisation of the novel protein-only RNase P from *Arabidopsis thaliana*
Supervisors: Prof.Dr. Roland Hartmann (Philipps University Marburg),
Prof.Dr. Peter Friedhoff (Justus Liebig University Giessen),
Dr. Elena Kubareva (Lomonosov University Moscow)

Diploma thesis

Title: Eutectics of butadionum and trisamine: improvement of dissolution, comparative *in vitro* pharmacokinetic studies
Supervisors: Dr. Michail Tkachenko (Samara State Medical University),
Dr. Ivan Levanjuk (Ozon Pharmaceutics, Samara)

Professional experience

2006-2007 Community pharmacist, Milana Pharmacy, Samara, Russia

Academic experience

• Teaching: Supervision of undergraduate students' lab courses in Biochemistry
• Graduate School Member of the International Research Training Group IRTG 1384 "Enzymes and multienzyme complexes acting on nucleic acids"

Scientific skills and methods

• Molecular biology: Work with genetically modified organisms (Bacteria), cloning, PCR, standard DNA techniques, radioactive and fluorescent labeling
• RNA methods: In vitro transcription, RNA ligation, RNA-protein chemical and UV-cross-linking, ribozyme kinetics
• Protein methods: Protein expression and purification using FPLC, Western blotting, enzyme kinetics
• Bioinformatics: PyMol, standard lab programs
• Soft skills: Seminars “English for Presentations”, ”Scientific Writing”, “Project Management in Research” attended in Marburg, Germany

Publications

• Pavlova L.V., Zhnyakina L.S., Smelova S.A., Tkachenko M.L. Solid dispersions of butadion and trisamine as a hydrophilic carrier. Pharmacy (Russia), 2006, 34: 31-35

•Turunen J.J., Pavlova L.V., Hengesbach M., Helm M., Hartmann R.K., Frilander M.J. Enzymatic RNA ligation. In:Handbook of RNA Biochemistry, 2nd Edition (eds.R.K.Harmann, A.Bindereif, A.Schön, E.Westhof), WILLY-VCH, Weinheim, Germany. Year of publication: 2012

• Khomykova E.I., Zubin E.M., Pavlova L.V., Kazanova E.V., Smirnov I.P., Pozmogova G.E., Müller S., Dolinnaya N.G., Kubareva E.A., Hartmann R.K., Oretskaya T.S. 2’-modified oligoribonucleotides, containing 1, 2-diol and aldehyde groups. Synthesis and properties. Russian Journal of Bioorganic Chemistry, 2012, 5: 1-14.

• Pavlova L.V., Gößringer M., Weber C., Buzet A., Rossmanith W. and Hartmann R.K. Catalysis by proteinaceous RNase P - effect of an *R*p-phosphorothioate substitution at the scissile phosphodiester (submitted to Nucleic Acid Research; NAR-01534-2012)

Languages

• Russian Native
• English Fluent
• German Good

Declaration

Ich versichere, dass ich meine Dissertation

Crosslinking studies of the bacterial RNase P holoenzyme and functional characterisation of the novel protein-only RNase P from *Arabidopsis thaliana*

selbstständig, ohne unerlaubte Hilfe angefertigt und mich dabei keiner anderen als der von mir ausdrücklich bezeichneten Quellen und Hilfen bedient habe.

Die Dissertation wurde in der jetzigen oder einer ähnlichen Form noch an keiner anderen Hochschule eingereicht und hat noch keinen sonstigen Prüfungszwecken gedient.

Marburg an der Lahn, 28.06.2012

(Ort/Datum) (Unterschrift mit Vor- und Zuname)